

**UNIVERSITY OF TURKISH AERONAUTICAL ASSOCIATION
INSTITUTE OF SCIENCE AND TECHNOLOGY**

**ENHANCED HEAT TRANSFER PERFORMANCE
OF A FLAT PLATE SOLAR COLLECTOR USING NANOFUIDS**



MASTER THESIS

Hassn Tarek JALEL

Institute of Science and Technology

Mechanical and Aeronautical Engineering Department

DECEMBER, 2017

**UNIVERSITY OF TURKISH AERONAUTICAL ASSOCIATION
INSTITUTE OF SCIENCE AND TECHNOLOGY**

**ENHANCED HEAT TRANSFER PERFORMANCE
OF A FLAT PLATE SOLAR COLLECTOR USING NANOFUIDS**



MASTER THESIS

Hassn Tarek JALEL

1406080006

Institute of Science and Technology

Mechanical and Aeronautical Engineering Department

Thesis Supervisor: Assist. Prof. Habib GHANBARPOURASL

Hassn Tarek Jalel, having student number 1406080006 and enrolled in the Master Program at the Institute of Science and Technology at the University of Turkish Aeronautical Association, after meeting all of the required conditions contained in the related regulations, has successfully accomplished, in front of jury, the presentation of the thesis prepared with the title of: "ENHANCED HEAT TRANSFER PERFORMANCE OF A FLAT PLATE SOLAR COLLECTOR USING NANOFLUIDS"

Supervisor : Assist Prof. Dr. Habib GHANBARPOURASL
University of Turkish Aeronautical Association

Jury Members : Assist Prof. Dr. Habib GHANBARPOURASL
University of Turkish Aeronautical Association

: Assist Prof. Dr. Mohamed Salem ELMENFI
University of Turkish Aeronautical Association

: Assist Prof. Dr. Rahim JAFARI
University of Atilim

Rahim Jafari

Thesis Defense Date : 12 .12.2017

**UNIVERSITY OF TURKISH AERONAUTICAL ASSOCIATION
INSTITUTE OF SCIENCE AND TECHNOLOGY**

I hereby declare that all the information in this study I presented as my Master's Thesis, called: "Enhanced Heat Transfer Performance of Flat Plate Solar Collector Using Nanofluids" has been present in accordance with the academic rules and ethical conduct. I also declare and certify with my honor that I have fully cited and referenced all the sources I made use of in this present study.



Hassn Tarek Jalel

12.12.2017

ACKNOWLEDGEMENTS

I am grateful to The Almighty GOD for helping me to complete this thesis. My Lord mercy and peace be upon our leader Mohammed peace be upon on him, who invites us to science and wisdom, and members of his family and his followers.

I would like to thank my parents, my brothers and my wife for supporting me throughout my academic career. Without their moral support, interest and encouragement for my academic work, the completion of this effort would not have been possible.

I would like to express my sincere gratitude to Assist. Prof. Dr. Habib GHANBARPOURASI at University of Turkish Aeronautical for his sound advice and constructive criticisms in the evaluation of the results. He has helped me at the final stage of my thesis and willingly sharing his knowledge and ideas with me.

My ambition to obtain a master degree was fulfilled mainly because of the support and guidance I received from Assist. Prof. Dr. Wisam Jaleel. He has helped me at various stages during my studies for achieving my objectives, and willingly sharing his knowledge and ideas with me. His active participation at every facet of my research work and mentoring has shaped my overall research outlook. I am extremely grateful to him.

Finally, I would present my fully gratitude to Eng. Hadi Roomi, for his unlimited support through help me in my thesis.

December 2017

Hassn JALEL

TABLE OF CONTENTS

ACKNOWLEDGEMENTS	iv
TABLE OF CONTENTS	v
LIST OF TABLES	vii
LIST OF FIGURES	viii
NOMENCLATURE.....	x
ABSTRACT	xii
ÖZET	xiv
CHAPTER ONE	1
1. INTRODUCTION	1
1.1 Motivation	1
1.2 Solar Energy	2
1.3 Solar Water Heating (SWH) Systems	3
1.4 Solar Thermal Collectors	3
1.5 Nano-fluid Technology Applications	6
1.6 Literature Review	6
1.6.1 Introduction	6
1.6.2 Experimental Studies	7
1.6.3 Theoretical Studies	9
1.7 Concluded Notes	13
1.8 Research Objectives	13
1.9 Thesis Outline	13
CHAPTER TWO	15
THEORY OF FLAT PLATE FORMULATION	15
2.1 Introduction	15
2.2 Flat Plate Thermal Efficiency	15
2.2.1 Heat Removal Factor.....	16
2.3 Collector Energy Losses.....	17
2.4 Useful Energy Gain.....	20
2.5 Reynolds Number.....	21
2.6 Nusselt Number.....	22
2.7 Prandtl Number	22
2.8 Useful Energy Gain for Nano-fluids	23
2.9 Empirical Relationship	24
CHAPTER THREE	25
3. EXPERIMENTAL WORK	25
3.1 Introduction	25
3.2 The Experimental Setup	25
3.2.1 Flat Plate Solar Collector (FPSC) Experimental Set-up	27
3.2.2 Glazing	28
3.2.3 Absorber Plate	28
3.2.4 Insulation	28

3.2.5 Pump.....	29
3.2.6 Storage Tank	29
3.3 The Measuring Devices.....	29
3.3.1 Thermocouples	29
3.3.2 Temperature Recorder	30
3.3.3 Flow Meter	31
3.3.4 Solar Power Meter.....	32
3.4 The Calibration of Measuring Devices	33
3.4.1 Calibration of Thermocouples	33
3.4.2 Calibration of Flow Meter	33
3.5 Nano-fluid Preparation	34
3.6 Experimental procedure	37
3.6.1 The Base Fluid Experiments	37
3.6.2 The TiO ₂ / Water Experiments	37
3.6.3 The CuO/Water Nano-fluid Experiments	38
3.7 Summary	40
CHAPTER FOUR	41
4. ANALYSIS OF DATA.....	41
4.1 Introduction	41
4.2 Experimental Results	41
4.2.1 Incident Solar Radiation Results	43
4.2.2 Temperature Difference Results	50
4.2.2.1 The Flow Rate Effect-The Base Fluid (Water)	50
4.2.2.2 The Fluid Type Effect-The Base Fluid (Water) and CuO/Water and TiO ₂ / Water Nano-fluids	51
4.2.2.3 The Flow Rate Effect – 0.2 % By vol. (CuO/Water Nano-fluid)	53
4.2.2.4 The Flow Rate Effect – 0.3 % By vol. CuO/Water Nano-fluid	54
4.2.2.5 The Effect of Nano-particles Volume Concentratio	55
4.3 Efficiency of Flat Plate Solar Collector	57
4.4 The Empirical Correlations	60
4.5 Summary	60
CHAPTER FIVE.....	62
5. CONCLUSIONS AND FUTURE WORK	62
5.1 Conclusion.....	62
5.2 Future Work	63
REFERENCESE	65
APPENDIX.....	69
APPENDIX-A:.....	70
APPENDIX-B:.....	83
CURRICULUM VITAE.....	87

LIST OF TABLES

Table 2.1 : Thermo Physical Properties of Base Fluid and Nano-particles	23
Table 3.1 : The Specification of Flat Plate Solar Collector Components.	27
Table 3.2 : The Solar Collector Network of Thermocouples Distribution.	30
Table 3.3 : Physical properties of Copper oxide (CuO) and Titanium oxide (TiO ₂) Nano-particles.	34
Table 4.1 : The Efficiency of Flat Plate Solar Collector Using Different Fluids.	58
Table 4.2 : The Dimensionless Relationship From Experimental Work.	60

LIST OF FIGURES

Figure 1.1	: Annual growth rates of world renewables supply from 1990 to 2013.....	1
Figure 1.2	: Usage for the solar energy.....	3
Figure 1.3	: The flat – plate collector.....	4
Figure 1.4	: The evacuated-tube collector.	5
Figure 1.5	: The concentrating collector.....	5
Figure 2.1	: Thermal network for a single cover collector in terms of (A) conduction, convection and radiation (B) resistance between plate, and (C) a simple collector network.....	18
Figure 2.2	: The heat transfer to a fluid flowing in a tube.....	21
Figure 3.1	: The schematic of flat plate solar collector experimental setup.....	26
Figure 3.2	: Experimental set-up of flat plate solar collector.....	26
Figure 3.3	: The flat plate solar collector (FPSC).....	27
Figure 3.4	: The insulated storage tank and the inlet and outlet pipes connected to the (FPSC).....	28
Figure 3.5	: The fluid pump.....	29
Figure 3.6	: The solar collector network of thermocouples distribution.....	30
Figure 3.7	: The temperature recorder.....	31
Figure 3.8	: The flow meter.....	32
Figure 3.9	: The solar intensity meter.....	32
Figure 3.10	: The flow meter calibration.....	34
Figure 3.11	: The sensitive balance.....	36
Figure 3.12	: (a) The Ultra – sonicator and (b) Mixing of the nano-fluids.....	36
Figure 3.13	: The chart of final experiments.....	39
Figure 4.1	: Incident solar radiation on May 29,2017.....	43
Figure 4.2	: Incident solar radiation on May 30,2017.....	44
Figure 4.3	: Incident solar radiation on May 31,2017.....	44
Figure 4.4	: Incident solar radiation on June 4,2017.....	45
Figure 4.5	: Incident solar radiation on June 8,2017.....	45
Figure 4.6	: Incident solar radiation on June 11,2017.....	46
Figure 4.7	: Incident solar radiation on June 12,2017.....	46
Figure 4.8	: Incident solar radiation on June 13,2017.....	47
Figure 4.9	: Incident solar radiation on June 14,2017.....	47
Figure 4.10	: Incident solar radiation on June 15,2017.....	48
Figure 4.11	: Incident solar radiation on June 18,2017.....	48
Figure 4.12	: Incident solar radiation on June 19,2017.....	49
Figure 4.13	: Incident solar radiation on June 20,2017.....	49
Figure 4.14	: The inlet – outlet temperature difference vs. time at different flow rates (1,1.5,2, and 3 Lpm) for the base (water).....	51

Figure 4.15 : The inlet – outlet temperature difference vs. time at 1.5 Lpm flow rate for water, CuO/water, and TiO ₂ /water nano-fluid with nano-particles volume concentration of ($\phi= 0.1$ %)	52
Figure 4.16 : The inlet – outlet temperature difference vs. time at 1.5, 2, and 3 Lpm flow rates for CuO/water with nano-particles volume concentration of ($\phi= 0.2$ %)	53
Figure 4.17 : .The inlet – outlet temperature difference vs. time at 1, 1.5, 2 and 3 Lpm flow rates for CuO/water with nano-particles voulme concentration of ($\phi = 0.3$ %)	54
Figure 4.18 : The inlet – outlet temperature difference vs. time at 1.5 Lpm flow rate for water and CuO/water nano-fluids of different concentration (0.1, 0.2, and 0.3 %).	55
Figure 4.19 : The inlet – outlet temperature difference vs. time at 2 Lpm flow rate for water and CuO/water nano-fluids of different concentration (0.2 and 0.3 %).	56
Figure 4.20 : The inlet – outlet temperature difference vs. time at 3 Lpm flow rate for water and CuO/water nano-fluids of different concentration (0.2 and 0.3 %)	57
Figür 4.21 : The efficiency of flat plate solar collector using diffrent nano-fluids	59

NOMENCLATURE

FPSC	: Flat plate solar collector
SWH	: Solar Water Heating
Lpm	: Liters per minutes
Ng	: Number of glass
V	: Average wind speed (m/s)
W	: Wall
nf	: Nanofluid
np	: Nanoparticles
ave.	: Average
f	: Correction of heat transfer coefficient by wind
c	: Correction coefficient of tilt angle
L	: Long of collector (m)
bf.	: Base fluid
to.	: Top of flat plate solar collector
bot.	: Bottom of flat plate solar collector
ed.	: Edge of flat plate solar collector
ba.	: Back of flat plate solar collector
Q_u	: Rate of useful energy gained (W)
Q_{loss}	: Total losses energy (W)
$Q_{to.}$: Top losses energy of flat plate solar collector (W)
$Q_{bo.}$: Bottom losses energy of flat plate solar collector (W)
$Q_{ed.}$: Edge losses energy of flat plate solar collector (W)
$t_{ba.}$: Thickness of back insulation (m)
$t_{ed.}$: Thickness of edge insulation (m)
$k_{ba.}$: Conductivity of back insulation ($W/m.K$)
$h_{c,b-a}$: Convection heat loss coefficient from back to ambient ($W/m^2.K$)
$h_{c,ed-a}$: Convection heat loss coefficient from edge to ambient ($W/m^2.K$)
\dot{m}	: Mass flow rate of fluid flow(kg/sec)
m	: Mass (g)
C_p	: Specific heat at constant pressure ($J/Kg.K$)
T_i	: Inlet fluid temperature of solar collector ($^{\circ}C$)
T_o	: Outlet fluid temperature of solar collector ($^{\circ}C$)
U_{in}	: Input velocity of fluid (m/sec)
q	: Heat transfer rate (w)
A_c	: Surface area of solar collector (m^2)
A_s	: Cross section area of pipe (m^2)
D_i	: Tube inside diameter (m)
D_o	: Tube outside diameter (m)
R_e	: Reynolds number
P_r	: Prandtl number

N_u	: Nusselt number
h	: Local heat transfer coefficient ($W/m^2.K$)
K	: Thermal conductivity ($W/m.K$)
U_L	: Overall heat loss coefficient based on collector area ($W/m^2.K$)
T_p	: Plate temperature ($^{\circ}C$)
T_a	: Ambient temperature ($^{\circ}C$)
T_{ave}	: Average temperature ($^{\circ}C$)
h_w	: Wind heat transfer coefficient ($W/m^2.K$)
G	: Radiation intensity (W/m^2)
F_r	: Heat removal factor
$T_{p,ave}$: Average plate temperature ($^{\circ}C$)
F'	: Collector efficiency factor
C_b	: Bond conductance
$T_{a,ave}$: Average ambient temperature ($^{\circ}C$)
w	: Distance between tubes (m)
h_{fi}	: Heat transfer coefficient inside absorber tube ($W/m^2.K$)
ρ	: Density (kg/m^3)
ϕ	: Weight fraction of nanoparticles in nanofluid (%)
μ	: Viscosity ($N.s/m^2$)
ν	: Kinematic viscosity (m^2/s)
ϵ_p	: Absorber plate emissivity
ϵ_g	: Glass emissivity
σ	: Boltz man constant = $5.67 * 10^{-8}$
β	: Tilt collector angle ($^{\circ}$)
η	: Collector efficiency
τ	: Transmittance
α	: Absorptance
δ	: Thickness of plate (m)

ABSTRACT

ENHANCED HEAT TRANSFER PERFORMANCE OF A FLAT PLATE SOLAR COLLECTOR USING NANOFLUIDS

JALEL, Hassn

M.Sc., Department of Mechanical Engineering

Supervisor: Assist. Prof. Dr. Habib GHANBARPOURASL

December 2017, 87 pages

A flat plate solar collector (FPSC) is considered a major component in solar water-heating systems. The harvested thermal energy from the solar radiation by the collector can be improved by adding a small amount of the nano-particles to the working fluid (water) to form what is called "nano-fluid". Hence, this project focuses on evaluating the heat transfer performance of the FPSC with a spiral tube arrangement using TiO₂/water and CuO/water nano-fluids as working fluids instead of the base fluid (water). The FPSC performance was evaluated based on the effect of the fluid type, the fluid flow rate, and the nano-particles volume concentration of the nano-fluids on the temperature difference between the inlet and outlet fluid streams and the FPSC thermal efficiency.

The results showed that the CuO/water nano-fluid as a working fluid in the FPSC exhibited higher heat transfer performance compared to TiO₂/water nano-fluid as well as the base fluid (water) due to the higher thermal conductivity of CuO nano-particles. The inlet-outlet temperature difference at 1.5 Lpm flow rate for water, CuO/water and TiO₂/water nano-fluids were 6.6 °C, 7.1 °C, and 7.9 °C, respectively. Furthermore, the maximum efficiency was reported to be 60% for 0.2% particle volume concentration of the CuO/water nano-fluid at a flow rate of 3 Lpm.

Finally, based on the raw experimental data, the empirical correlations (Nusselt number as a function of Reynolds number and Prantal number) for the base fluid (water), CuO/water nano-fluid, TiO₂/water nano-fluid were obtained utilizing Statistica software.

Keywords: Renewable energy, Flat plate solar collector, Nanofluid, CuO/Water and TiO₂ /Water Nanofluids, Solar thermal energy, Water heating systems.



ÖZET

NANOFLUIDS KULLANARAK BİR PLAF SOLAR KOLLEKTÖRÜNÜN, ISI TRANSFER PERFORMANSINI GELİŞTİRMEK

JALEL, Hssan

Yüksek Lisans, Makine Mühendisliği Bölümü

Danışman: Doçent Dr. Habib GHANBARPOURASL

Aralık 2017, 87 sayfa

Düz plaka güneş kolektörü (FPSC), güneş enerjili su ısıtma sistemlerinde önemli bir bileşen olarak düşünülür. Kolektör tarafından, güneş radyasyonundan elde edilen ısı enerjisi, "nano-fluid/nano akışkan" olarak adlandırılanları oluşturmak için küçük miktarda nanopartiküllerin çalışma sıvısına (suya) eklenmesiyle geliştirilebilir. Bu nedenle, bu proje, FPSC'nin ısı transfer performansını, orijinal sıvı (su) yerine çalışma sıvıları olarak TiO₂ / su ve CuO / su nano akışkanlarını kullanarak spiral boru düzeni ile değerlendirmeye odaklanmaktadır. FPSC performansı, akışkanın tipinin, akışkanın akış oranının ve nanofluidlerin nanopartikül hacim konsantrasyonunun, giren ve çıkan akışkanların akımları arasındaki sıcaklık farkı ve FPSC termal verimliliği üzerindeki etkisine dayanarak değerlendirildi.

Sonuçlar, FPSC'de bir çalışma sıvısı olarak CuO / su nano-fluidinin, CuO nano parçacıklarının daha yüksek olan termal iletkenliğinden dolayı, orijinal sıvı (su) kadar TiO₂ / su nano-fluid'e kıyasla daha yüksek ısı transfer performansı sergilediğini gösterdi. Su, CuO / su ve TiO₂ / su nano yakıtları için 1.5 litre / dakika akış hızındaki giriş-çıkış sıcaklık farkı sırasıyla 6.6 ° C, 7.1 ° C ve 7.9 ° C idi. Ayrıca, maksimum verimlilik 3 litre / dakikalık bir akış oranında CuO / su nano-fluidinin (%0.2) partikül hacmi konsantrasyonu için % 60 olarak rapor edilmiştir.

Son olarak, ham deney verileri temel alınarak, baz sıvısı (su), CuO / su nanoakışkanı ve TiO₂ / su nano akışkanı için ampirik korelasyonlar (Nusselt sayısı Reynolds sayısı ve Prantal sayısına bağılı olarak) STAYISTICA yazılımı kullanılarak elde edildi.

Anahtar Kelimeler: Yenilenebilir enerji, Düz plaka güneş kolektörü, Nanofluid, CuO / Su ve TiO₂ / Su Nanoflüleri, Güneş enerjisi, Su ısıtma sistemleri.



CHAPTER ONE

INTRODUCTION

1.1 Motivation

The coupled challenges of the fast developments in a world population, which is doubling the world's energy needs, and the increasing demands for clean energy sources resulted in increased worldwide interest in the possibilities of utilizing renewable sources as a long-term solution for a secure energy future as shown in Fig. (1.1) [1-4]. Compared to fossil fuels, the solar energy as one of the most available renewable energy sources is an environmentally clean source of energy and it is a very suitable energy source for solar water heating (SWH) applications, which is considered the most effective approach for utilizing the solar heat [1]. Hence, in the recent years, there is a great potential in utilizing the solar energy due to the problems associated with the depletion of fossil fuels as well as the environmental concerns such as global warming and air pollution.

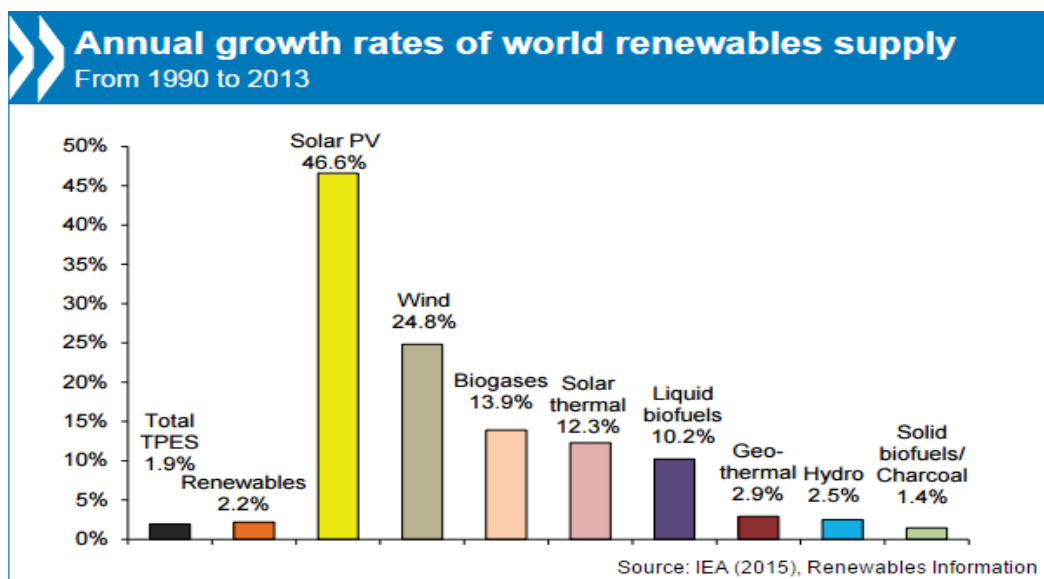


Figure 1.1: Annual growth rates of world renewables supply from 1990 to 2013[2].

The solar collectors are considered a special type of heat exchangers that are absorb the incoming solar radiation and convert it into heat, which is transferred to a fluid such as air, water, oil, and ethylene glycol flows through the collector [3]. The major applications of these units are (SWH) systems in homes, solar space heating, air-conditioning, and some others industrial processes [3]. Among various types of the solar collectors, the FPSC is commonly used today for the collection of low temperature solar thermal energy. Although the FPSC is simple, cheap, and most productive collector, it comparatively suffers from the low efficiency. Hence, it is very important to find new, effective, and convenient approaches to enhance the efficiency of FPSC. One of the most efficient approaches is to replace the base fluid (water) with a higher thermal conductivity fluid containing solid nano-particles known as nano-fluids [1-4].

1.2 Solar Energy

Different technologies such as photovoltaic, solar thermal energy, solar architecture, and can be utilized to harness the solar energy (radiant light and heat) from the Sun. The solar energy is considered as one of the most common, important, and valuable source for renewable energy field. The technologies of the solar energy are classified as passive and active solar based on how these technologies capture and distribute the solar energy or convert it into solar power. The photovoltaic, concentrated solar power and solar water heating systems are active solar technique, which are used to harness the solar energy as shown in Fig. (1.2). While designing spaces that naturally circulate air, orienting a building to the Sun, and selecting materials with favorable thermal mass or light-dispersing properties are considered as passive solar techniques [5-6].

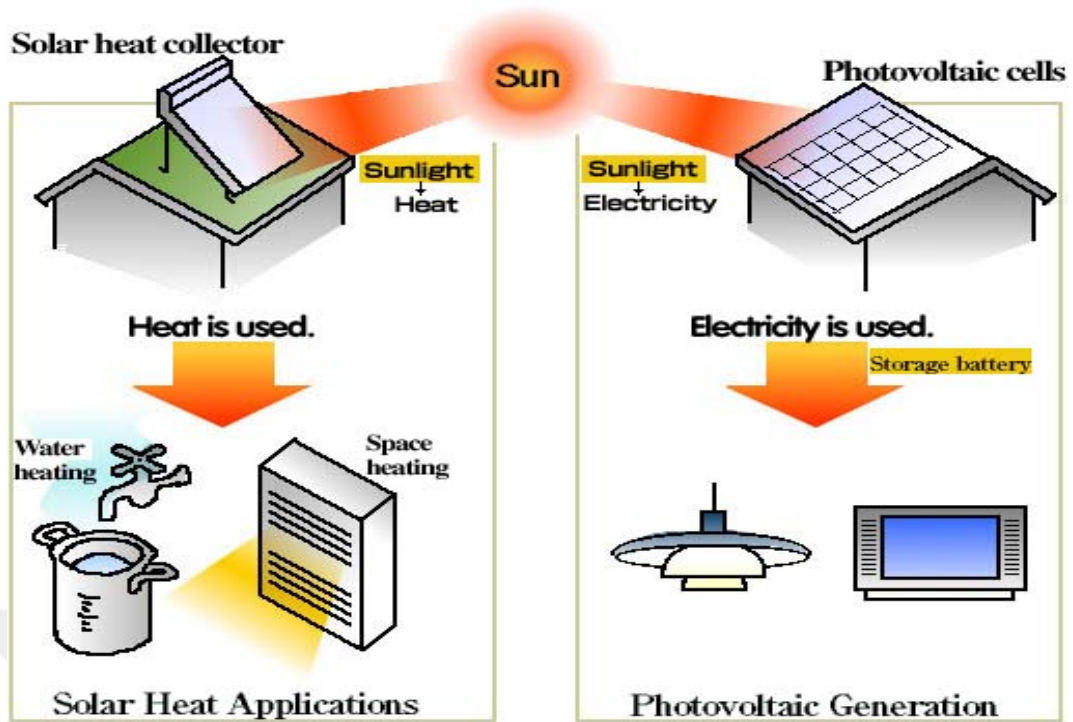


Figure 1.2: Usage for the solar energy [7]

1.3 Solar Water Heating (SWH) Systems

To provide homes and businesses with hot water, solar thermal water heating systems are utilized to harness the sun's energy. These systems are simple, durable, reliable, and cost-effective. The heart of the SWH is the solar collectors that are used to heat up the water by capturing the sunlight and convert it to heat. The SWH systems are widely used in residential and industrial applications [8]. There are two types of the SWH systems, which are active (pumped) and passive (convection-driven). The working fluid passes through the solar collector and it is heated by the direct exposure to the sunlight or via light-concentrating mirrors heat it. These collectors can independently operate or as hybrids with gas or electric heaters [9]. China, Japan, and India are leading the global solar thermal market [10].

1.4 Solar Thermal Collectors

There are three basic styles of collectors: (flat-plate, concentrating, and evacuated-tube). A FPSC is an insulated, climate-evidence field containing a darkish absorber plate underneath one or greater obvious or translucent covers Fig. (1.3) Small tubes run through the field and bring the warmth switch fluid. The tubes are attached

to the dark absorber plate. As warmth builds up in the collector, it heats the fluid passing in the tubes. that is the most not unusual sort of collectors.

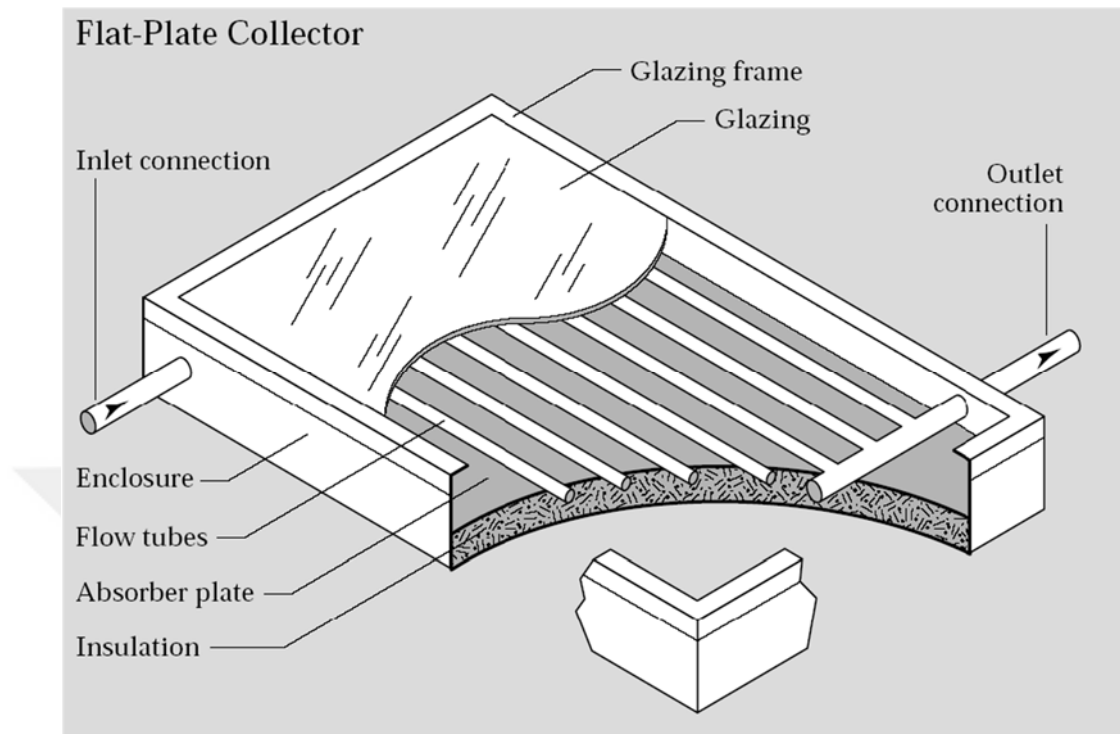


Figure 1.3: The flat-plate collector [11]

Figure (1.4) evacuated-tube collectors are made of rows of parallel, obvious glass tubes stored in a rigid box. Each tube consists of a pitcher outer tube and an inner tube, or absorber, included with a selective coating that absorbs sun electricity. The air is evacuated from the distance among the tubes to form a vacuum, which removes conductive and convective warmth loss. The fluid in those tubes may additionally reach extremely high temperatures which lead them to suitable for business or industrial uses.

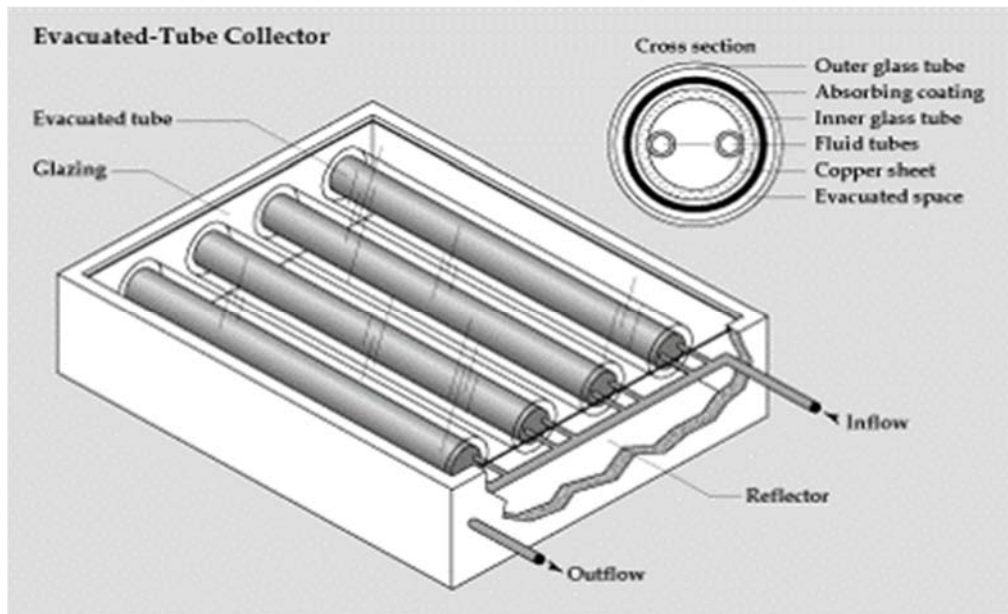


Figure 1.4: The evacuated-tube collector [12]

Figure (1.5) concentrating collectors are generally parabolic troughs that use mirrored surfaces to pay attention the sun's strength on a tube containing the warmth-switch fluid [13].

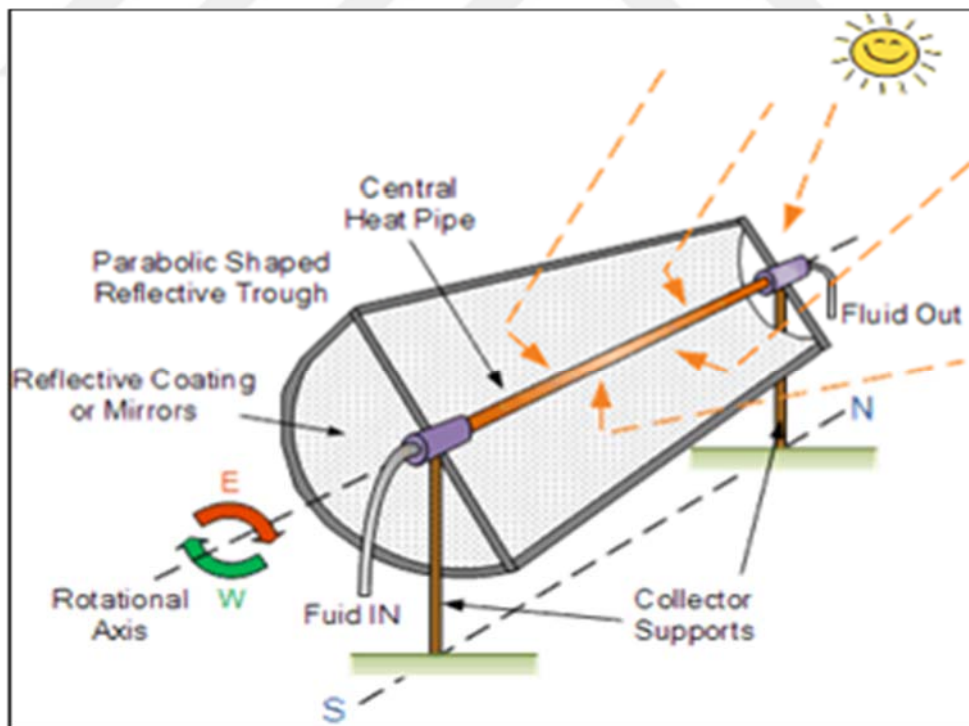


Figure 1.5: The concentrating collector [14]

1.5 Nano-fluid Technology Applications

A nano-fluid is a fluid containing nanometer-sized particles (less than 100 nm), which are commonly manufactured from metals and metal-oxides, and metal-carbides [15]. The carbon nanotubes have been also utilized as dispersed particles in the base fluid [15]. Choi first coined the term nano-fluid by 1995 [16]. The common base fluids include (water), ethylene glycol, and oil [15].

Nano-fluids have novel residences that make them potentially beneficial in lots of programs in warmth switch, along with microelectronics, pharmaceutical, gasoline cells, techniques, and hybrid-powered engines, engine cooling/vehicle thermal control, chiller, home refrigerator, heat exchanger, in grinding, machining and in boiler flue gas temperature discount [15]. They display superior thermal conductivity and the convective warmth switch coefficient as compared to the bottom fluid. Know-how of the rheological conduct of nano-fluids is discovered to be very crucial in determining their suitability for convective warmth switch programs [15].

Nano-fluids are generally used for their stronger thermal residences as coolants in heat transfer system that includes warmth exchangers, digital cooling gadget (which includes FPSC) and radiators. Many researchers have analyzed warmth switch over FPSC. However, they may be also beneficial for his or her controlled optical homes. Nano-fluids in solar collectors is some other utility wherein nano-fluids are employed for the tunable optical residences [15].

1.6 Literature Review

1.6.1 Introduction

Several experimental and numerical studies investigated the prospects of improving the efficiency of FPSCs using nano-fluids. Hence, this section presents an overview of the literature related to the effect of applying nano-fluids as working fluids on the thermal performance of FPSCs. The survey focuses on the experimental and theoretical studies in which CuO/water and TiO₂/water nano-fluids were used.

1.6.2 Experimental Studies

The nano-fluid term was first coined by Choi [16] which is defined as a suspension formed by mixing (metallic or nonmetallic) nano-particles with a base fluid (water). The enhanced thermos-physical properties such as liquid viscosity, liquid thermal conductivity, and heat transfer coefficient are the unique specifications of nano-fluids. It is well known that liquids have lower thermal conductivities than metals in solid phase [17].

Navid Bozorgan et al. (2012) [18] studied numerically the heat transfer performance, under turbulent conditions, of a radiator of Chevrolet Suburban diesel engine using 20 nm in diameter CuO nano-particles added to the base fluid (water) with the 0.2% volume concentration of the nano-particles. The radiator performance was evaluated based on the effects of the automotive speed and Reynolds number (Re) of the nano-fluid in the different volume concentrations. Compared to the base fluid (water), the results showed that the 0.2% volume concentration CuO/water nano-fluid exhibited higher overall heat transfer coefficient and pumping power by approximately (10% and 23.8%), respectively, at circulating through the flat tubes with ($Re_{enf} = 6000$) while the automotive speed is (70 km/hr).

Ravindra Kolhe et al. (2013) [19] investigated experimentally the effect of adding the aluminum oxide (Al_2O_3) and copper oxide (CuO) nano-particles (35-50 nm in diameter) to the base fluid (water) on the thermal efficiency of FPSC. The concentration of the nano-fluids was varied between (0.3% to 0.9 %wt.). In addition, the effect of coolant rate and the inclination angle of the FPSC were also studied. In general, the nano-fluids showed better thermal efficiency than water. It was found that increasing the coolant rate has positive effect on the thermal performance up to certain levels. Moreover, thermal efficiency of FPSC increases as the concentration increases for both Al_2O_3 and CuO. They concluded that the optimal inclination angle of FPSC would be close from 50 degrees. In another experimental study, Chaji et al. 2013 [20] introduced TiO_2 nano-particles to the base fluid and evaluated the efficiency of a small FPSC. The results revealed that there is an enhancement in the efficiency of 15.7% was observed of the TiO_2 /water nano-fluid compared to pure water. Furthermore, Jamal et al. (2013) [21] the 0.05 wt% and 0.1 wt% Cu/water nano-fluids were synthesized by a One-Step method and used as a working fluids in a FPSC. It was reported that the Cu/water nano-fluid with nano-particles weight concentration of

0.05% enhances the FPSC efficiency by 24% compared to the base fluid (water). In addition, increasing the weight concentration of Cu nano-particles in the nano-fluids increases the FPSC efficiency.

Hossein Chaji et al. (2013) [20] studied experimentally the thermal efficiency of FPSC using TiO_2 /water nano-fluids. Different flow rates (36,72 and 108 $\text{lit}/\text{m}^2\cdot\text{hr}$) and nano-particles concentrations (i.e. 0% wt%, 0.1%wt%, 0.2%wt% and 0.3 % wt) of the nano-fluid were examined for their effect on the thermal efficiency of FPSC. Compared to the base fluid (water), the initial efficiency of FPSC using the nano-fluid was improved between 3.5% and 10.5% and the index of FPSC total efficiency between 2.6% and 7%. In another experimental work, Ali Jabari Moghadam et al. (2014) [22] investigated the heat transfer performance of CuO/water nano-fluids as a working fluid in a FPSC. The average diameter of CuO nano-particles was about (40 nm). The mass flow rate of the fluids was varied within the range of 1 kg/min to 3 kg/min. and the nano-particles volume concentration was fixed at 0.4%. At a flow rate of 1 kg/min, the results showed that found that the CuO-water nano-fluid enhances the FPSC efficiency by about 21.8% in comparison with the base fluid (water). The heat transfer enhancement was attributed to the enhanced thermos-physical properties of the nano-fluids compared to the base fluid.

Goudarzi K. et al. (2014) [23] designed and manufactured a cylindrical FPSC with receiver helical tube to investigate its thermal efficiency using de-ionized water and CuO/ H_2O nano-fluid as working fluids based on ASHRAE standard in collector testing. In this study, the FPSC efficiency was evaluated based the mass flow rate of fluid, nano-particle mass concentration, and the effect of adding surfactant. The sodium dodecyl sulfonate (SDS) was used as a surfactant. The nano-particles mass concentration was varied within the range of (0.1-0.4%) and the mass flow rate of fluid changed from 0.0083 kg/sec. to 0.033 kg/sec. Compared to the base fluid (water), the results showed that CuO/water nano-fluids significantly enhanced the efficiency. At a flow rate of 0.0083 kg/sec, the CuO/water nano-fluid with a nano-particles concentration of 0.1 wt% exhibited an increase in the thermal efficiency by 25.6%. In addition, using the surfactant (SDS) with the nano-fluid enhances the FPSC efficiency by 24.2% in comparison with the case without surfactant

Z. Said et al. (2015) [1] presented an experimental study of the heat transfer enhancement of a FPSC using TiO_2 /water nano-fluid and polyethylene glycol

dispersant compared to the base fluid (water). The nano-fluids were prepared with nano-particles volume fractions 0.1% and 0.3% with the mass flow rates of the nano-fluid varied from 0.5 kg/min. to 1.5 kg/min, respectively. The results showed an increase of 76.6% in energy efficiency for 0.1% volume fraction and 0.5 kg/min flow rate, while the nano-fluid of 0.1% volume fractions and 0.5 kg/min flow rate gives exergy efficiency of (16.9%). Moreover, the results revealed that the pressure drop and of TiO₂ nano-fluid was very close to the base fluid (water) for the studied volume fractions. In the same year, Michael and Iniyani et al. (2015) [24] carried out an experimental study to investigate the effect of using CuO/water nano-fluid as the working fluid on the performance of a FPSC under natural and forced circulations. The natural circulation (thermosyphon) shows a higher enhancement of the FPSC performance compared to the forced circulation. Compared to the base fluid (water), the CuO/water nano-fluid enhances the collector efficiency by 6.3%.

Sujit Kumar Verma et al. (2017) [25], studied experimentally the performance of a FPSC using different working fluids. The thermal performance of the FPSC was evaluated based on constant nano-particles concentration of 0.75% with a flow rate of (0.025 kg/sec). A wide spectrum of the nano-fluids were used, which are Multi walled carbon nanotube/water, Copper Oxide water, Graphene/water, Aluminum Oxide/water, Silicon oxide/water, and Titanium oxide/water. At these parameters, the multivalued carbon nanotube/water exhibited the highest rise in energy efficiency of a FPSC that is 23.47%, followed by (16.97%, 12.64%, 8.28%, 5.09% and 4.08%), respectively for graphene/water, Copper oxide/water, Aluminum oxide/water, Titanium oxide /water, and Silicon oxide/water in comparison with the (base fluid).

1.6.3 Theoretical Studies

Rehena Nasrin et al. (2014) [26], carried out a numerical study to the forced convective flow and heat transfer of a FPSC using different nano-fluids. The FPSC has the flat plate cover and sinusoidal wavy absorber. They used different nano-fluids which are (Ag/water) (Cu/water) (Al₂O₃,/water) and (CuO/water) nano-fluid. The finite element method using Galerkin's weighted residual scheme was used to solve the governing partial differential equations with suitable boundary conditions. The performance of FPSC was numerically evaluated for different nano-fluids based on the effect of temperature and velocity distributions, radiative and convective heat

transfer, and mean temperature and velocity of the nano-fluid This is in addition to the effect of the effect of nano-fluids concentration on the performance of FPSC. It was found that the best heat transfer performance was obtained with (5% solid volume fraction of (Ag/water nano-fluids) since the Ag nano-particles have higher thermal conductivity than other fluids as justified by the authors.

E. EKramian et al. (2014) [27], performed a numerical investigation of heat transfer performance of various nano-fluids flow inside a FPSC. In this study, the heat transfer coefficients and thermal efficiency of the FPSC using the base fluid as well as the suggested nano-fluids (MWCNT/water, Multi Wall Carbon Nano-Tube), (Al_2O_3 /water, and CuO/water nano-fluids) were predicted numerically. numerical simulation was used for prediction of heat transfer coefficients and thermal efficiency of water and various nano-fluids in a FPSC. The (MWCNT/water), (Al_2O_3 /water), and (CuO/water) nano-fluids with mass percent's of (1 wt%, 2 wt%, and 3 wt%) were used as working fluids. The effects of temperature and mass flowrate on the thermal efficiency of FPSC using pure water and nano-fluids were investigated, and the numerical results of the FPSC efficiency under different operating conditions were compared to the experimental data available in the literature. It was found that there is a perfect agreement between the numerical predictions and, the experimental data. The CuO/water nano-fluid exhibits higher heat transfer coefficient and thermal efficiency compared to other working fluids. It should be noted that this finding contracted that the experimental results by Sujit Kumar Verma et al. (2017) [25], in which the MWCNT/water exhibited better performance than (graphene/water), (CuO/water), (Al_2O_3 /water), (TiO_2 /water), and (SiO_2 /water) instead of the base fluid.

The authors concluded the following:

1. Compared to the conventional working fluids, the heat transfer performance is enhanced due to the higher thermal conductivity of nano-fluids and Brownian motion of nano-particles.
2. Increasing the nano-fluid concentration results in improving the Brownian motions and chaotic movement of nano-particles, which in turn increases the thermal efficiency of the FPSC.
3. The coolant outlet temperature and the absorber temperature decrease with increasing the mass flowrate. However, the collector thermal efficiency enhances by increasing the flowrate.

4. The temperature difference between the absorber plate and the transparent glass cover decreases as the inlet temperature increases. This results in more thermal losses in the collector, consequently thermal efficiency of FPSC reduces.
5. The specific heat of nano-fluids has a very important role on the thermal efficiency of the FPSC. CuO/water nano-fluid has lowest specific heat compared with Al₂O₃ /water and CNT/water nano-fluids. Therefore, based on the results the heat transfer coefficients and thermal efficiency of CuO/water nano-fluid are greater than those of other nano-fluids. The average heat transfer coefficient of CuO /water nano-fluid is about (4% and 2%) higher than those of Al₂O₃ /water and CNT/water nano-fluids respectively. For constant mass flowrate, thermal efficiency of 1% wt CuO /water nano-fluid is about (3%, 6% and 9%) higher than those for (CNT/water) (Al₂O₃ /water) and pure water, respectively.

Rehena Nasrin a et al. (2015) [28] evaluated numerically the thermal performance of a FPSC under forced convection conditions using Cu/water nano-fluid as working fluid. The governing differential equations with boundary conditions were solved using Finite Element Method using Galerkin's weighted residual scheme. The solar irradiation (I) and diameter (D) of the riser pipe were analyzed and their effects on the forced convection heat transfer were simulated. Based on the above parameters, the results of comprehensive average output temperature, Nusselt number, mean velocity, the FPSC efficiency percentage for both nano-fluid and base fluid (water) through the absorber tube were presented. In general, the authors concluded that the nano-fluids with highest solar irradiation and lowest pipe diameter exhibited the highest heat transfer rate.

For low temperature residential applications, the FPSC is widely used to heat the water. For that purpose, Jee Joe et al. (2015) [24] used copper acetate to prepare copper oxide/water nano-fluid, which is then used as a working fluid in a FPSC. The thermal performance of the indirect-type FPSC water heater was investigated experimentally on a 100 Lit/day thermosiphon. The results showed that the (thermosiphon) circulation exhibited significant improvement of the collector performance in comparison with the forced circulation. To get a better dispersion stability in comparison with pure water and Triton X-100 surfactant suspensions, the CuO/water nano-fluid was also

prepared with the presence of (sodium-dodecyl-benzene-sulfonate) surfactant. Moreover, the authors carried out an experimental and a theoretical comparison of the thermos-physical properties of the synthesized nanoparticle and prepared nano-fluid.

Wail Sami et al. (2015) [29] presented previous studies related to the use of the nano-fluid as working fluids instead of the base fluids and evaluate their performance in FPSCs. Based on the review, the authors concluded the following: (1) the performance of the FPSCs effectively enhanced using the nano-fluids, (2) the highest FPSC efficiency was reached using the nano-fluids based on carbon nanostructures, (3) at high temperature, the surfactant stability in the nano-fluids requires more in depth investigation, and (4) the cost, viscosity, stability, and pumping power are the main challenges facing the nano-fluid technology.

Recently, Nang Khin Chaw Sint. et al. (2017) [30] analyzed the efficiency of a FPSC using CuO/water nano-fluid as a working fluid. The FPSC efficiency for a domestic (SWH) system was calculated using MATLAB software. The weather conditions of a city in Myanmar was considered in this study. Three aspects were considered in this work which are as follows: (1) at the optimum tilted angle of the FPSC, the estimation of the maximum solar energy availability was conducted, (2) the effect of volume concentration and size of the nano-particle on the convective heat transfer coefficient of nano-fluid was investigated, and (3) A method of iteration was used to calculate the overall heat loss coefficient of the FPSC. The results showed that the nano-particles volume concentration up to 2% enhances the FPSC efficiency, while a marginal effect of the nano-particle size on the efficiency was observed. As a summary, the CuO/water nano-fluid exhibited better collector efficiency with the nano-particles concentration up to 5% compared with that of water under the same ambient, radiant, and operating conditions

Maouassia A. et al. (2017) [31] illustrated a numerical study of using TiO₂ nano-particles to simulate the efficiency of FPSC under laminar and forced convections conditions. The dynamic and thermal properties were evaluated based on different 1%, 3%, 5%, and 10 % and Reynolds number range of (25-800) and the effectiveness of TiO₂/water nano-fluids was compared to conventional coolant (water). The results presented by the following parameter: pressure drop coefficient, average temperature, and Nusselt number. Finally, the authors concluded that heat transfer enhanced by increasing both nano-particles concentration and Reynolds number.

1.7 Concluded Notes

Based on the above literature, it is clear that there are relatively few studies carried out for investigating numerically and experimentally the thermal performance of FPSC using TiO₂/water and CuO/water nano-fluids. This is in addition to some contradictions in reporting the effectiveness of these nano-particles, especially for CuO. The conventional FPSC was used in all the research work available in the literature. Therefore, the aim of this study is to compare the performance of FPSC with a spiral pipe arrangement using TiO₂/water and CuO/water nano-fluids relative to the base fluid (water) under outdoor conditions. The comparison will be done at a volume concentration 0.1 % and a flow rate of 1.5 Lpm. Based on the results, the nano-fluid with the best performance will be considered for a detailed study in comparison with water.

1.8 Research Objectives

The main objective of this work is to investigate experimentally the thermal performance of FPSC (with a spiral pipe arrangement) in term of inlet-outlet for both base fluid (water) and water/CuO and water/TiO₂ nano-fluids. This study is considered one of the few studies that performed in IRAQ in which nano-fluids are utilized as working fluids in FPSC, which has different geometry compared to the conventional collectors, under outdoor conditions. In order to achieve this goal, the thermal performance of the FPSC uses the proposed nano-fluids (CuO and TiO₂) is evaluated by changing their volume concentrations (0.1-0.3%) and flow rates (1 Lpm to 3 Lpm). The results of the nano-fluids are compared with the reference fluid water.

1.9 Thesis Outline

Five chapters are covered in the thesis aiming to provide a complete and clear picture about this project. The background knowledge about the importance of solar thermal energy, solar water heating systems (SWH), solar thermal collectors (STC), and the nano-fluid technology and applications are presented in Chapter 1, and gives detailed description of the updated literature related to the studies focused on the investigation of the performance of FPSC using nano-fluids. Chapter 2 presents the

required equations that are used in calculation the thermal efficiency of the FPSC. In Chapter 3, the components of the experimental setup of the FPSC as well as the experimental procedure used in this study are described in details. The results of the proposed nano-fluids flow in the FPSC are discussed in Chapter 4. Finally, conclusions of this work and recommendations for future work are given in Chapter 5.



CHAPTER TWO

THEORY OF FLAT PLATE FORMULATION

2.1 Introduction

This chapter presents the required equations that are used in calculating the thermal efficiency of the FPSC using the base fluid (water) as well as the nano-fluids CuO/water and TiO₂/water nano-fluids. Prior to the thermal efficiency calculations, the thermos-physical properties for both the base fluid (water) and nano-fluids should be determined. At the end of the chapter, the empirical correlations for calculating the Nusselt numbers for the water and the nano-fluids in the FPSC are formulated using Statistica software based on the raw experimental.

2.2 Flat Plate Thermal Efficiency

Thermal efficiency of the FPSC is the ratio of the useful heat gain to the total input energy. can be calculating from the following equation [32]:

$$\eta = F_r \left[(\tau\alpha) - \frac{U_L(T_i - T_a)}{G} \right] \quad (2-1)$$

where

F_r : - Heat removal factor

$\tau\alpha$: -Transmittance- Absorptance product

T_i : - Inlet fluid temperature of (FPSC) ($^{\circ}C$)

T_a : - Ambient temperature ($^{\circ}C$)

G : - Radiation intensity (W/m^2)

U_L : - Solar collector overall heat loss coefficient of (FPSC) ($W/m^2 \cdot ^{\circ}C$)

When the collector is perpendicularly facing the sun, the product of the transmittance-absorptance ($\tau\alpha$) in Eq. (2.1) for the solar collector corresponds to the radiation beam at normal incidence.

2.2.1 Heat Removal Factor

One of important factor the heat removal factor which represents the ratio of the actual output energy when output plate temperature is equal to fluid inlet temperature, it can be calculated by given equation [32].

$$F_r = \frac{\text{Actual output}}{\text{Output for plate temperature} = \text{fluid inlet temperature}}$$

The heat removal factor is expressed as [32].

$$F_r = \frac{\dot{m} C_p}{A_c U_L} \left[1 - \exp \left[- \frac{U_L F' A_c}{\dot{m} C_p} \right] \right] \quad (2-2)$$

The FPSC efficiency factor can be calculating from this equation [32].

$$F' = \frac{\frac{1}{U_L}}{w \left[\frac{1}{U_L [D_o + (w - D_o) F]} + \frac{1}{C_b} + \frac{1}{\pi D_i h_{fi}} \right]} \quad (2-2-a)$$

where

w : - distance between pipes (m)

h_{fi} : - heat transfer coefficient inside absorber pipe ($W/m^2 \cdot ^\circ C$)

D_o : - tube inside diameter (m)

D_i : - tube outside diameter (m)

C_b : - Bond conductance

For straight fin with rectangular profile, the fin efficiency can be calculating from this equation:

$$F = \frac{\tanh[m(w-D)/2]}{m(w-D)/2} \quad (2-2-b)$$

$$m = \sqrt{\frac{U_L}{K.\delta}} \quad (2-2-c)$$

2.3 Collector Energy Losses

In the solar thermal systems, most of the solar radiation is absorbed by the solar collectors and transferred to the working fluid, and then it is utilized as a useful energy, while some of the absorbed heat is usually lost to the environment by different heat transfer modes (conduction, convection, and radiation) as shown in Fig. (1.4a). The FPSC back temperature is (T_b), the temperature of the plate is (T_p) and the absorbed solar radiation is S . Figure (1.4c) shows the heat losses from the solar collector can be combined into a simple resistance R_L , so that the energy losses from the collector can be written as:

$$Q_{Loss} = \frac{T_p - T_a}{R_L} = U_L A_c (T_p - T_a) \quad (2-3)$$

where

T_p : - Plate Temperature ($^{\circ}C$)

One of the most complicated function of the solar collector construction and its operating conditions is the heat-transfer loss coefficient, which is given by the following expression:

$$U_{Loss} = U_{to} + U_{bo} + U_{ed} \quad (2-4)$$

where

U_{to} : - Top loss coefficient ($W/m^2 \cdot K$)

U_{bo} : - Bottom heat loss coefficient ($W/m^2 \cdot K$)

U_{ed} : - Heat loss coefficient from the collector edges ($W/m^2 \cdot K$)

It should be noted that all the heat-transfer loss coefficients are evaluated separately and Fig. (1.4) does not show the edge losses.

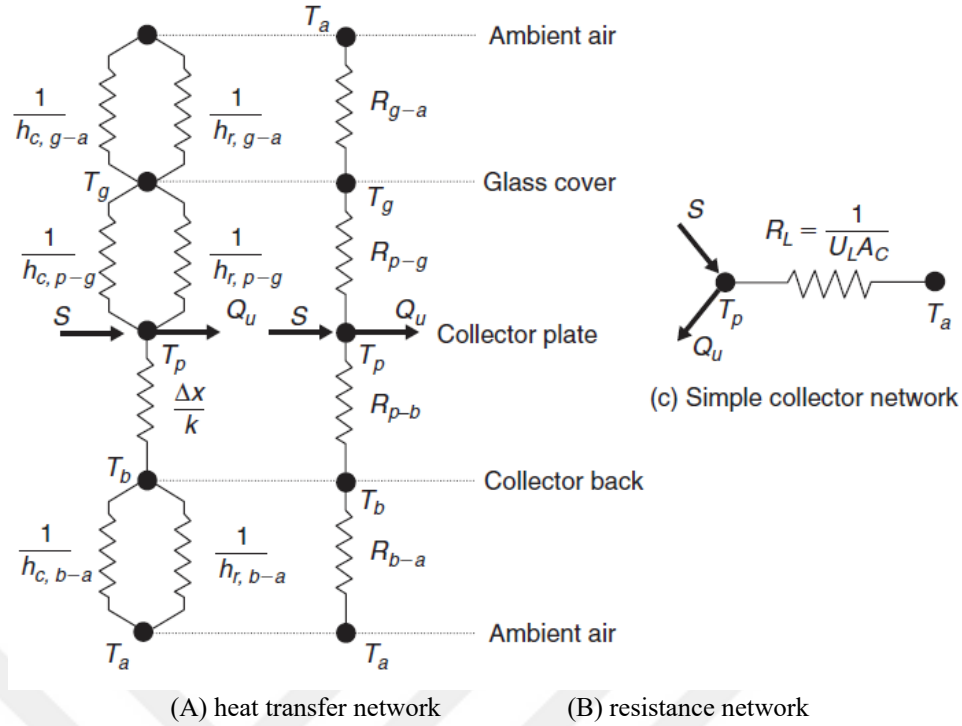


Figure 2.1: Thermal network for a single cover FPSC in terms of (A) conduction, convection, and radiation (B) resistance between plates, and (C) a simple collector network

A- Calculate the top losses energy of the FPSC [32]:

$$Q_{top\ loss} = U_t A_c (T_p - T_a) \quad (2-5)$$

For design purposes with a sufficient accuracy, the top heat-transfer loss coefficient (U_t) can be calculated by the following empirical equation (Klein, 1975) [32]:

$$U_{to} = \frac{1}{\frac{Ng}{\frac{c}{T_p} \left[\frac{T_p - T_a}{Ng + f} \right]^{0.33}} + \frac{1}{h_w}} + \frac{\sigma(T_p^2 + T_a^2)(T_p + T_a)}{\left[\frac{1}{\varepsilon_p + 0.05 Ng(1 - \varepsilon_p)} \right] + \left[\frac{2Ng + f - 1}{\varepsilon_g} \right] - Ng} \quad (2-5-a)$$

where

Ng = number of glass covers = 1

T_p : - average plate temperature ($^{\circ}C$)

T_a : - average ambient temperature ($^{\circ}C$)

ε_p = absorber plate emissivity

ε_g = glass emissivity

σ : - stefan-boltzmann constant = $5.65 \cdot 10^{-8} \text{ W/m} \cdot K^{-4}$

The factor (f) of correction of heat transfer coefficient by wind is calculated by the following formula:

$$f = (1 - 0.04 h_{wi} + 0.0005 h_{wi}^2) (1 + 0.09 Ng) \quad (2-5-b)$$

The factor (c) of correction coefficient of tilt angle is calculated by the following formula:

$$C = 365.9 (1 - 0.0083 \beta + 0.0001298 \beta^2) \quad (2-5-c)$$

Based on the literature, there is no well-established research work carried out on calculating the wind heat transfer coefficient, therefore, Equation (2.5-d) can be considered ($h_w = 5 \text{ W/m}^2 \cdot \text{°C}$).

$$h_w = \frac{8.6 * V^{0.6}}{L^{0.4}} \quad (2-5-d)$$

where

L: - collector length (m)

V: - wind velocity (m/s)

B- Calculate the bottom losses energy of the FPSC [32].

$$Q_{bo.} = U_{bo.} A_c (T_p - T_a) \quad (2-6)$$

It should be noted that the energy loss is first transferred through the insulation material by conduction and to the ambient air by the combination of convection and infrared radiation. Thus, the energy loss can be calculated by the following equation with an assumption of neglecting the radiation term ($h_{c,b-a}$) since the bottom temperature of the casing is low:

$$U_{bot.} = \frac{1}{\frac{t_{ba.}}{k_{ba.}} + \frac{1}{h_{c,bo-a}}} \quad (2-6-a)$$

where

$t_{ba.}$ = Thickness of back insulation (m)

$k_{ba.}$ = Conductivity of back insulation (W/m.k) for wood.

$h_{c,b-a}$ = convection heat loss coefficient from back to ambient ($\text{W/m}^2 \cdot \text{k}$).

C- Calculate the edge losses energy of the FPSC [32]:

$$Q_{ed.} = U_{ed} A_c (T_p - T_a) \quad (2-7)$$

It was reported that the energy loss from the back surface of the collector plate rarely exceeds 10% of the upward loss [32]. The back surface heat loss coefficient has typical values of 0.3 – 0.6 W/m² K. Similarly, the heat loss coefficient of the collector edges is expressed as follows:

$$U_{ed} = \frac{1}{\frac{t_{ed.}}{k_{ed.}} + \frac{1}{h_{c,ed.-a}}} \quad (2-7-a)$$

where

$t_{ed.}$ = Thickness of edge insulation (m)

$k_{ba.}$ = Conductivity of back insulation (W/m.k) for play wood = 0.12

$h_{c,ed.-a}$ = convection heat loss coefficient from edge to ambient (W/m².k)

The typical values of the edge heat loss coefficient are (1.5 – 2) (W/m².k).

2.4 Useful Energy Gain

For the steady-state flow of a fluid in a tube, the energy conservation equation is given by (see Fig. 2.2):

$$Q_u = \dot{m} \times C_p \times (T_o - T_i) \quad (2-8)$$

where (T_i) and (T_o) are the mean fluid temperatures at the inlet and outlet of the tube, respectively, and Q_u is the rate of heat transfer to or from the fluid. In the case of no energy interactions through the wall of the tube occur, the fluid temperature in a tube remains constant.

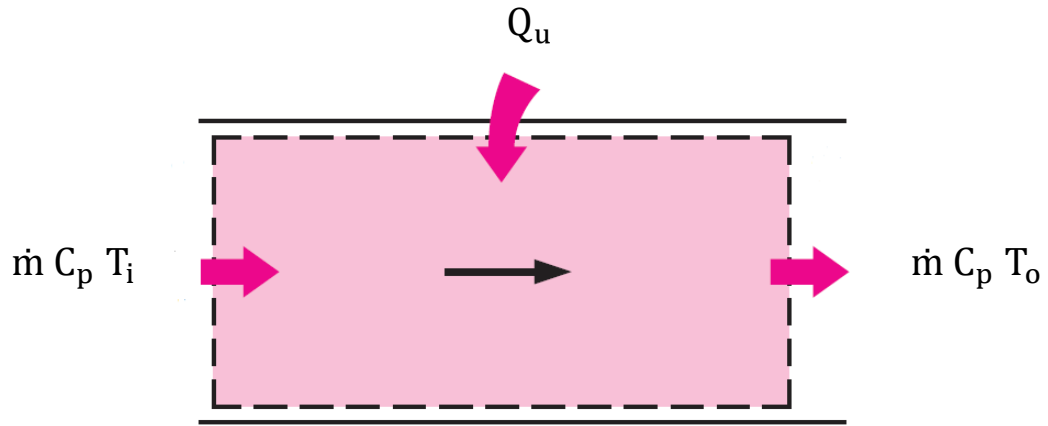


Figure 2.2: The heat transfer to a fluid flowing in a tube

The properties of water are determined at average temperature, which is:

$$T_{ave} = \frac{(T_o + T_i)}{2} \quad (2-9)$$

The water velocity inside the FPSC can be calculated by the following formula:

$$u_{in} = \frac{q}{A_s} \quad (2-10)$$

$$q = \frac{\dot{m}}{\rho} \quad (2-10-a)$$

The cross section area of pipe can be calculated by the following formula:

$$A_s = \frac{\pi}{4} d_{in}^2 \quad (2-10-b)$$

2.5 Reynolds Number

The transition from laminar to turbulent flow depends on the surface geometry, surface roughness, free-stream velocity, surface temperature, and type of fluid, among other things. The Reynolds number is defined as [32]:

$$Re = \frac{\rho U_{in} d_i}{\mu} \quad (2-11)$$

Under most practical conditions, the flow in a tube is laminar for ($Re < 2300$), turbulent for ($Re > 10,000$) and transitional in between. That is,

$$\begin{aligned} Re < (2300) & \text{ Laminar Flow} \\ (2300) \leq Re \leq (10,000) & \text{ Transitional Flow} \\ Re > (10,000) & \text{ Turbulent flow} \end{aligned}$$

The viscosity (μ) of the fluid is calculated by the following formula:

$$\mu = v \times \rho \quad (2-11-a)$$

2.6 Nusselt Number

The Nusselt number represents the enhancement of heat transfer through a fluid layer as a result of convection relative to conduction across the same fluid layer.

$$Nu = \frac{h D}{K} \quad (2-12)$$

where k is the thermal conductivity of the fluid and D is the characteristic diameter, and h it is viewed as the dimensionless convection heat transfer coefficient.

$$h = \frac{Q_u}{\pi D_i L (T_w - T_{ave})} \quad (2-12-a)$$

2.7 Prandtl Number

The relative thickness of the velocity and the thermal boundary layers is best described by the dimensionless parameter Prandtl number, defined as [33].

$$Pr = \frac{c_p \mu}{K} \quad (2-13)$$

2.8 Useful Energy Gain for Nano-fluids

For the nano-fluids, the total useful energy gain of the FPSC is given by:

$$Q_{U.(nf)} = \dot{m}. C_{p,nf}(T_0 - T_i) \quad (2-14)$$

In this thesis, density (ρ_{nf}) and special heat capacity ($c_{p,nf}$) of nano-fluid have been calculated based on empirical correlations proposed by Pak [34].and Xuan [34].as follows:

$$C_{p,nf} = \frac{(1-\phi)\rho_{bf}c_{p,bf}+\phi\rho_p c_{p,np}}{\rho_{np}} \quad (2-14-a)$$

$$\rho_{nf} = (1 - \phi)\rho_{bf} + \phi\rho_{np} \quad (2-14-b)$$

The viscosity (μ_{nf}) of the nano-fluids is calculated by the following formula developed by Drew and Passman [36]:

$$\mu_{nf} = \mu_{bf}(1 + 2.5 \phi) \quad (2-15)$$

The effective thermal conductivity of nano-fluids is calculated using a relation based on Maxwell's work [37]. The calculated properties of the nano-fluid are listed in (Table 1.2).

$$k_{nf} = k_{bf} \left[\frac{k_{np}+2k_{bf}-2\phi(k_{bf}-k_{np})}{k_{np}+2k_{bf}+\phi(k_{bf}-k_{np})} \right] \quad (2-16)$$

Table 2.1 Thermo-physical properties of base fluid and nano-particles

No.	property	CuO	TiO ₂	water
1	$c_p(\text{J. kg}^{-1}. \text{k}^{-1})$	535.6	689	4197
2	$\rho[\text{kg. m}^{-3}]$	6500	4500	997.1
3	$k(\text{W. m}^{-1}. \text{k}^{-1})$	20	8.4	0.669
4	$d_p(\text{nm})$	30	30	-

The Reynolds and Prandtl numbers are calculated with considering the nano-fluid properties as follows:

$$Re_{nf} = \frac{\rho_{nf} \cdot u_{nf} \cdot D_{h,nf}}{\mu_{nf}} \quad (2-17)$$

$$Pr = \frac{c_p \mu}{K} \quad (1-18)$$

The Nusselt number is calculated with considering the nano-fluid properties by:

$$Nu = \frac{h_{nf} D}{k_{nf}} \quad (2-19)$$

The heat transfer coefficient for nano-fluids and water is expressed by the following equation:

$$h_{nf} = \frac{Q_{u,nf}}{\pi D_i L (T_w - T_{ave})} \quad (2.19-a)$$

2.9 Empirical Relationship

Finally, from the raw experimental data, the following steps can formulate the empirical correlations or power-law correlations for heat transfer coefficient ($Nu = a Re^b Pr^{1/3}$) of the base fluid (water) and nano-fluids:

1. Statistica program (version 10) can be used to analyze the experimental data and find the parameters of the power-law correlation.
2. Open statistica program, from file menu, choose a new data and start to input experimental data (Nu, Re, and Pr).
3. From analysis menu, choose the other statistics, from a new open screen, choose the non-linear estimation.
4. From a new open screen, choose the user-specified regression.
5. From a new open screen, start to write the function to be estimated as follows: -

$$Nu = (a Re^b) (Pr^{1/3}) \quad (2.20)$$

CHAPTER THREE

EXPERIMENTAL WORK

3.1 Introduction

The experimental work was carried out for the research aim of improving heat transfer in FPSC using nano-fluids instead of the base fluid (water). The following sections describes the details of the experimental set-up, measuring and auxiliary devices, nano-fluid preparation, experimental procedure.

3.2 The Experimental Setup

Figure (3.1) and (3.2) demonstrate the schematic and some photos of the experimental setup. During the operation, the solar radiation gets through the glass cover to the collector plate and tubes where the solar radiation is absorbed. The plate and tubes of the collector are painted with a black painting to improve the absorption of the short-wavelength solar radiation as well as reducing the loss of the long wavelength radiation from the absorbing surface. The heat extracted from the solar radiation is transferred and stored in a heat transfer fluid. The working fluid is circulating through the FPSC closed system using a tank and submersible water pump.

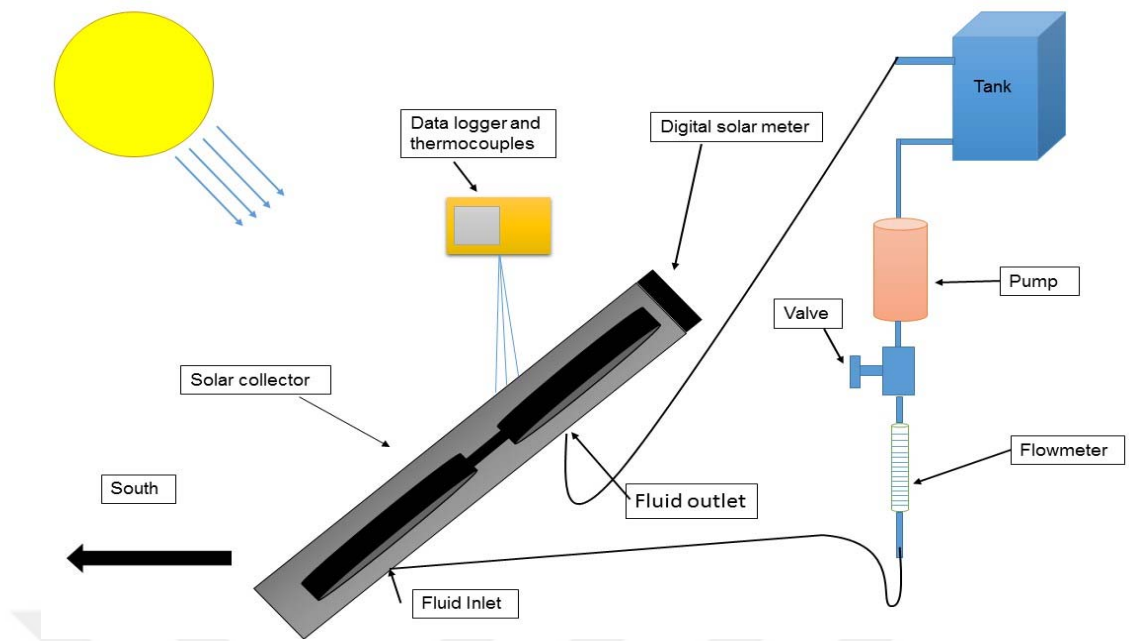


Figure 3.1: The schematic of (FPSC) experimental setup



Figure 3.2: Experimental set-up of FPSC

3.2.1 Flat Plate Solar Collector (FPSC) Experimental Set-up

The FPSC consists of box made from wood with dimensions of {1.07 m, 0.57 m, 0.1 m} as shown in Fig.(3.3). The specifications of FPSC are presented in (Table 3.1). The transparent glass was fixed on the top of the FPSC that contains the absorber plate and the flow tube. The wood was used in the industry of enclosure as a heat insulator with thermal conductivity of {0.19 w/m. c}.



Figure 3.3: The flat plate solar collector (FPSC).

Table 3.1: The specification of (FPSC) components

Component	Dimension	Remarks
Collector	1.07 m x 0.57 m x 0.1 m	(Gross area= 0.6099 m ²)
Absorber plate	1.07m x 0.57 m x 0.002 m	Material (black painted) Galvanized plate
Transparent cover	3 mm thick	Material (window glass)
Number of pipe coils	diameter =0.015875 m	Material: copper Length pipe = 15 m Number of coils = 12
Bottom-insulation	0.3 m thick	Material (glass wool)
Edges-insulation	0.15 m thick	Material (glass wool)

3.2.2 Glazing

The glass – type (window glass) was used with thickness of 3 mm and dimensions of (1.07 m and 0.57 m). It has high degree of transparency and poor refraction or reflection percentage that was fixed on the front face of the wooden box.

3.2.3 Absorber Plate

The absorber plate is a piece made from galvanized iron stainless steel with thickness of 2 mm and dimensions of (1.07 m,0.57 m) in a shape of rectangle painted in the dark black color which is highly absorbent to the waves of solar radiation and its high reflectivity to the long wave.

3.2.4 Insulation

To decrease the thermal losses, the glass wool was used with thickness of 2 cm and thermal conductivity of (0.25 w/m.c) to insulate the storage tank and the inlet and outlet pipes connected to the solar collector as demonstrated by Fig. (3.4).



Figure 3.4: The insulated storage tank and the inlet and outlet pipes connected to the FPSC

3.2.5 Pump

Figure (3.5) shows the pump with three speeds work, voltage (230 V), and frequency (50 HZ). The pump was used for continuity of flow at a fixed flow rate for the closed loop of solar collector flat plate unit.



Figure 3.5: The fluid pump

3.2.6 Storage Tank

The storage tank was made from galvanized iron with dimensions of (0.60m, 0.35m, 0.35 m) fixed on height of 1.5 m and insulated from all sides. The tank was used to supply water by the pump to the solar collector.

3.3 The Measuring Devices

3.3.1 Thermocouples

A chromel – constantan called Type – K thermocouple was used to measure temperatures at different places of the FPSC set-up as shown in Fig. (3.6) These points are described in Table (3.2).

Table 3.2: The solar collector network of thermocouples distribution

No.	Location	Note
1	Absorber plate	thermocouple attached backside
2	Tube top surface	-
3	Air gap between the (plate and glass)	-
4	Ambient	attached outside
5	Glass cover	-
6	Inlet tube	-
7	Outlet tube	-

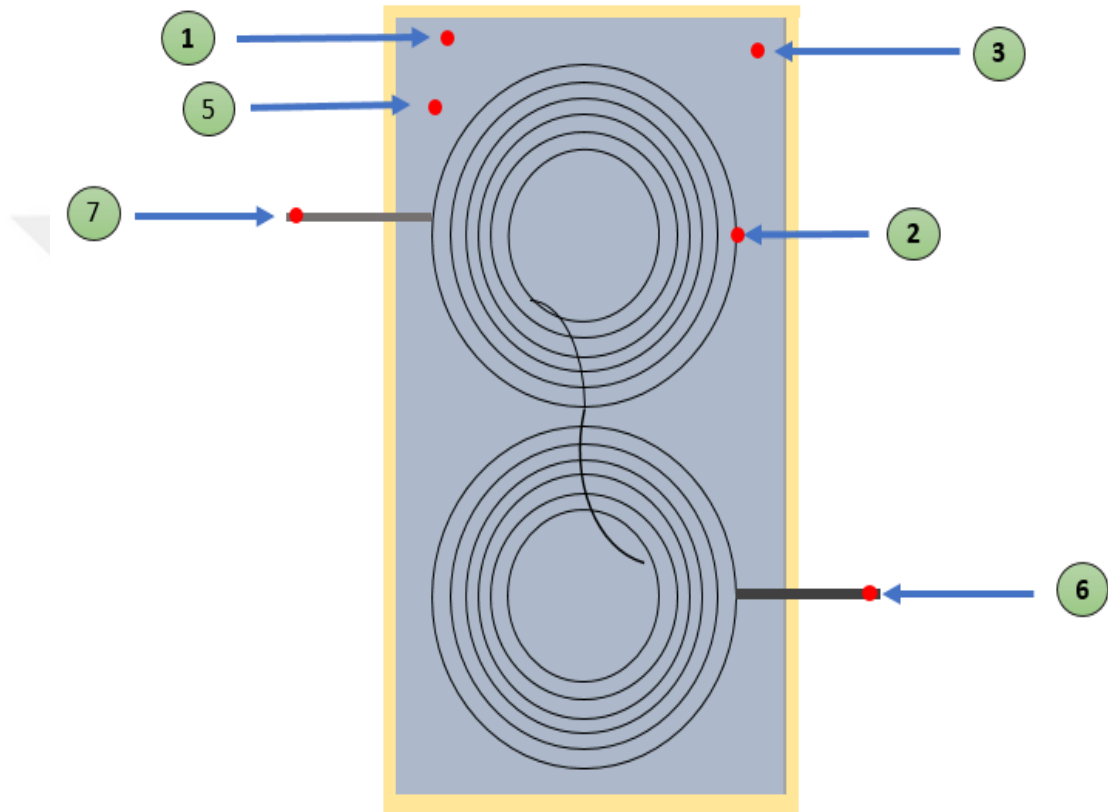


Figure 3.6: The solar collector network of thermocouples distribution

3.3.2 Temperature Recorder

The readings of thermocouples were collected and stored in a computer through a temperature recorder (Make-Lutron-BTM-42085D-12 channels (USB disk storage), basic accuracy $(0.2 \% \pm 1^{\circ} \text{C})$ shown in (Fig. 3.7). The software program of the temperature meter is (AT45X-EN) software-EXE.



Figure 3.7: The temperature recorder

3.3.3 Flow Meter

The flow meter device shown in the (Fig. 3.8) was used to measure the flow rate of water and nano-fluids during the experiments work. The flow meter range is 0.5-4 Lpm, with an accuracy of $\pm 5\%$.

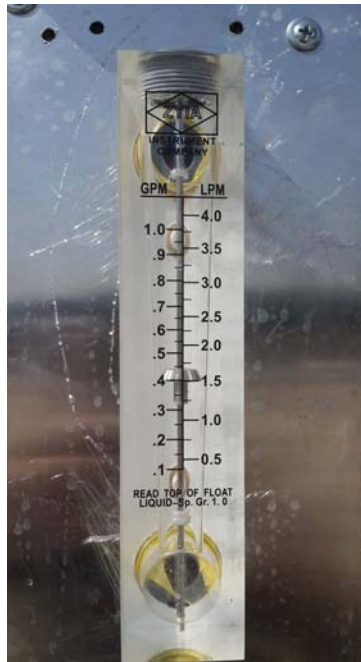


Figure 3.8: The flow meter

3.3.4 Solar Power Meter

Figure (3.9) shows the solar radiation intensity measuring device (A digital solar power meter), (Make-EZDO-Electrical Electronics), (model-sp216), Range-12000 (w/m^2), accuracy ($\pm 5\%$) of measurement in units (w/m^2). It was placed with the same angle of the solar collector (45°) to measure radiation intensity throughout the experiment duration for the time period of (10:00 AM) until (12:30 PM).



Figure 3.9: The solar intensity meter

3.4 The Calibration of Measuring Devices

Before starting the experiments, all the measuring devices were calibrated as described by the following sections:

3.4.1 Calibration of Thermocouples

All thermocouples were calibrated by connecting one end of thermocouple to digital thermometer and the other end inside water and de-ionized water for comparison at boiling point., The water was placed in a bowl, and a heat source was focused on the bowl, when the water begins to boil, a thermocouple is placed in order to measure the degree of boiling. It should be note that the boiling degree of de-ionized water ($100^{\circ}C$) and it was used the inertia degree of water ($0^{\circ}C$) and the boiling degree of water was ($100^{\circ}C$) from the practical experiments, and then the comparison is made among thermocouples and it was noted that the there is no difference in temperature for thermocouple.

3.4.2 Calibration of Flow Meter

The flow meter used to measure the flow rate (Lpm) of liquid is calibrated using a graded glass cylinder and stop watch. Volume flow rate of 0.5,1 and 2 liters per minutes is used in calibrating the flow meter as shown in Fig. (3.10) with the following steps:

- 1- A volume of water is accumulated in the graded cylinder after passed throw the flow meter (which reads 1 Lpm)
- 2- During a known period of time recorded by the watch (60 seconds).
- 3- The volume flow rate gives by dividing the volume by time.

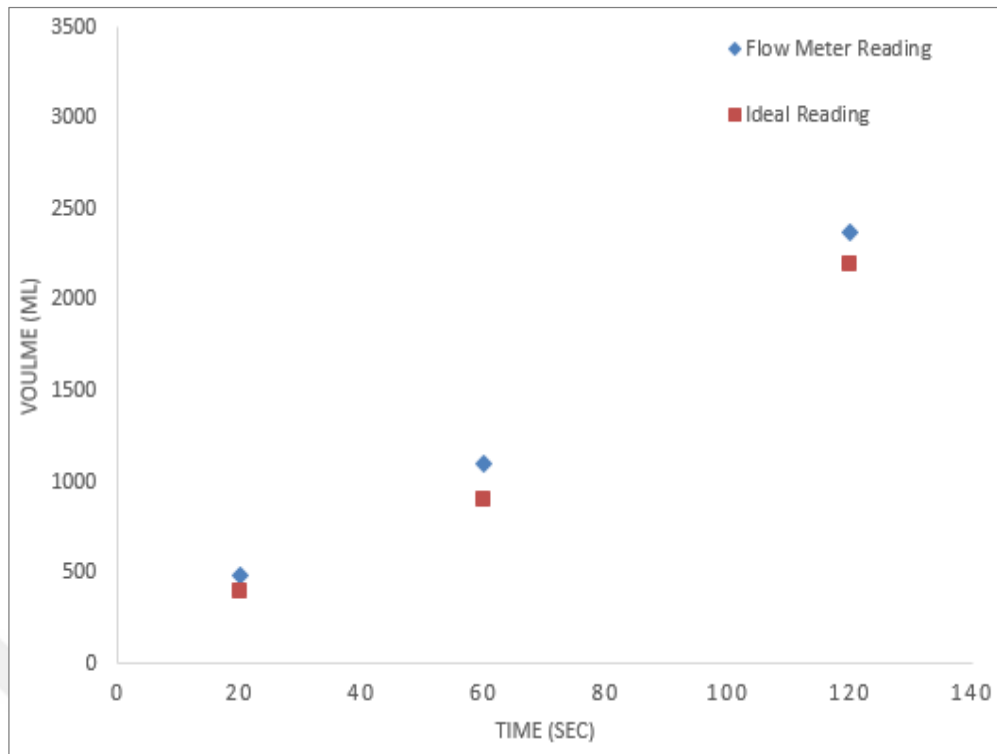


Figure 3.10: The flow meter calibration

3.5 Nano-fluid Preparation

In this research, dry powder of CuO and TiO₂ nano-particles of 99.9 % purity and average size (20-60) nm purchased from (Nanografi Nano Technology, Turkey base company) are dispersed in deionized water as base fluid (water) for the nano-fluid preparation. The CuO and TiO₂ nano-particles were selected to prepare the water-based nano-fluids in this study due to their good chemical stability and the enhanced thermal properties compared to the base water. The properties of the CuO and TiO₂ nano-particles are listed in (Table 3.3).

Table 3.3: Physical properties of copper oxide (CuO) and Titanium oxide (TiO₂) Nano-particles

No.	Technical properties	CuO	TiO ₂
1	Purity %	99.99	99.99
2	Average particle size (nm)	20-60	20-60
3	Specific surface area (m ² /g)	35	50
4	Bulk density (g/cm ³)	0.8	0.3
5	True density (g/cm ³)	6500	4500
	Color	black	white
6	Morphology	nearly spherical	nearly spherical

To enhance the heat transfer performance of the conventional fluids, it is necessary to obtain a good dispersion and stability of the nano-particles in the base water. There are two techniques of preparing the nano-fluids which are two step and one step methods. In the two-step method, the nano-particles or nanotubes are first prepared in a form of dry powder by various methods as physically, chemically, and laser based techniques. The produced nano-particle is mixed with water and then are sonicated to get uniform and stable suspension [38]. A special type of surfactants may be used to get well dispersion of the nano-particles in the base fluid. This depends on the depend on the boundary properties among nano-particles and base fluid [39]. However, it was reported that adding surfactants may result in decreasing the thermal performance of the nano-fluids due to the formation of the bubbles [25]. This method is widely applied for producing nano-fluid since the commercial availability of nano-particle powders for the time being. This method is limited by the nano-particles agglomeration during the process, packing, and transport, causing problems in the subsequent dispersing in fluid step. On the other hand, the one-step method utilized to diminish the agglomerating of nano-particles during the drying, storage, and transportation processes, leading to difficulties in the following dispersion stage of the two-step method [39].

To weigh the Nano powder very accurately, a sensitive balance (Mettler-Sartorius) (model-234-IS) (resolution-0.1 mg) shown in Fig. (3.11) was used. The mass in grams of the nano-particles required for preparation of nano-fluids with different volume concentration is calculated using equation (3.1) [40].

$$Vol \%(\phi) = \frac{m/\rho}{100ml\ water + m/\rho} \quad (3.1)$$

This equation calculates the mass of CuO and TiO₂ nano-particles dispersed into (100 ml) of water, volume concentration of (0.1% Vol.), (0.2% Vol.), and (0.3% Vol.) were prepared and used in the study.

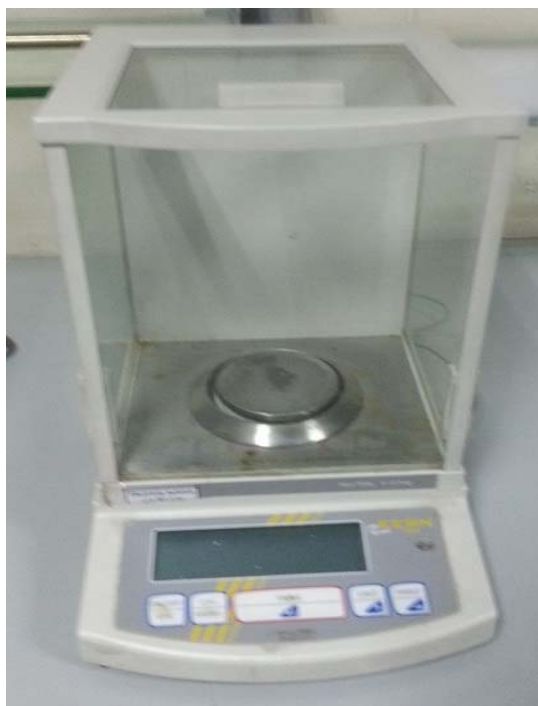


Figure 3.11: The Sensitive balance

Ultrasonic sonic mixing was applied for (one and half hour) to disperse the weighed amount of CuO and TiO₂ nano-particles in (de-ionized water) using ultrasonic mixing (made-QSONICA-Sonicators, power-500 W frequency 20 ±3KHz) as shown in Fig. (3.12).



Figure 3.12: (a) The Ultra-sonicator and (b) mixing of the nano-fluids

3.6 Experimental procedure

Before running the experiments, the following preparations were carried out as follows:

1. The tank was filled with de-ionized water.
2. The FPSC was oriented to south (using a compass) with a tilt angle ($\beta = 45^\circ$) in Baghdad at (33.2° latitude and (44.3° longitudes))
3. The pump is connected from two sides, exterior from the upper tank and interior to flow meter and then to solar collector to ensure that the flow rate is not changed.
4. The thermocouples were connected to temperature recording device for measuring the temperatures at different points during experiments.
5. The solar radiation intensity measure device is placed on the upper side of solar collector at angle (45°) to measure solar radiation intensity during experiment time.

At this stage, the experimental setup is ready to proceed with the following experiments:

3.6.1 The Base Fluid Experiments

The deionized water was used as a reference base fluid which is introduced into the FPSC setup at a flowrate of (1 Lpm). The average temperature readings for different points on the experimental system shown in Fig. 3.6 were taken every five minutes during two and a half hours starting from (10:00 AM) until (12:30 PM). This experiment was repeated with water as a base fluid but with different flowrate (1.5, 2, and 3 Lpm).

For fair comparison, it should be noted that all the experiments were performed under the same experimental conditions with changing the fluid type, nano-particles concentration, and the fluid flowrate.

3.6.2 The TiO_2 / Water Experiments

The base water was replacing by TiO_2 /water nano-fluids. At the beginning, the TiO_2 /water nano-fluids with fraction concentration 0.1% was used as a working fluid

at different flowrate of 1.5 Lpm. Based on the available literature, we decided to carry out the comparison at low nano-particles volume concentration (0.1%) and low fluid flow rate of 1.5 lit/min. This decision was considered to avoid the reduction in the thermal efficiency caused by (1) the enhanced fluid viscosity that causes frictional dissipation and the possibility of nanoparticles agglomeration at high nano-particles concentration [1] and (2) the shorter residence time of the fluid into the FPSC that result in lower inlet-outlet temperature difference at high fluid flow rate [20]. to be compared with the base fluid at the same conditions.

3.6.3 The CuO/Water Nano-fluid Experiments

The CuO/water nano-fluids was used as a working fluid with a volume fraction concentration of 0.1% and a flow rate of 1.5 Lpm under the same experimental condition of the base fluid experiment. Based on the comparison between the base fluid, CuO (0.1 %V) /water, and TiO₂ (0.1 %V) nano-fluids at a flowrate of 1.5 Lpm, we decided to select the nano-fluid with the best thermal performance to conduct a systematic study by changing the flow rates and the nano-particles concentrations and compare the results with the base fluid. Based on the literature, we selected the range of nano-particles volume concentration was 0.1-0.3% that is considered in most of the relevant work [1-20-27].

The thermal performance of FPSC was evaluated using CuO (0.2 %V)/water nano-fluid at flowrate of 1.5, 2, and 3 Lpm. Then, the concentration was increased to 0.3 %V and the effect of the flowrate was studied at 1, 1.5, 2, and 3 Lpm. Finally, the results of CuO/water nano-fluids were compared to the base water. The schematic of the experiments is shown in (Fig. 3.13), which contains a summary of the experiments.

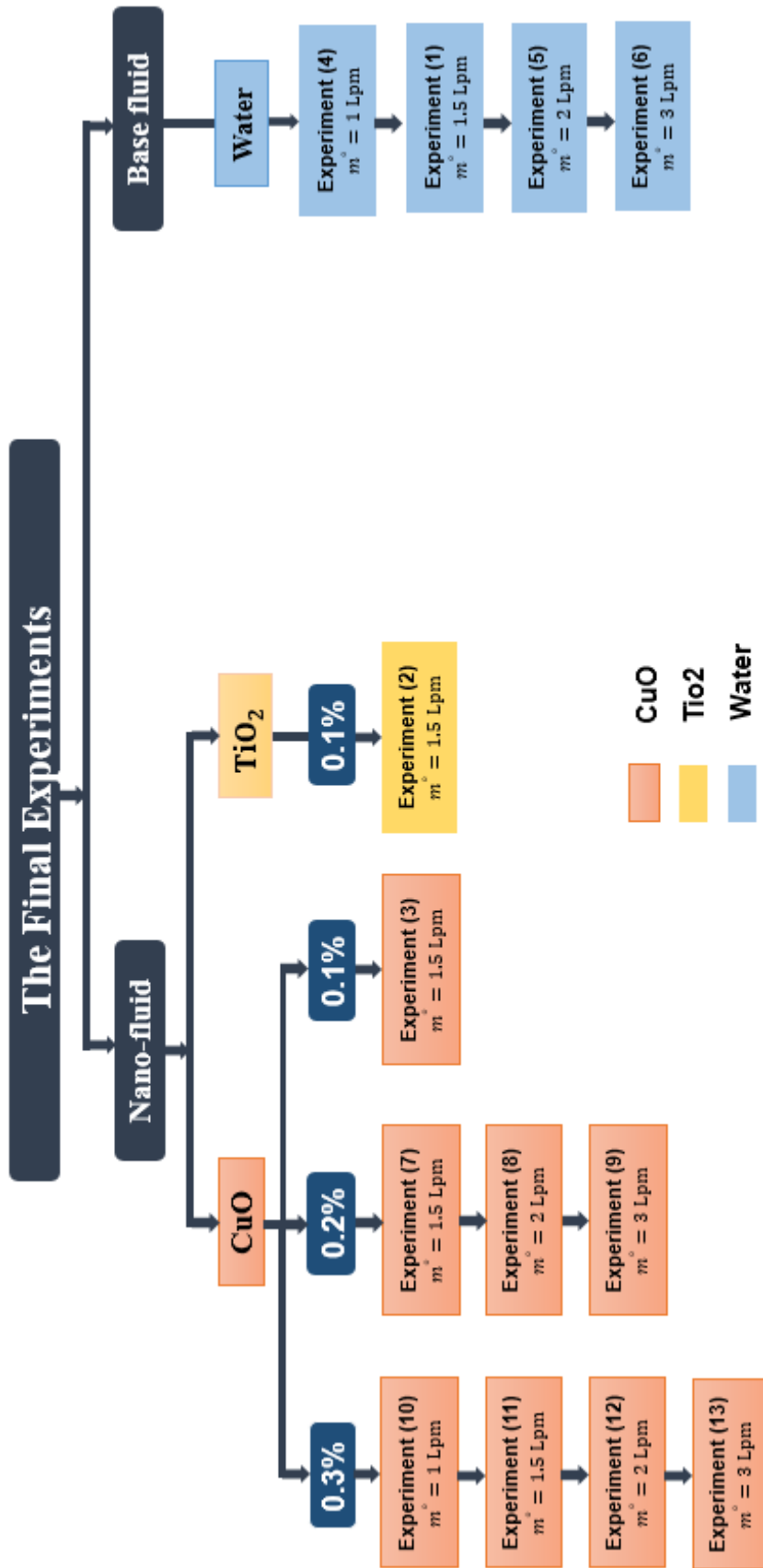


Figure 3.13: The chart of the final experiments

3.7 Summary

The aim of this chapter is to explain in details the experimental work that includes the experimental setup assembly, calibration of the devices, nano-fluid preparation, and experimental procedure. Finally, a detailed explanation of how to conduct the experiments is presented. The plan of the experiments includes:

- 1- The deionized water was used as a reference base fluid, which is introduced into the FPSC setup at different flow rates (1, 1.5, 2, and 3 Lpm).
- 2- The TiO_2 / water nano-fluids with volume fraction concentration 0.1% was used as a working fluid in the FPSC at a flow rate of (1.5 Lpm).
- 3- The CuO / water nano-fluids with volume fraction concentration of (0.1%) (0.2%), and (0.3%) was introduced into the FPSC at different flow rates (1,1.5, 2, and 3 Lpm).

CHAPTER FOUR

ANALYSIS OF DATA

4.1 Introduction

The experimental heat transfer results of the proposed nano-fluids CuO/water and TiO₂/water as well as the results of base fluid (water) in the manufactured FPSC were presented and discussed in this chapter. The results of the different fluids are evaluated based on the effect of varying volume concentration (0.1%-0.3%) of the nano-fluids and flow rates (1-3 Lpm) on the performance of FPSC. The FPSC performance is expressed by the temperature difference of the flowing fluid in FPSC, Nusselt number, and the collector thermal efficiency. Finally, the empirical correlations for calculating Nusselt number of the flowing fluids in the FPSC were developed based on the experimental data using STATISTICA Software.

4.2 Experimental Results

The experiments were conducted during two months (May and June 2017) from 10 AM to 12:30 PM. The FPSC with a spiral pipe arrangement was manufactured by teamwork at Iraq. Two nano-fluids CuO/water and TiO₂/water were proposed and their results were compared with the base fluid (water). The flow rates of the fluids and the nano-particles volume concentration of the nano-fluids were varied within the range of (1-3 Lpm) and (0.1%-0.3%), respectively. The thermocouple readings of the inlet, outlet, and the fixed points as well as the solar radiation intensity on the FPSC were taken every five seconds. However, five minutes' intervals were considered in recording the solar radiation intensity and the thermocouples readings.

The experiments of the base fluid (deionized water) flows in the FPSC were carried out on May 29, 30, and 31 as well as June 20, 2017 for fluid flow rates of (1, 1.5, 2, and 3 Lpm), respectively, and the results are listed in Tables (A.1, 2, 3, and 4) that are included in Appendix (A). The maximum weather temperature was recorded to be about 41.7 °C during the run with a small variation.

The TiO₂ nano-fluid with the nano-particles concentration of 0.1% was introduced into the FPSC to study its effect on the performance of the FPSC. The nano-fluid experiments were performed on June 8, 2017 at the same experiments conditions mentioned previously. Table (A.6) in Appendix (A) presents the measured temperature by thermocouples and the solar radiation intensity during at 0.1% volume concentration of TiO₂/water nano-fluids with the flow rate of (1.5 Lpm). The maximum ambient temperature of about 43.7 °C was recorded for TiO₂ nano-fluids.

Tables (A.5) in Appendix (A) represents the experimental results of 0.1 % by volume CuO/water nano-fluid. The experiments were conducted on June 4, 2017 with the nano-fluid flow rate of 1.5 Lpm. The maximum weather temperature was 42.8 °C, with average temperature of about 39 °C during the run with a small variation. It should be noted that CuO/water nano-fluid exhibited higher heat transfer performance than TiO₂/water nano-fluid at 0.1% nano-particles and flow rate of (1.5 Lpm). Hence, we decided to conduct a systematic study using CuO nano-particles as a working fluid for the experimental investigation of the FPSC performance at different nanoparticles concentrations and flow rate. Based on the above conclusion, the experiments of 0.2 % and 0.3% by volume CuO/water nano-fluid were carried out on June 11, 12, and 13, 2017 and June 14, 15, 18, and 19, respectively. The experimental results were included in Tables A. 7, 8, and 9 and Tables A. 10, 11, 12, and 13 for 0.2% and 0.3% concentrations, respectively, with flow rates range of 1-3 Lpm. The maximum weather temperature was 44.3 °C, with average temperature of about 42 °C during the run with a small variation.

4.2.1 Incident Solar Radiation Results

All the experiments were carried out on selected days during summer 2017 in Iraq based on the weather conditions as the clear sky. The incident solar radiation was measured and the collected data are shown in Figures (4.1-4.13). During the experiments, it can be observed that the incident solar radiation increases within the period of (10 AM-12:30 PM) with some fluctuations due to the presence of clouds from time to time.

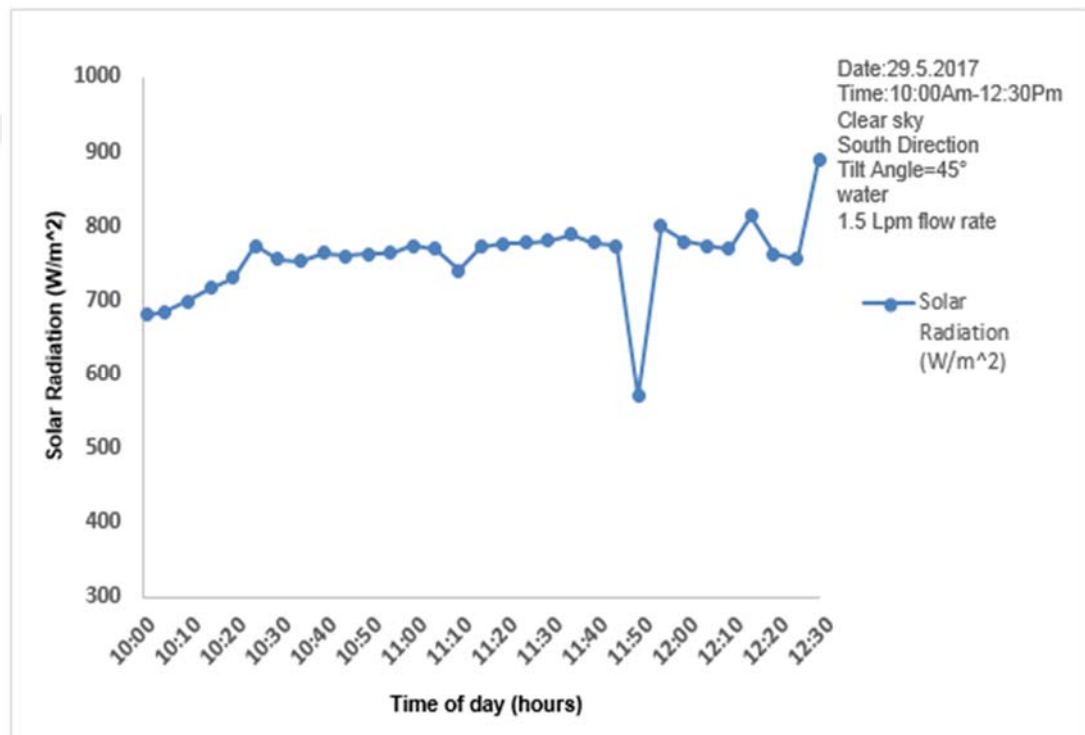


Figure 4.1: Incident solar radiation on May 29, 2017

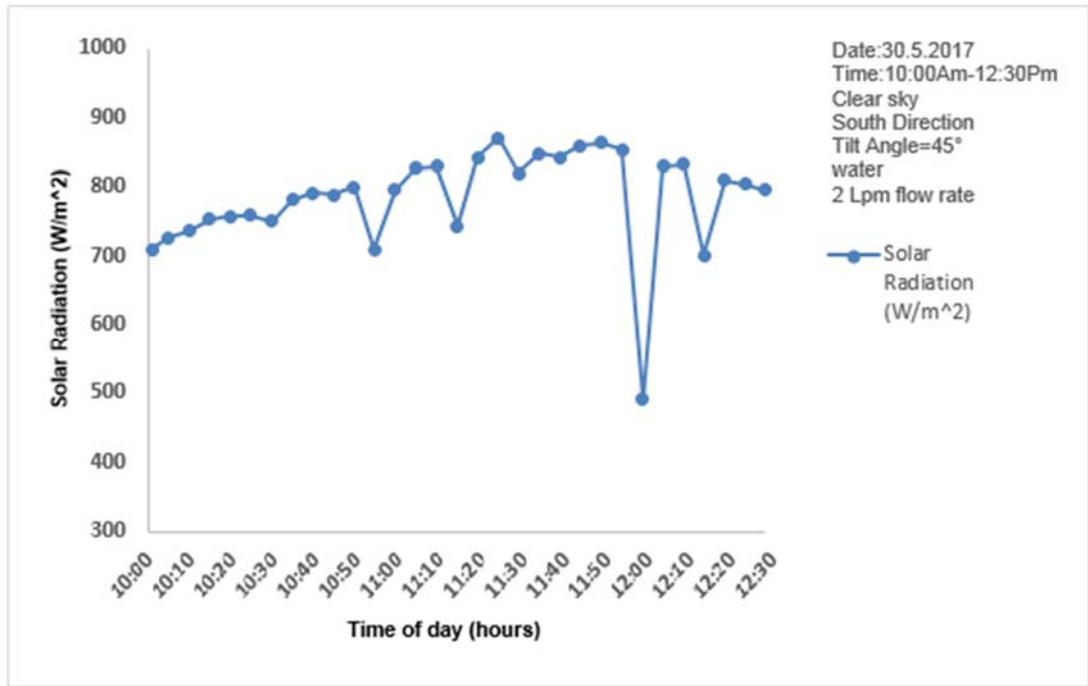


Figure 4.2: Incident solar radiation on May 30, 2017.

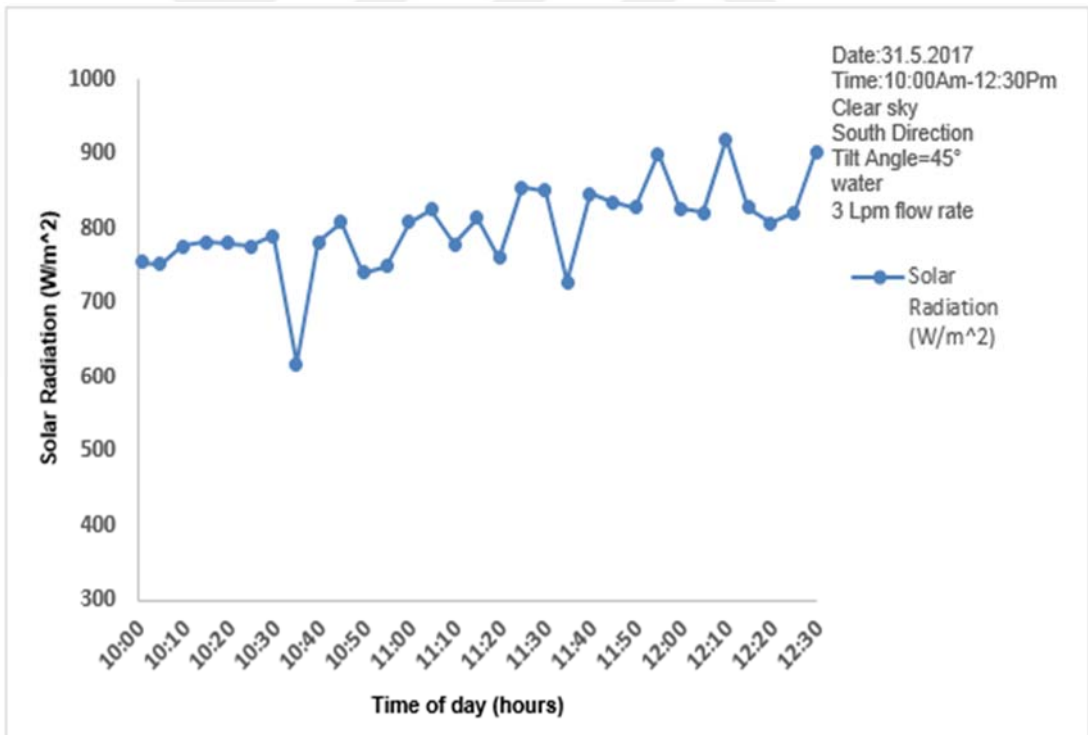


Figure 4.3: Incident solar radiation on May 31, 2017.

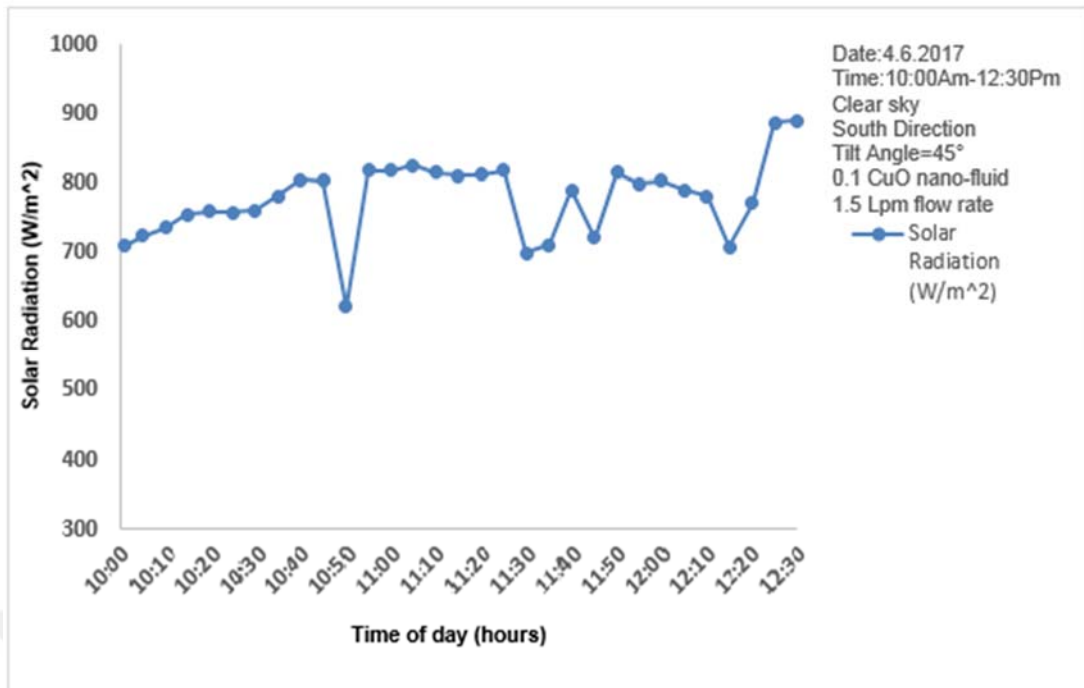


Figure 4.4: Incident solar radiation on June 4, 2017.

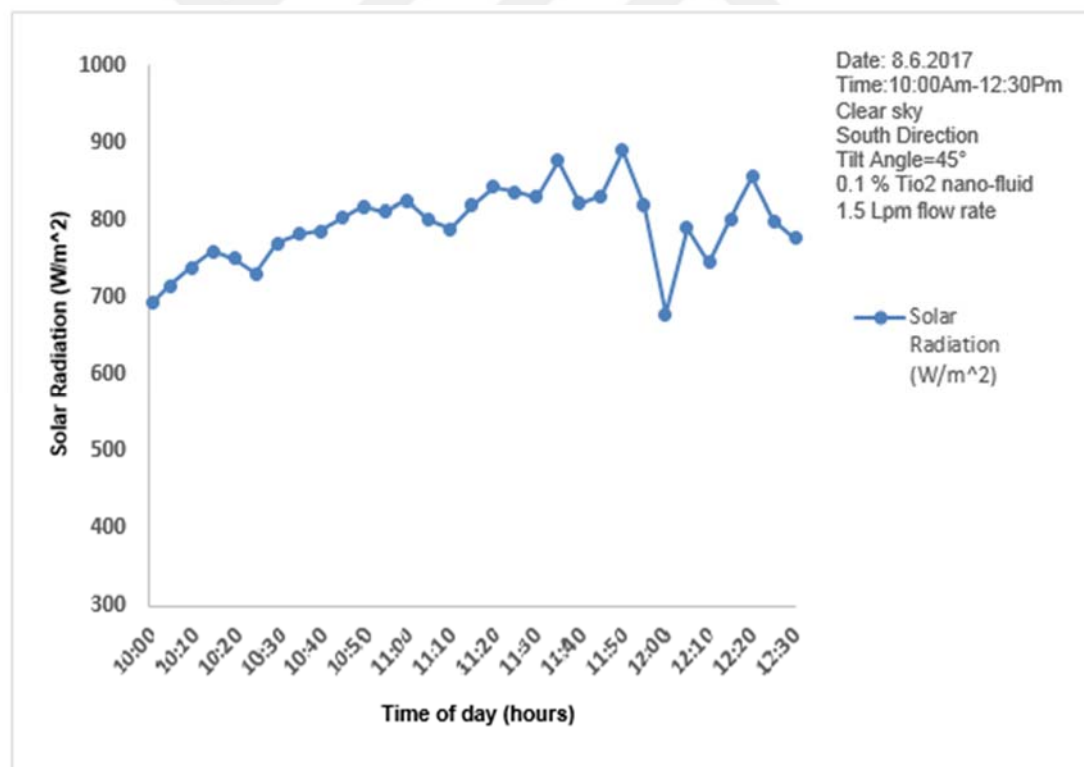


Figure 4.5: Incident solar radiation on June 8, 2017.

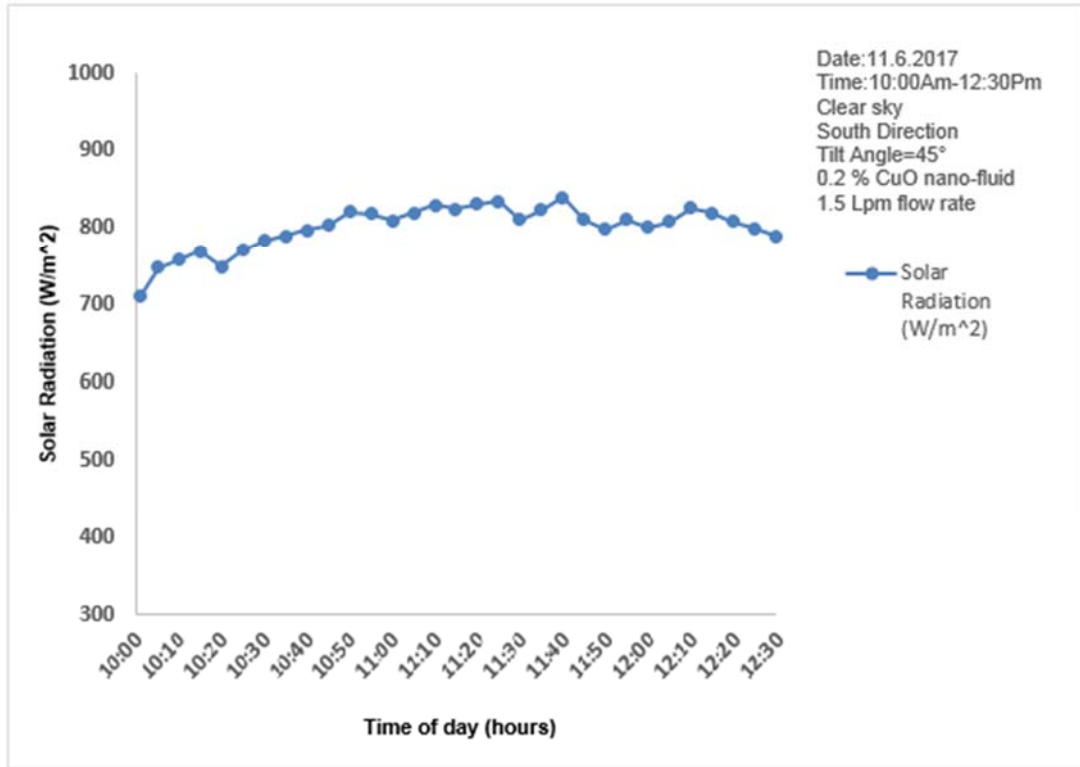


Figure 4.6: Incident solar radiation on June 11, 2017.

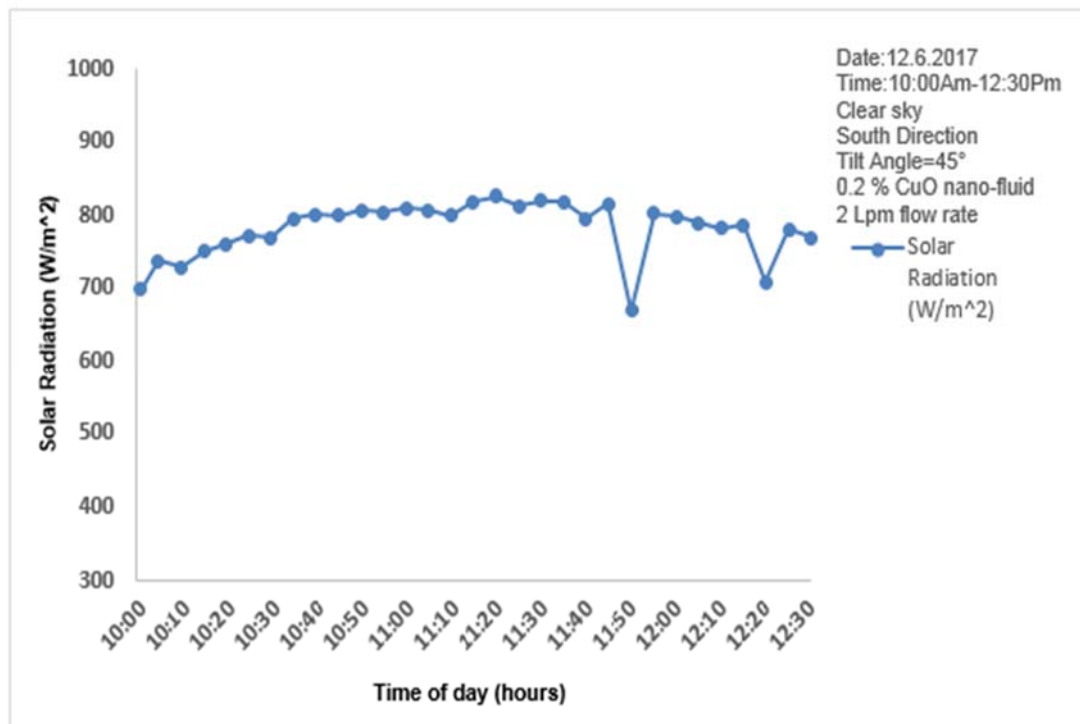


Figure 4.7: Incident solar radiation on June 12, 2017.

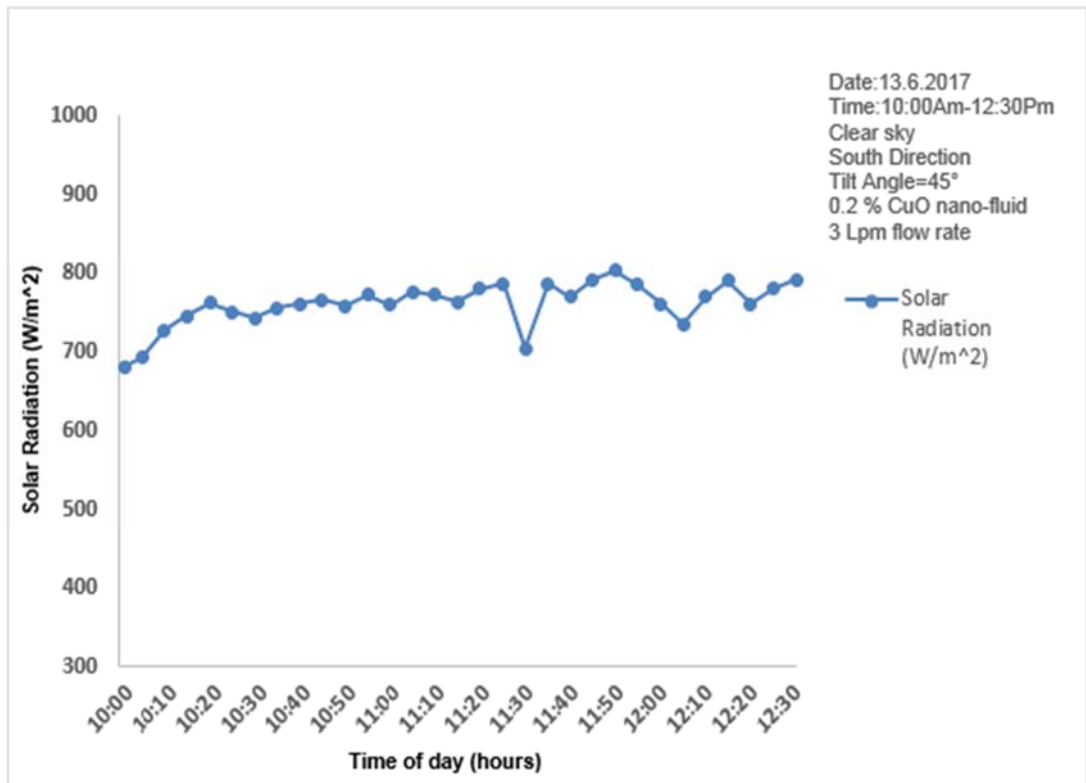


Figure 4.8: Incident solar radiation on June 13, 2017.

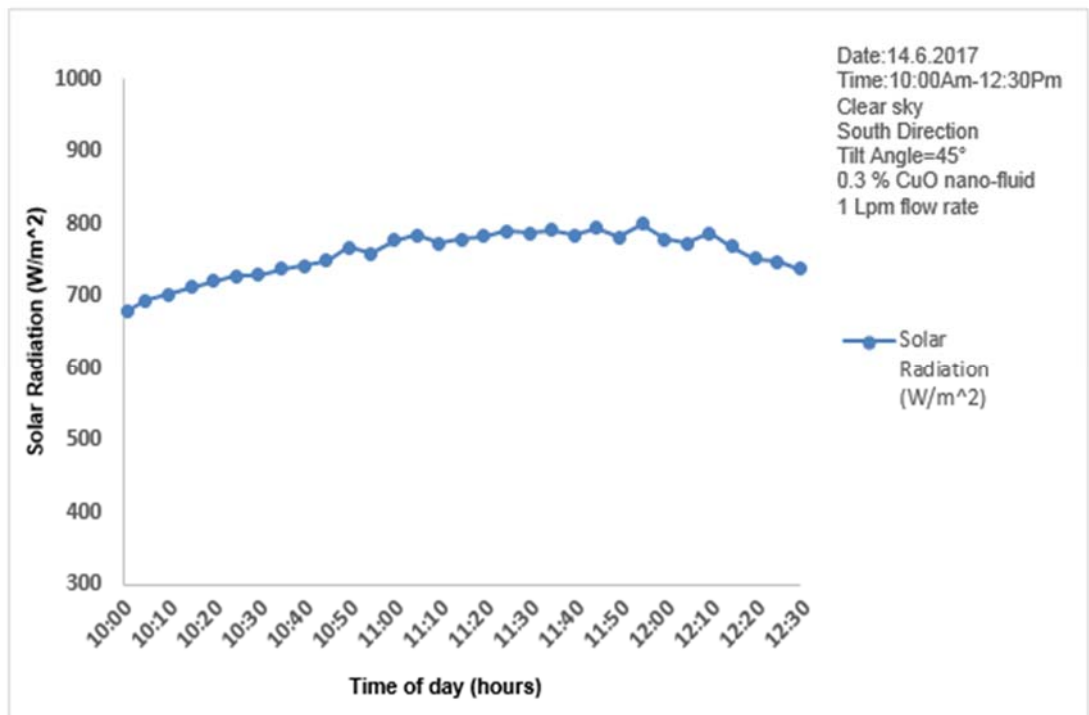


Figure 4.9: Incident solar radiation on June 14, 2017.

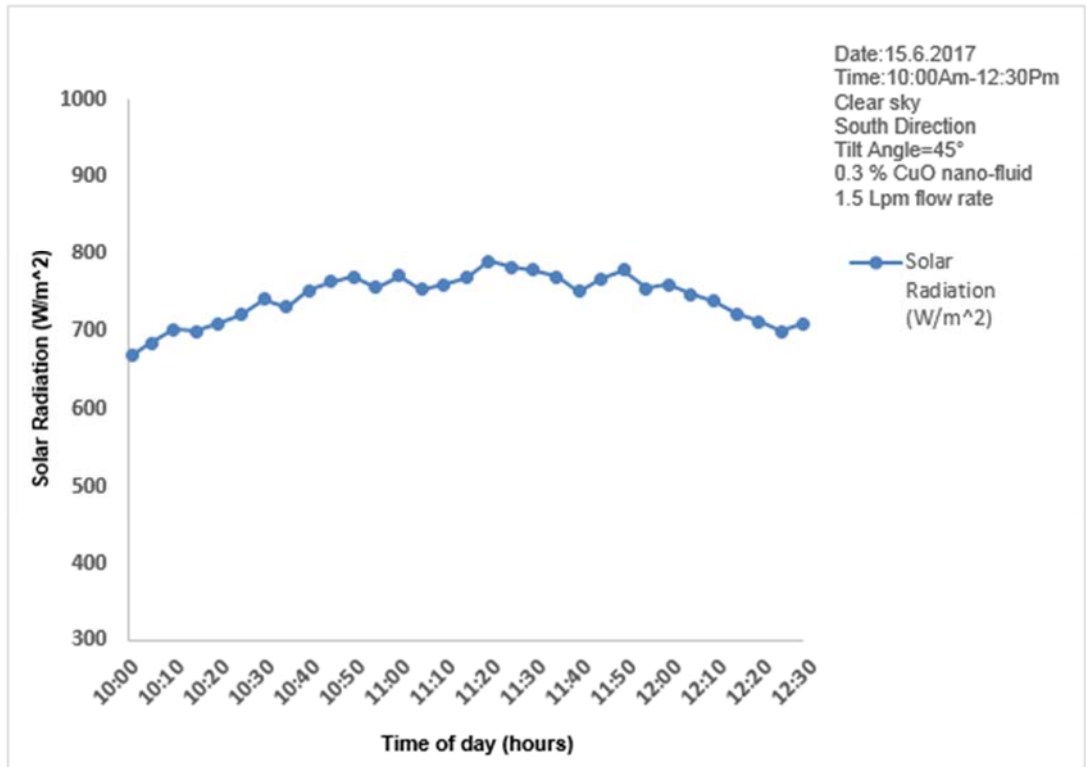


Figure 4.10: Incident solar radiation on June, 15, 2017.

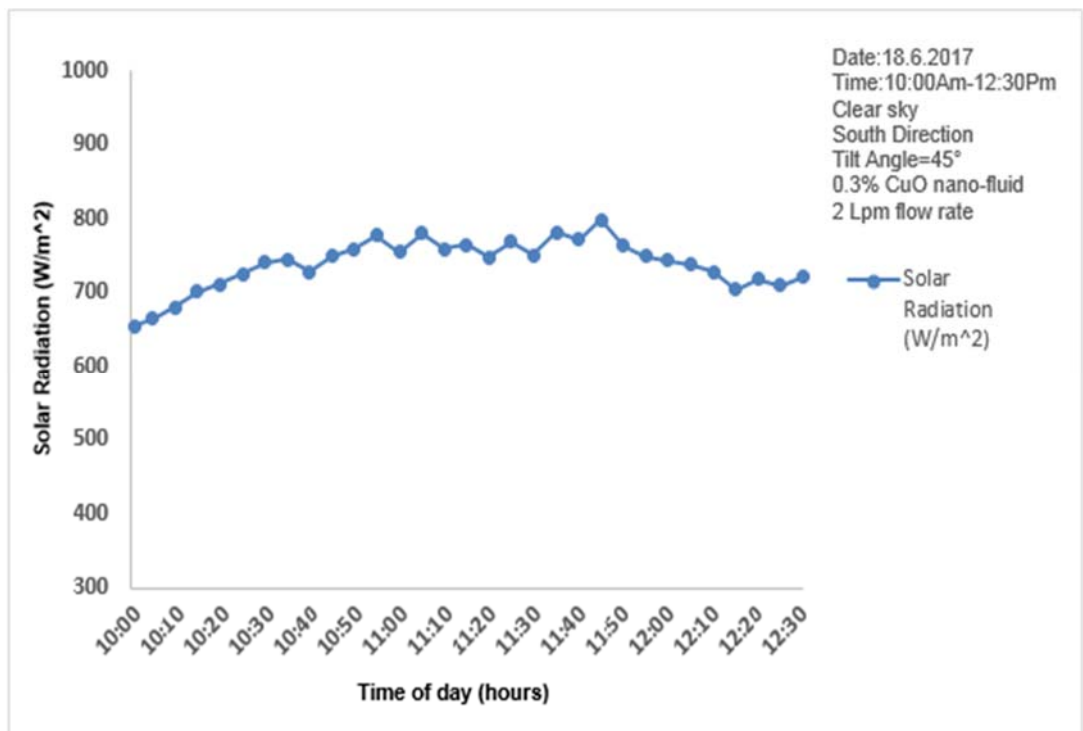


Figure 4.11: Incident solar radiation on June 18, 2017.

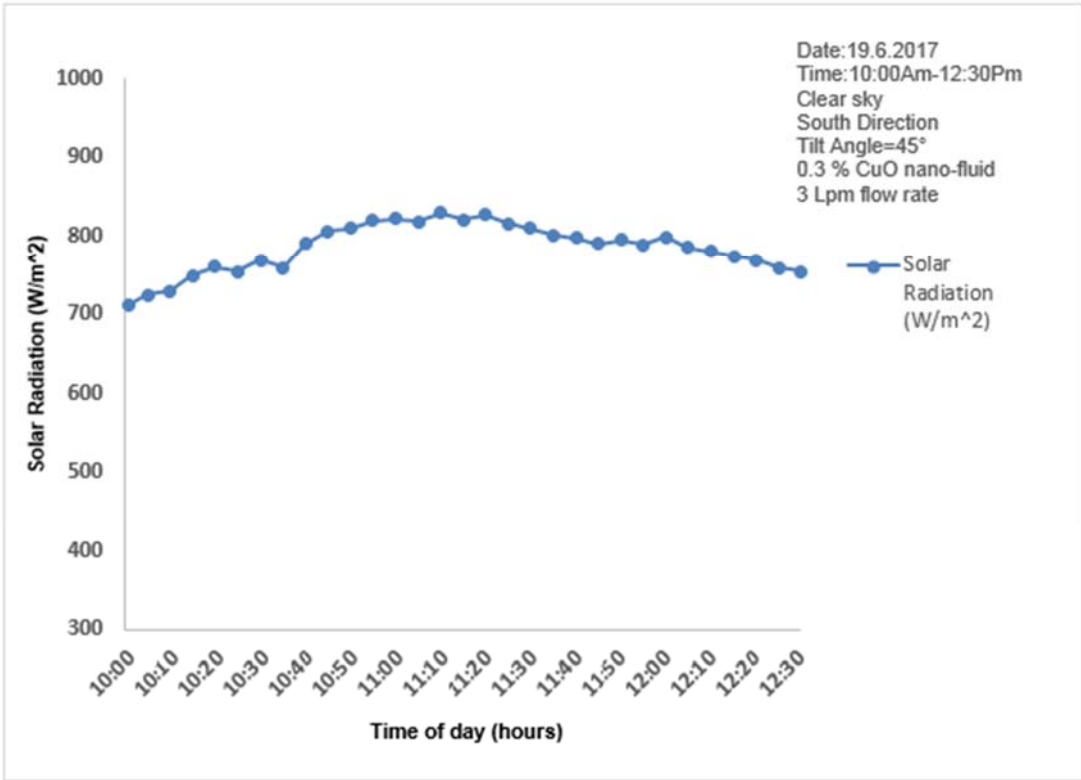


Figure 4.12: Incident solar radiation on June 19, 2017.

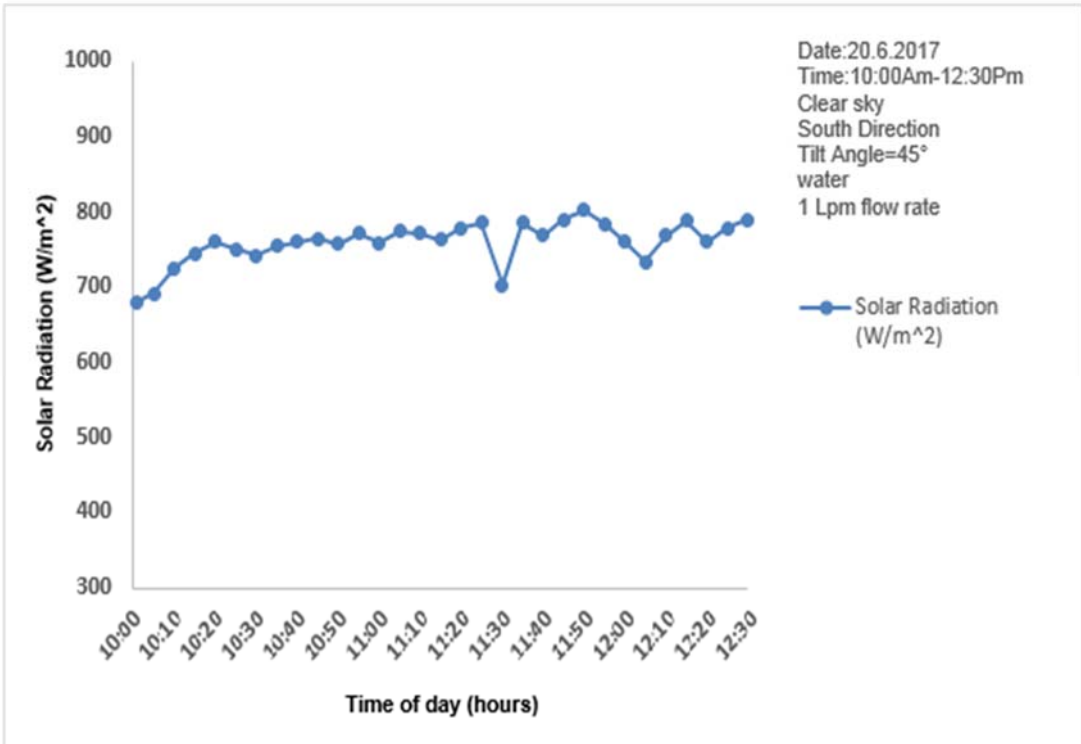


Figure 4.13: Incident solar radiation on June 20, 2017.

4.2.2 Temperature Difference Results

The effects of two type of fluid water and nano-fluids flow rate, the nano-fluid types, and the nano-particles volume concentration of the nano-fluids on the outlet-inlet temperature difference of the FPSC. These effects will be discussed in more details in the following sections.

4.2.2.1 The Flow Rate Effect-The Base Fluid (Water)

The effect of the mass flow rate of the fluids on the temperature difference was evaluated for the following cases: (1) base fluid (water), (2) TiO₂/water nano-fluid with 0.1% volume concentration, and (3) CuO/water nano-fluids with 0.1%, 0.2%, and 0.3 % volume concentrations.

Figure (4.14) shows the outlet-inlet temperature difference of water with the flow rates of (1, 1.5, 2, and 3 Lpm). It was observed that the temperature differences of about 7.3 °C, 6.6 °C, 5.2 °C, and 4 °C for 1, 1.5, 2, and 3 Lpm at was obtained. From Appendix (A), these readings were reported when the solar radiation reaches its highest value approximately about 787 W/cm² (at 11:15 AM), 788 W/cm² (at 11:35 AM), 870 W/cm² (at 11:25 AM), and 779 W/cm² (at 11:10 AM) for 1, 1.5, 2, and 3 Lpm, respectively. Based on the above results, it is obvious that the outlet-inlet temperature difference decreases with increasing the flow rate of the working fluid. This is attributed to the fact that at low flow rate, the residence time of the working fluid is longer than that of high flow rate so that more solar radiation can be absorbed by the FPSC allowing more temperature rise.

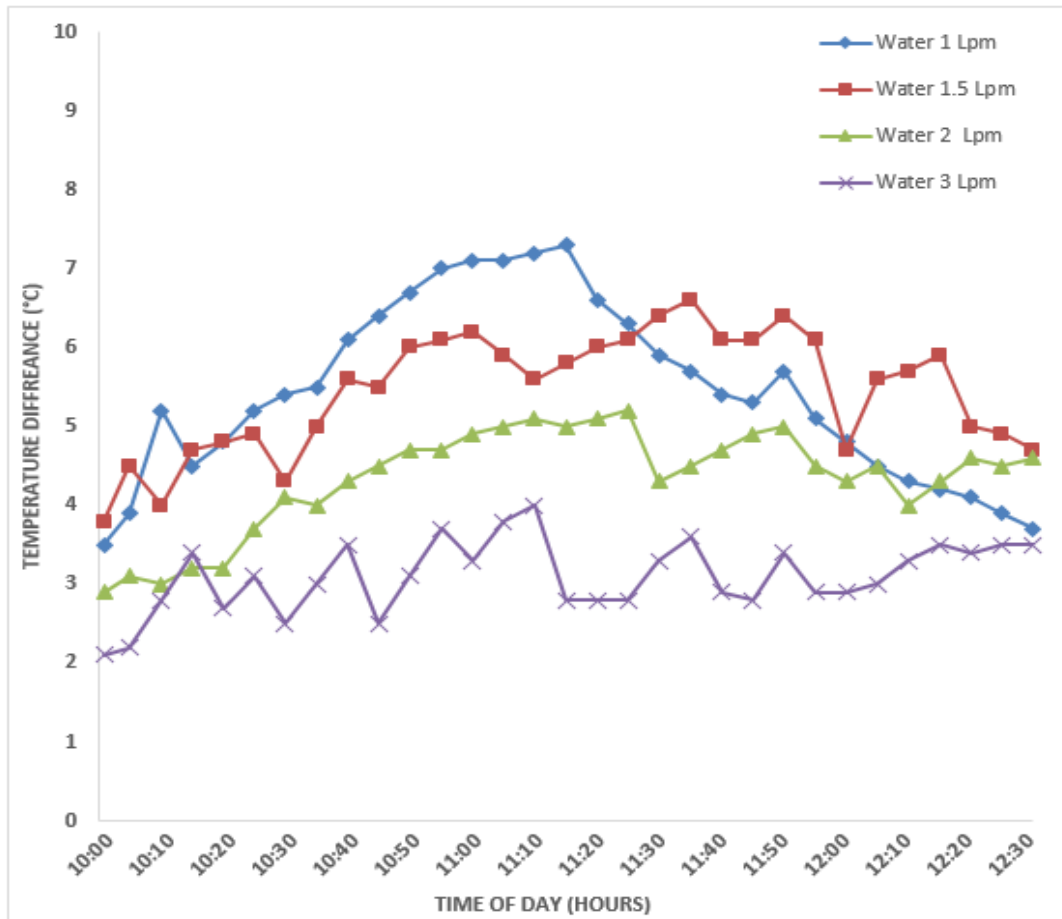


Figure 4.14: The inlet-outlet temperature difference vs. time at different flow rates (1, 1.5, 2, and 3 Lpm) for the base fluid (water)

4.2.2.2 The Fluid Type Effect-The Base Fluid (Water) and CuO/Water and TiO₂ / Water Nano-fluids

The effect of fluid type on the outlet-inlet temperature difference of the FPSC is demonstrated in Fig. (4.15). At 1.5 Lpm, the experimental results indicated that the temperature differences of about 6.6 °C, 7.1 °C, and 7.9 °C for water, TiO₂, and CuO was reported. From Fig. (4.15) and Appendix (A), these readings were reported when the solar radiation reaches its highest value approximately about 788 W/cm² (at 11:35 AM), 788 W/cm² (at 11:10 AM), and 811 W/cm² (at 11:15AM) for water, TiO₂, and CuO, respectively. Hence, the 0.1 % volume concentration CuO/water nano-fluid exhibited higher temperature difference than that of both 0.1 % volume concentration TiO₂/water nano-fluid and the base fluid (water). The TiO₂/water nano-fluid has a higher temperature difference compared to water. The heat transfer enhancement of the nano-fluids is attributed to the enhanced (thermosphysical) properties such as

thermal conductivity and heat transfer coefficient caused by adding the CuO and TiO₂ nano-particles to water. In addition to the above reason, it was noted that adding nano-particles to the water has many advantages: (1) results in a decrease in the heat capacity of the water so that less energy is required for the nano-fluid in comparison with water; in other words, the temperature difference of the nano-fluids is larger than that of water if the same amount of heat is provided, (2) the heat transfer area is increased by mixing a little amount of the nano-particles with the base fluid (water), and (3) the mass migration phenomenon of the nano-particles in the nano-fluid working media further improves the heat transfer enhancement. On the other hand, the higher temperature difference of the CuO/water nano-fluid in comparison with TiO₂/water nano-fluid is due to the higher thermal conductivity of CuO nano-particles.

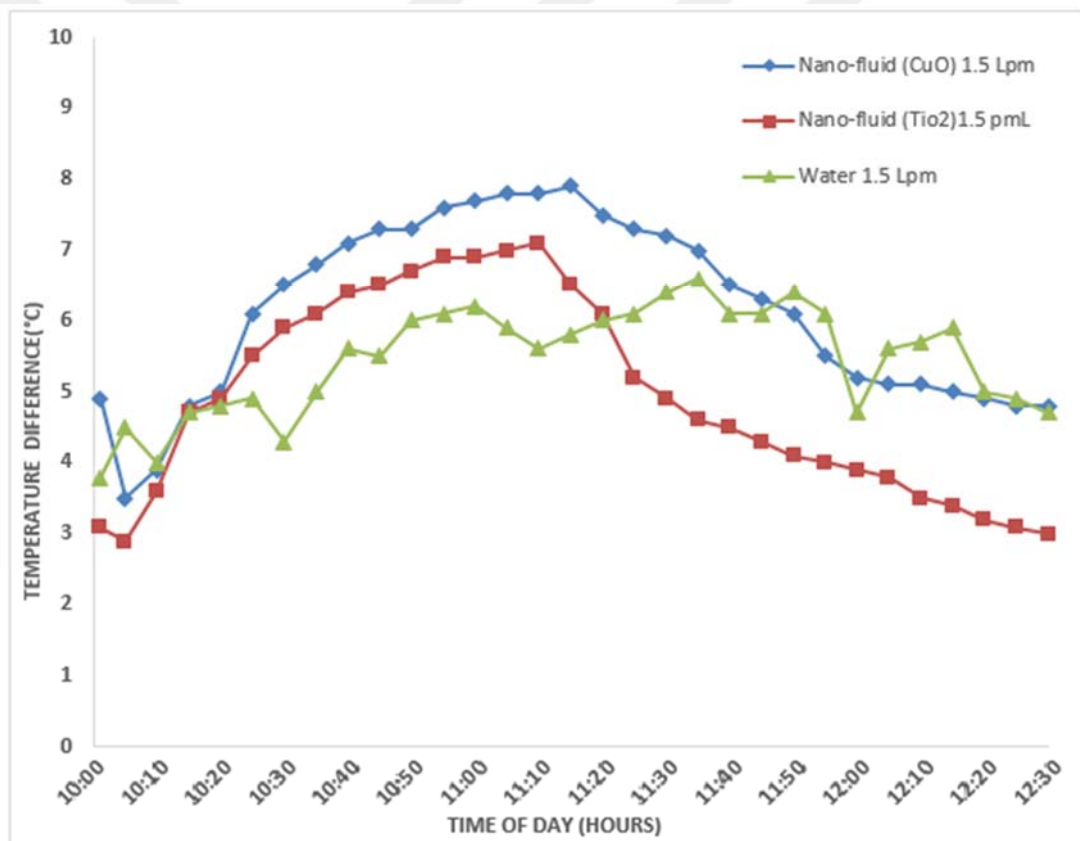


Figure 4.15: The inlet-outlet temperature difference vs. time at 1.5 Lpm flow rate for water, CuO/water, and TiO₂/water Nano-fluids with Nano-particles volume concentration of ($\phi = 0.1\%$)

4.2.2.3 The Flow Rate Effect – 0.2 % By vol. (CuO/Water Nano-fluid)

The experimental results of the CuO/water nano-fluid with nano-particles volume concentration 0.2% at 1.5, 2, and 3 Lpm are presented in Fig. (4.16). It was found that the maximum temperature difference of about 8.4, 7.5, and 6.3 °C were reported for the flow rate of 1.5, 2, and 3 Lpm, respectively. These results are consistent with the observation of the base fluid (water); the temperature difference decreases with increasing the nano-fluid flow rate because of the significant reduction in the residence time of the nano-fluid in the FPSC that leads to lower the absorbed solar energy during the same time interval. From Fig. (4.16) and Appendix A, these readings were recorded when the solar radiation reaches its highest value approximately about 825 W/cm² (at 11:15 AM), 799 W/cm² (at 11:10 AM), and 779 W/cm² (at 11:20AM) for the flow rate of 1.5, 2, and 3 Lpm, respectively. Generally, the (1.5 Lpm) flow rate provides the highest temperature difference compared to higher flow rates (2 and 3 Lpm) for 0.2% by vol. CuO/ water nano-fluid.

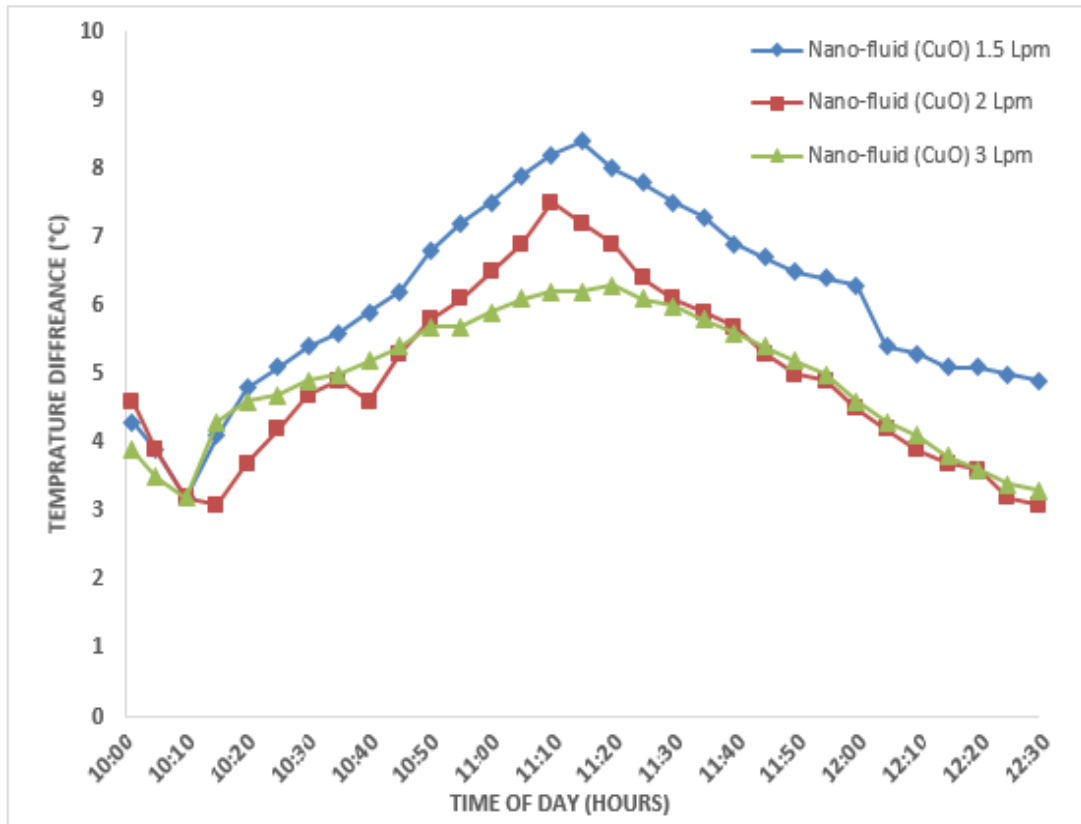


Figure 4.16: The inlet-outlet temperature difference vs. time at 1.5, 2, and 3 Lpm flow rates for CuO/water with Nano-particles volume concentration of ($\phi = 0.2\%$)

4.2.2.4 The Flow Rate Effect – 0.3 % By vol. CuO/Water Nano-fluid

The same trend has been observed for the effect of the fluid flow rate on the temperature difference for CuO /water nano-fluid with nano-particles concentration 0.3% at different flow rates (1, 1.5, 2, and 3 Lpm). From Fig. (4.17), the lowest flow rate (1 Lpm) provides the highest temperature difference (9.8 °C) compared to 8.9, 8.5, and 7.6 °C for 1.5, 2, and 3 Lpm, respectively. From Fig. (4.16) and Appendix A, these readings were recorded when the solar radiation reaches its highest value approximately about 785 W/cm² (at 11:05 AM), 768 W/cm² (at 11:15 AM), 755 W/cm² (at 11:00AM), and 819 W/cm² (at 11:05AM) for the flow rate of 1, 1.5, 2, and 3 Lpm, respectively.

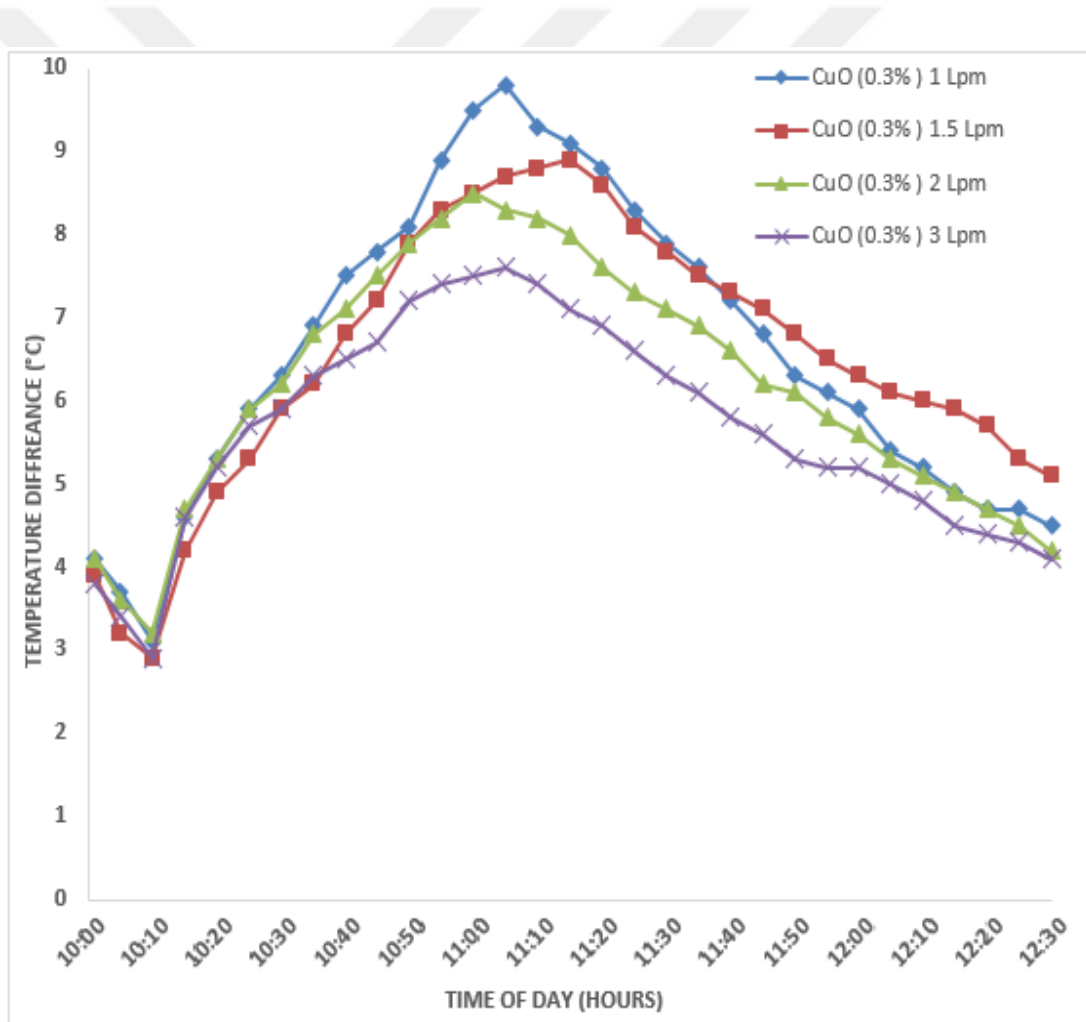


Figure 4.17: The inlet-outlet temperature difference vs. time at 1, 1.5, 2, and 3 Lpm flow rates for CuO/water with Nano-particles volume concentration of ($\phi = 0.3\%$)

4.2.2.5 The Effect of Nano-particles Volume Concentration

Figure (4.18) presents the experimental results in terms of the temperature difference of the base fluid (water) and 0.1, 0.2, and 0.3% by vol. CuO/water nano-fluid at a flow rate of 1.5 Lpm. The results show that the temperature difference increases as the nano-fluid concentration increases. The CuO/water nano-fluid with 0.3% by vol. gives the highest temperature difference of about 8.9 °C in comparison with 6.6, 7.9, and 8.4 °C for water, 0.2% and 0.3% by vol. CuO/water nano-fluid, respectively. As discussed above in section (4.2.2.2), adding the nano-particles to the water results in improving the (thermo-physical) properties of the water, decreasing the heat capacity of the water, enlarging the heat transfer area, and the mass migration phenomenon further improves the heat transfer enhancement.

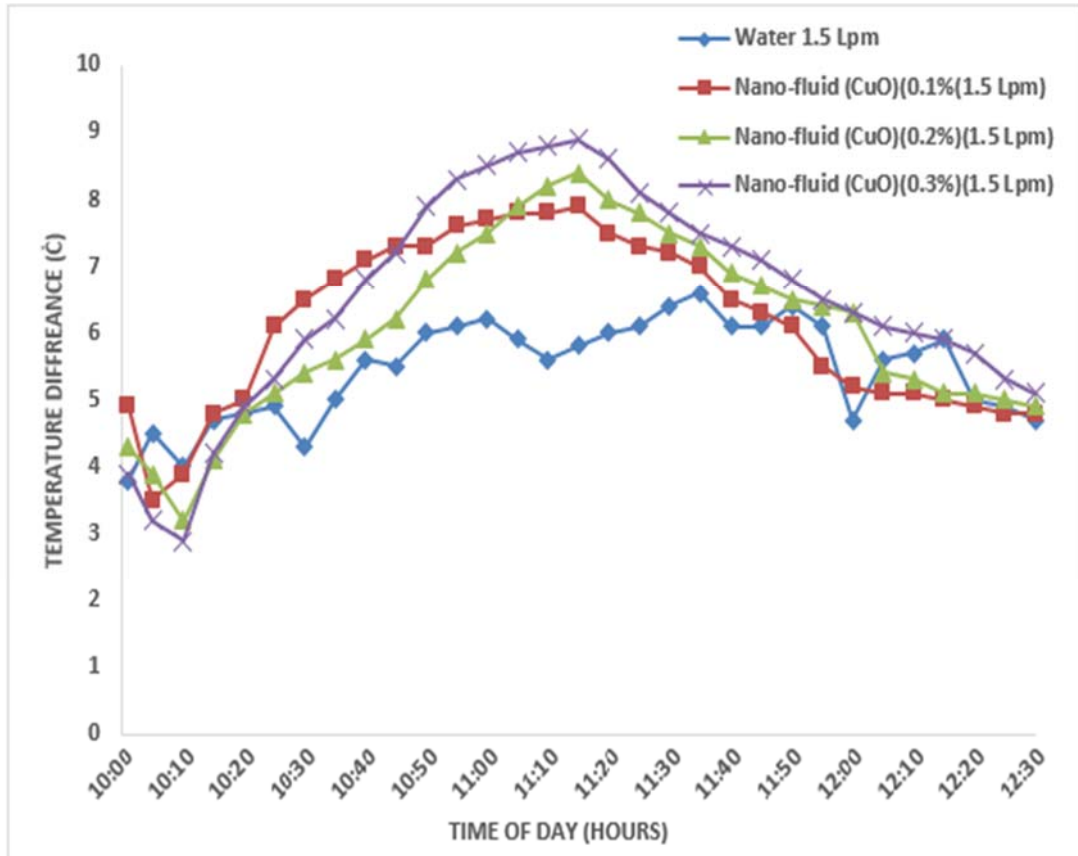


Figure 4.18: The inlet-outlet temperature difference vs. time at 1.5 Lpm flow rate for water and CuO/water Nano-fluids of different concentrations (0.1, 0.2, and 0.3%)

The same trend has been observed in Fig. (4.19) where the temperature difference increases as the nano-fluid concentration increases. The experimental temperature difference results of 0.3% by vol. CuO/water nano-fluid is obviously higher than that of 0.2% by vol. nano-fluid as well as the base fluid (water). From Fig. (4.19), the temperature differences were 8.5, 7.5, and 5.2 °C for 0.3% by vol. CuO/water, 0.2% by vol. CuO/water, and water, respectively.

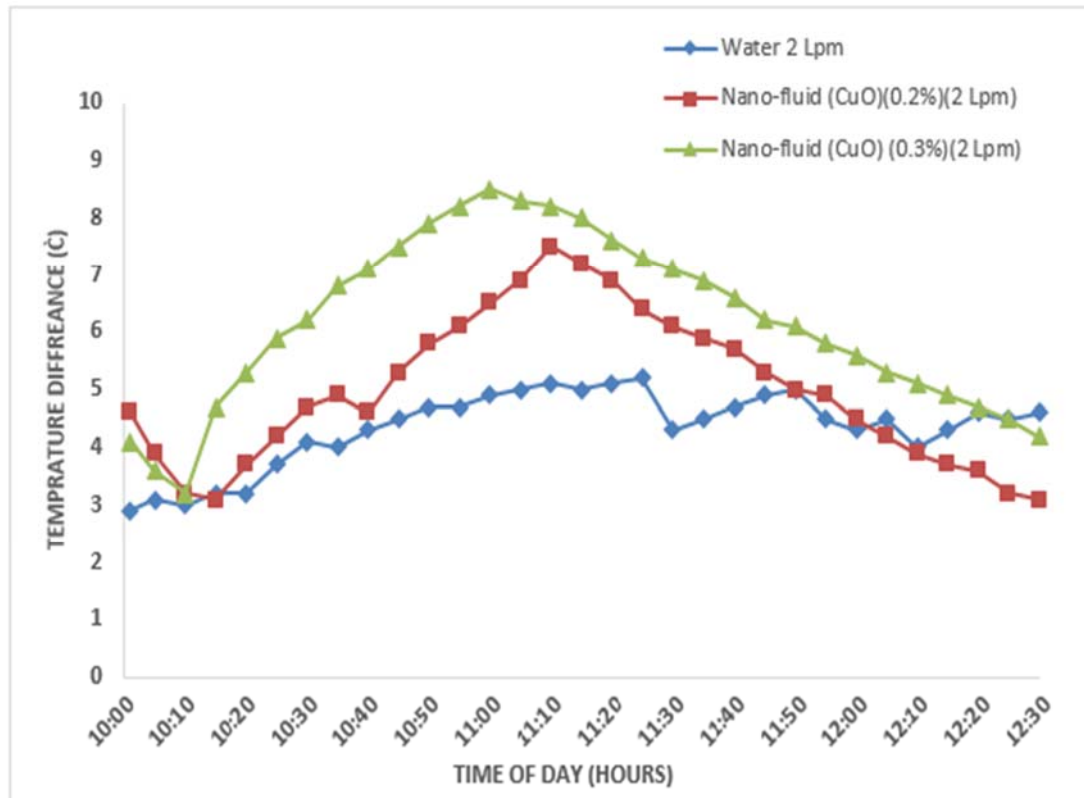


Figure 4.19: The inlet-outlet temperature difference vs. time at 2 Lpm flow rate for water and CuO/water Nano-fluids of different concentrations (0.2 and 0.3%)

Figure (4.20) the trend of the positive effect of increasing the volume concentration on the heat transfer enhancement is further confirmed by increasing the flow rate to (3 Lpm). The experimental results of the temperature difference for water, 0.2% by vol. CuO/water, and 0.3% by vol. CuO/water at a flow rate of 3 Lpm. The 0.3% by vol. CuO/water exhibited the higher temperature difference of about 7.6 °C in comparison with 6.3 and 4 °C for the 0.2% by vol. CuO/water and water, respectively.

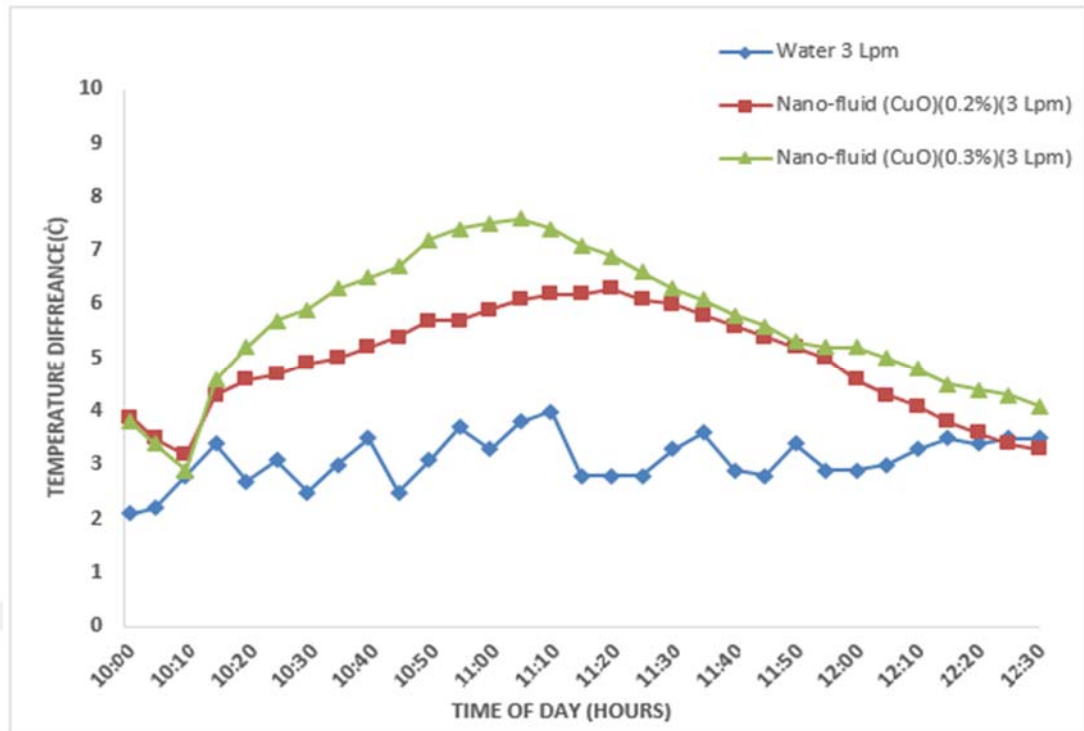


Figure 4.20: The inlet-outlet temperature difference vs. time at 3 Lpm flow rate for water and CuO/water Nano-fluids of different concentrations (0.2 and 0.3%)

4.3 Efficiency of Flat Plate Solar Collector

Figure 4.21 and Table (4.1) present the FPSC efficiency as a function of the fluid type, nano-particles volume concentration of the nano-fluids, and the fluid flow rates. At 1.5 Lpm, the 0.1 % by vol. CuO/water nano-fluids exhibited higher efficiency (54.3%) compared to 53.8% and 50% for 0.1 % by vol. TiO₂/water and the base fluid (water), respectively. This is attributed to the higher thermal conductivity of CuO compared to TiO₂ and water. For the base fluid (water), it was found that the FPSC efficiency increases slightly with increasing the flow rate from (1 to 3 Lpm). The reported efficiency was 49, 50, 51, and 52.6 for 1, 1.5, 2 and 3 Lpm, respectively. At constant particles volume concentration, similar trend was observed for CuO/water nano-fluid. These observations are in good agreement with the reported data in the literature [1-4-20-25]. However, it was reported that at a very high flow rate, there is a decrease in the efficiency of the fluid due to the significant reduction in the temperature difference of the inlet and outlet fluid [25].

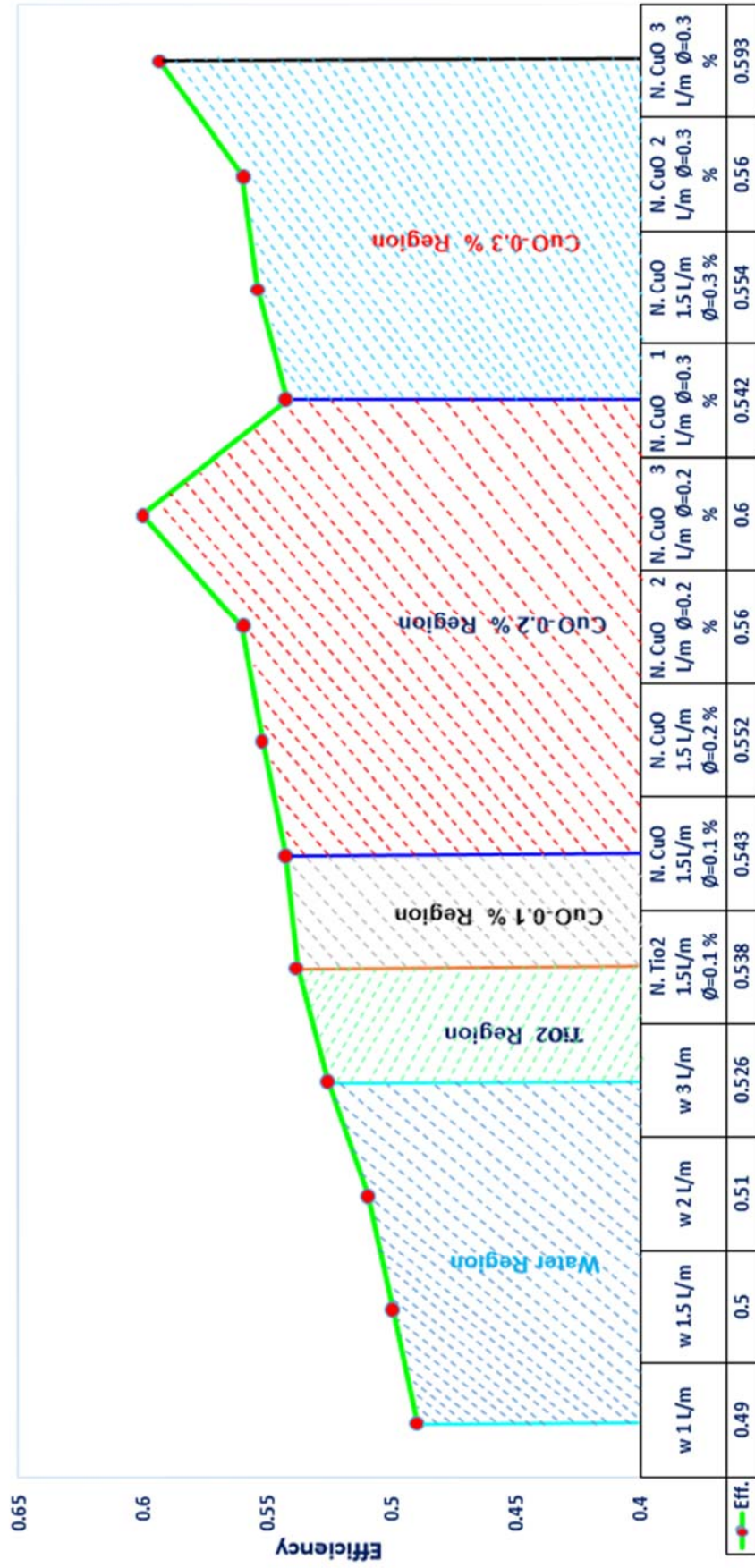
To evaluate the effect of the nano-particles volume concentration on the FPSC efficiency, the CuO/water nano-fluids were prepared with (0.1%, 0.2%, and 0.3%. At

1.5 Lpm flow rate, the results showed that the efficiency was improved from 54.3% to 55.2% with an increase in the concentration from 0.1% to 0.2%, respectively. The maximum efficiency was reported to be (60%) for 0.2% particle volume concentration of the CuO/water nano-fluid at a flow rate of 3 Lpm. In general, increasing the particle concentration of the nano-fluid leads to an increase in the efficiency due to the enhanced thermal conductivity of the nano-fluid that rises the convective heat transfer coefficient. However, it should be noted that as the particle concentration of the nano-fluid increases from 0.2% to 0.3%, the efficiency approximately remains constant or reduces slightly. This indicates that increasing the particle volume concentration up to or more than 0.3% may results in a reduction in the efficiency due to the enhanced fluid viscosity that causes frictional dissipation and the possibility of nano-particles agglomeration. Our results are in a good agreement with the available results reported in the literature [1-20-25-26]. Based on the literature, it should be noted that the suggested FPSC with spiral tube arrangement in this project showed approximately the same efficiency of the conventional FPSC [20].

Table 4.1: The efficiency of (FPSC) using different fluids

Number of Experimental	Type of fluid	Mass flow rate	Efficiency %
1	water	1 Lpm	49
2	water	1.5 Lpm	50
3	water	2 Lpm	51
4	water	3 Lpm	52.6
5	Nano-fluid (Tio2-0.1%)	1.5 Lpm	53.8
6	Nano-fluid (CuO-0.1%)	1.5 Lpm	54.3
7	Nano-fluid (CuO-0.2%)	1.5 Lpm	55.2
8	Nano-fluid (CuO-0.2%)	2 Lpm	56
9	Nano-fluid (CuO-0.2%)	3 Lpm	60
10	Nano-fluid (CuO-0.3%)	1 Lpm	54.2
11	Nano-fluid (CuO-0.3%)	1.5 Lpm	55.4
12	Nano-fluid (CuO-0.3%)	2 Lpm	56
13	Nano-fluid (CuO-0.3%)	3 Lpm	59.3

Efficiency Chart.



Type of Fluid

Figure 4.21: The efficiency of FPSC using Different fluids

4.4 The Empirical Correlations

Using the experimental data, the non-dimensional relationships (Nusselt number as a function of Reynolds number and Prantal number) were obtained utilizing Statistica software as shown in Table (4.2). For water, the constants (n_1 and n_2) of the correlation $Nu = n_1 Re^{n_2} Pr^{0.3}$ at different flow rates (1, 1.5, 2, and 3 Lpm) were calculated by taking the average values of the estimated constants for each run. While for the nano-fluids, the average values of the constants were considered for each concentration with different flow rates. The power of the Prantal number was taken to be 0.3 for all the experiments. The empirical correlations were tested by calculating the Nusselt numbers using the values of the Reynolds number and Prantal number. The results were compared with the calculated Nusselt numbers from Eq. (2.12) and (2.19), the level of confidence was about [95.0 %].

Table 4.2: The dimensionless relationship from experimental work (*Model: $Nu = n_1 Re^{n_2} Pr^{0.3}$*)

Number of Experimental	Type of fluid	Mass flow rate	Dimensionless Relationship
1	Water	1 Lpm	$Nu = .6015e^{-3} Re^{1.22189} Pr^{0.3}$
2	Water	1.5 Lpm	
3	Water	2 Lpm	
4	Water	3 Lpm	
5	Nano-fluid (Tio2-0.1%)	1.5 Lpm	$Nu = .00182 Re^{1.072973} Pr^{0.3}$
6	Nano-fluid (CuO-0.1%)	1.5 Lpm	$Nu = .982e^{-3} Re^{1.118938} Pr^{0.3}$
7	Nano-fluid (CuO-0.2%)	1.5 Lpm	$Nu = .329e^{-3} Re^{1.22003} Pr^{0.3}$
8	Nano-fluid (CuO-0.2%)	2 Lpm	
9	Nano-fluid (CuO-0.2%)	3 Lpm	
10	Nano-fluid (CuO-0.3%)	1 Lpm	$Nu = .4221e^{-3} Re^{1.221005} Pr^{0.3}$
11	Nano-fluid (CuO-0.3%)	1.5 Lpm	
12	Nano-fluid (CuO-0.3%)	2 Lpm	
13	Nano-fluid (CuO-0.3%)	3 Lpm	

4.5 Summary

This chapter presents the evaluation of the FPSC efficiency based on the fluid type, the flow rate of the fluid, and the nano-particles volume concentration of the

nano-fluids. The CuO/water and TiO₂/water nano-fluids were used as working fluids in the FPSC and their performance was compared with that of the (base fluid/deionized water). The results can be summarized as follows:

- 1. The fluid type effect:** The CuO/water and TiO₂/water nano-fluids demonstrated higher thermal efficiency of the FPSC compared to the deionized water. It should be noted that CuO/water nano-fluid gives the highest thermal efficiency.
- 2. The fluid flow rate:** At a constant particles volume concentration, it was found that the FPSC efficiency increases slightly with increasing the flow rate from 1 to 3 Lpm. However, it was reported that at a very high flow rate, there is a decrease in the efficiency of the fluid due to the significant reduction in the temperature difference of the inlet and outlet fluid.
- 3. The Nano-particles volume concentration of the Nano-fluids:** In general, increasing the particle concentration of the nano-fluid leads to an increase in the efficiency up to a certain limit of the nano-particles concentration after which there will be a drop in the collector efficiency.

CHAPTER FIVE

CONCLUSIONS AND FUTURE WORK

5.1 Conclusion

This project focuses on evaluating the heat transfer performance of the FPSC with a spiral tube arrangement using TiO₂/water and CuO/water nano-fluids as working fluids instead of the base fluid (water). The FPSC performance was evaluated based on the effect of the fluid type, the fluid flow rate, and the nano-particles volume concentration of the nano-fluids on the temperature difference between the inlet and outlet fluid streams and the FPSC thermal efficiency. To show the effect of the fluid type on the inlet-outlet temperature difference, the base fluid (water) and (0.1% vol.) CuO/water and TiO₂/water nano-fluids were introduced into the FPSC. The results showed that the temperature difference at 1.5 Lpm flow rate for water, (CuO/water TiO₂/water nano-fluids were (6.6 °C) (7.1 °C) and (7.9 °C) respectively. This is due to the enhanced thermophysical properties of the nano-fluids compared to the water. On the other hand, the higher temperature difference for CuO/water nano-fluid in comparison with other fluids is attributed to higher thermal conductivity of CuO nano-particles.

Based on the above results, we decided to conduct a systematic study for evaluating the effects of nano-particles volume concentration (0.1%, 0.2%, and 0.3% of CuO and the flow rates (1, 1.5, and 3 Lpm) on the inlet-outlet temperature difference and the thermal efficiency of FPSC and the results were compared with those of the base fluid (water). The results of 0.2% and 0.3% CuO/water nano-fluid showed that increasing the fluid flow-rate results in a decrease in the inlet-outlet temperature difference. On the other hand, the effect of nano-particles volume concentration was evaluated and a comparison was carried out between water and (0.1%, 0.2%, and 0.3%)

of CuO/water nano-fluid. At a flow rate of 1.5 Lpm, the CuO/water nano-fluid with 0.3% by vol. gives the highest temperature difference of about 8.9 °C in comparison with 6.6, 7.9, and 8.4 °C for water, 0.1% and 0.2% by vol. CuO/water, respectively. Furthermore, the lowest flow rate (1 Lpm) of 0.3% vol. CuO/water nano-fluid provides the highest temperature difference (9.8 °C) compared to 8.9, 8.5, and 7.6 °C for 1.5, 2, and 3 Lpm, respectively.

The effect of the fluid type on thermal efficiency of FPSC was also investigated experimentally. It was found that at 1.5 Lpm, the 0.1 % by vol. CuO/water nano-fluid exhibited higher efficiency (54.3%) compared to 53.8% and 50% for 0.1 % by vol. TiO₂/water and the base fluid (water), respectively. Furthermore, the effect of fluid flow rate on the thermal efficiency of FPSC was also evaluated. At constant particles volume concentration, it was found that the FPSC efficiency increases slightly with increasing the flow rate from 1 to 3 Lpm. However, it was reported that at a very high flow rate, there is a decrease in the efficiency of the fluid due to the significant reduction in the temperature difference of the inlet and outlet fluid.

To evaluate the effect of the nano-particles on the FPSC efficiency, the CuO/water nano-fluids were prepared with 0.1, 0.2, and 0.3%. At 1.5 Lpm flow rate, the results showed that the efficiency was improved from 54.3% to 55.2% with an increase in the concentration from 0.1% to 0.2%, respectively. The maximum efficiency was reported to be 60% for 0.2% particle volume concentration of the CuO/water nano-fluid at a flow rate of 3 Lpm. In general, increasing the particle concentration of the nano-fluid leads to an increase in the efficiency due to the enhanced thermal conductivity of the nano-fluid that rises the convective heat transfer coefficient. However, it should be noted that as the particle concentration of the nanofluid increases from 0.2% to 0.3%, the efficiency approximately remains constant or reduces slightly. This indicates that increasing the particle volume concentration up to or more than 0.3% may results in a reduction in the efficiency due to the enhanced fluid viscosity that causes frictional dissipation and the possibility of nano-particles agglomeration.

5.2 Future Work

Based on the encouraging results of this work, it is necessary to conduct more in depth research work in order to have a full understanding of how to further enhancing

the thermal efficiency of the FPSC. It is believed that this goal can be achieved by conducting the following road map:

1. A wider range of the fluid flow rate and nano-particles volume concentration may be considered to conduct more in depth experimental investigation on their effects on the thermal efficiency of the FPSC.
2. Using a various type of the nano-particles to prepare the nano-fluids such as carbon nanotubes/water, Fe_2O_3 /water, SiO_2 /water, MgO /water, and ZnO /water nano-fluids. It is also possible to use the nano-composite nano-particles to prepare a special type of the nano-fluids.
3. Studying the effect of the tube arrangement of the FPSC on the thermal efficiency. Based on the literature, it should be noted that the suggested FPSC with spiral tube arrangement in this project showed approximately the same efficiency of the conventional FPSC.
4. Carrying out a numerical study to simulate the performance of the FPSC and comparing the simulated results with those obtained from this and other experimental research.

REFERENCESE

- 1- Z. Said., M. A. Sabiha., R. Saidur., A. Hepbasli., N. A. Rahim., S. Mekhilef, "*Performance enhancement of a Flat Plate Solar collector using Titanium dioxide nanofluid and Polyethylene Glycol Dispersant*", Journal of Cleaner Production, 92,(2015),pp.343-353.
- 2- <http://www.oecd.org>
- 3- Abbas S. Shareef, Mohammed H. Abood, and Sura Q. Kadhim, "*Experimental Investigation for Flow Rate Effect on a Flat Plate Solar Collector with the Using of Al₂O₃ Nanofluids as a Heat Transfer Fluid*", International Journal of Mechanical & Mechatronics Engineering (IJMME-IJENS), Vol. 16, No. 01, pp. 42-48, February 2016.
- 4- S. Arun Babu and M. Raja," *An experimental investigation on the effect of ZnO/water nanofluid on the efficiency of flat-plate solar collector*", Advances in Natural and Applied Sciences, 10 (7), pp. 40-48, June 2016.
- 5- Solar Energy Perspectives: Executive Summary (PDF), "*International Energy Agency*", 2011, Archived from the original (PDF) on 3 December 2011.
- 6- Energy, <http://www.rsc.org>.
- 7- <http://www.nepalb2b.com/blog/use-solar-energy>.
- 8- C. Marken (2009). "*Solar collectors: Behind the glass*" Home Power, 133, Pages 70–76.
- 9- Abhishek Verma. And Vishal Kumar, "*Solar water heating* ", International Journal of Research in Aeronautical and Mechanical Engineering, Vol.3, Issue 1,pp. 53-63, January 2015.
- 10- Wei Li. Tzameret H.Rubin. Onyina, Paul A,"*Comparing Solar Water Heater Popularization Policies in China Israel and Australia: The Roles of Governments in Adopting Green Innovations*", Published online in Wiley online Library.

- 11- <http://www.solar-energy-scene.com>
- 12- <http://www.daviddarling.info>
- 13- Hadi. R. Roomi, "*Natural convection from single finned tube immersed in a tilted enclosure*" Journal of Engineering, Vol. 13, No. 3, September 2006.
- 14- <http://www.alternative-energy>
- 15- Robert Taylor.Sylvain Coulombe. Todd Otanicar. Patrick Phelan. Andrey Gurawan,"*Small particles, big impacts: A review of the diverse applications of nanofluids*", Journal of Applied Physics 113, 011301, January (2013).
- 16- Stephan U.S. Choi and J. A. Eastman, "*Enhancing Thermal Conductivity of Fluids with Nanoparticles*", International Mechanical Engineering Congress and Exposition, conference, 951135-29, January 1995.
- 17- A. Bejan, A.D. Kraus, Heat Transfer Handbook, J. Wiley, Sons Inc, Hoboken, NJ, 2003.
- 18- Navid Bozorgan., Komalangan Krishakumar, Nariman Bozorgan "*Numerical Study on Application of CuO-Water Nanofluid in Automotive Diesel Engineering Radiator*" Scientific Research, Modern Mechanical Engineering, pp.130-136, November 2012.
- 19- Ravindra Kolhe, J. H. Bhangale, Tushar Thakare, "*An Experimental Investigation on the Effect of Al₂O₃-H₂O and CuO-H₂O Nanofluid on the Efficiency of Flat-plate Solar Collectors*", International Journal of Science, pp. 2319-7064, October 2013.
- 20- Hossein Chaji, Yahya Ajabshirchi, Esmaeil. Esmailzadeh, Saeid. Zeinali-Haris, Mahdi. Hedayatizadeh, Mostafa. Kahani, "*Experimental study on thermal efficiency of flat plate solar collector using TiO₂-Water nanofluid*", Modren. Applied. Science, Vol. 7, No. 10, September 2013.
- 21- Milad Tajik Jamal-Abad, A. Zamzamian, E. Imani, M. Mansouri, "*Experimental study of the performance of a flat-plate collector using Cu-water nanofluid*", Journal of Thermophysics and Heat Transfer, Vol. 27, pp. 756-760, 2013.
- 22- Ali Jabari Moghadam, Mahmood Farzane-Gord, Mahmood Sajadi, Monireh Hoseyn-Zadeh, "*Effects of CuO/water nanofluid on the efficiency of a flat-plate solar Collector*", Experimental Thermal and Fluid Science Vol.58, pp.9-14, June 2014.

- 23- Goudarzi K, Shojaeizadeh E, Nejati F. " *An experimental investigation on the simultaneous effect of CuO–H₂O nanofluid and receiver helical pipe on the thermal efficiency of a cylindrical solar collector* "Applied Thermal Engineering, July 2014.
- 24- Jee Joe Michael. And S. Iniyar "*performance of copper oxide / water nanofluid in a flat plate solar water heater under natural and forced circulation*", Energy conversion and management 95, pp. 160-169, February 2015.
- 25- Sujit Kumar Verma, Arun Kumar Tiwari, Durg Singh Chauhan, " *Experimental evaluation of flat plate solar collector using nanofluid*" s, Energy conversion and Management 134, pp.103-115, January 2017.
- 26- Rehena Nasrin, Salma Parvin and M.A Alim, "*Heat transfer by nanofluids through a flat solar collector*" Science Direct, Procedia Engineering 90, pp.364-370, 2014.
- 27- E. Ekramian, S.Gh. Etemad, M. Haghshenasfard, " *Numerical Investigations of Heat Transfer Performance of nanofluids in a Flat Plate Solar Collector*", International Journal of Theoretical and Applied Nanotechnology, Vol. 2, Journal ISSN:1929-1248, pp.30-39,2014.
- 28- Rehena Nasrin and M.A. Alim "*Thermal Performance of Nanofluid solar flat plate collector*", International Journal of Heat and Technology, Vol.33, No.2, pp. 17-24,2015.
- 29- Wail Sami Sarsam, S.N.Kazi, A.Badarudin, "*A review of studies on using nanofluid in flat plate solar collector* ", ScienceDirect, Solar Energy 122, pp. 1245-1265, October 2015.
- 30- Nang Khin Chaw Sint, I.A. Choudhury, H.H. Masjuki, H.Aoyama, "*Theoretical analysis to determine the efficiency of a CuO-water nanofluid based-flat plate solar water heating system in Myanmar* ", Solar Energy 155, pp. 608 -619, June 2017.
- 31- Maouassi A, Beghidja A, Zeraibi N, " *Numerical study of Nanofluid heat transfer Tio₂ through a Solar Flat Plate Collector*", Science Direct, Procedia Environmental Sciences 00(2017)000-000.
- 32- "*Solar Energy engineering, Academic Press is an imprint of Elsevier*" 30 Corporate Drive, Suite 400, Burlington, MA 01803, USA 525 B Street, Suite 1900, San Diego, California 92101-4495, USA84 Theobald's Road, London WC1X 8RR, UK.
- 33- "*Heat Transfer*" BOOK YUNUS A. CENGEL, SECOND EDITION.

- 34- B. C. Pak and Y.I Cho, "*Hydrodynamic and Heat Transfer Study of Dispersed fluids with submicron metallic oxide particles* ", Experimental Heat Transfer, Vol.11, No.2, 1998, pp.151-170.
- 35- Y. Xuan and W. Roetzel, "*Conception of heat transfer correlation of nanofluids*" International Journal of Heat and Mass Transfer, Vol. 43, No. 19, 2000, pp. 3701-3707.
- 36- D. A. Drew, S. L. Passman, Theory of multicomponent fluids, Springer, Berlin, (1999).
- 37- W. Yu, U.S. Choi, "*The role of interfacial layers in the enhanced thermal conductivity of nanofluids*", A renovated Maxwell model, Journal Nanoparticles Research 5 (2003), pp. 167-171.
- 38- Han Zenghu. "*Nanofluids with Enhanced Thermal Transport Properties*", Ph.D. thesis, University of Maryland, 2008.
- 39- Das. S. K. Choi. S.U.S., Yu, W., and Pradeep, T., "*NANOFLUIDS*": Science and Technology, John Wiley & sons, Inc., (2008).
- 40- Duanfei. Thermal property measurement of Al₂O₃-water nanofluids. chapter 15 in Smart Nanoparticles Technology "*book edited by Abbass Hashim* ", pp. 336-352, Intechopen, 2012.

APPEDIX

APPENDIX-A: The Data	70
APPENDIX-B: Nanografi Nano Techonogy	83



APPENDIX-A: The Data

Table A.1: The experimental results of the flat plate solar collector with working fluid (Water) (20– 6 – 2017)

Mass flow rate 1 Lpm

Time (minutes)	T-plate (1) [°c]	T-pipe (2) [°c]	T-space (3) [°c]	T-ambient (4) [°c]	T-glass (5) [°c]	T-in (6) [°c]	T-out (7) [°c]	$\Delta T = T7-T6$ [°c]	Solar Radiation [W/m^2]
10:00	73.5	56.7	64.6	36.7	57.2	37.8	41.3	3.5	688
10:05	75.8	57.9	65.7	38.5	57.4	43.7	47.6	3.9	697
10:10	75.9	58.5	65.2	38.8	57.5	50.4	55.6	5.2	714
10:15	74.5	59.4	65.1	39.5	57.4	51.5	56	4.5	720
10:20	74.8	60.4	65.8	39.3	57.2	52.5	57.3	4.8	734
10:25	75.6	61.6	66.3	39.5	57.4	53.5	58.7	5.2	740
10:30	76	62.5	67	39.3	57.3	54.4	59.8	5.4	750
10:35	76.7	63.4	67.8	39.4	58.5	55.4	60.9	5.5	756
10:40	77.2	64.1	68.4	39.5	58.7	56.6	62.7	6.1	769
10:45	77.3	64.3	68.7	39.5	58.7	56.8	63.2	6.4	775
10:50	76.9	65.1	68.8	39.6	57.9	57.6	64.3	6.7	767
10:55	76.7	65.3	69	39.6	58.1	58.5	65.5	7	773
11:00	78.4	66	69.5	39.7	59.3	59.1	66.2	7.1	785
11:05	78.7	66.8	70.3	39.8	59.9	59.6	66.7	7.1	790
11:10	78.9	67.2	71.1	39.9	59.6	60.4	67.6	7.2	798
11:15	79.3	68	71.8	39.9	59.4	60.9	68.2	7.3	787
11:20	79.5	68.4	72.1	39.2	59.8	59.6	66.2	6.6	776
11:25	79.5	68.6	71.7	39.5	59.3	58.9	65.2	6.3	771
11:30	79.8	68.7	72.4	39.9	60.5	58.5	64.4	5.9	788
11:35	80.2	69.2	71.6	39.8	60.7	58.3	64	5.7	783
11:40	79.7	69.4	71.9	38.6	60.7	58.2	63.6	5.4	802
11:45	79.2	69.9	72.7	41.7	60.4	58	63.3	5.3	790
11:50	79.1	70.6	71.9	39	59.5	57.7	63.4	5.7	784
11:55	78.8	70.4	72.1	40.7	60.1	57.3	62.4	5.1	773
12:00	78.4	69.9	72.6	39	59.5	57.1	61.9	4.8	768
12:05	78.6	71.2	70.3	39.6	59.4	56.7	61.2	4.5	775
12:10	78.3	72.4	71.5	39.7	58.8	56.5	60.8	4.3	761
12:15	78.4	69.5	72.9	40.9	59.8	56.3	60.5	4.2	754
12:20	77.3	69.5	72.9	39.7	59.5	56.1	60.2	4.1	745
12:25	76.4	69.7	71.7	39.8	59.2	55.8	59.7	3.9	740
12:30	76.9	70.1	71.3	41.7	58.6	55.2	58.9	3.7	768

Table A.2: The experimental results of the flat plate solar collector with working fluid (Water) (29– 5 – 2017)

Mass flow rate 1.5 Lpm

Time (minutes)	T-plate (1) [°c]	T-pipe (2) [°c]	T-space (3) [°c]	T-ambient (4) [°c]	T-glass (5) [°c]	T-in (6) [°c]	T-out (7) [°c]	$\Delta T = T7-T6$ [°c]	Solar Radiation [W/m^2]
10:00	72.8	52	62.5	39.8	53.9	43.5	47.3	3.8	680
10:05	72.6	52.1	62.3	40.3	54.9	43	47.5	4.5	685
10:10	72.5	52.1	62.2	40.5	55.2	44	48	4	699
10:15	72.6	53	62.1	40.1	55.6	43.5	48.2	4.7	717
10:20	72.7	53.6	62.4	40.3	55.3	43.3	48.1	4.8	731
10:25	73.2	54.3	62.5	40.2	55.9	44	48.9	4.9	774
10:30	73.7	54.9	63.2	40.5	55.3	44.1	48.4	4.3	755
10:35	74.2	55.7	63.7	42	57.2	45.6	50.6	5	753
10:40	74.7	56.2	64.5	40.4	56.8	46.2	51.8	5.6	764
10:45	74.9	56.4	64.3	40.4	56.8	46.6	52.1	5.5	760
10:50	75	56.6	64.5	40.5	56.7	46.3	52.3	6	762
10:55	75.1	56.7	64.7	39.8	56.2	46	52.1	6.1	764
11:00	76.5	58.9	66.5	40.8	60.4	48.1	54.3	6.2	773
11:05	76.8	59.5	66.8	41.4	60.1	49.2	55.1	5.9	769
11:10	77.1	59.3	66.8	41.2	67.5	51.3	56.9	5.6	740
11:15	77.2	59.5	66.9	42.8	67.7	51.9	57.7	5.8	772
11:20	77.4	59.9	67	43.1	67.7	51.9	57.9	6	776
11:25	77.4	60.2	67.1	41.3	67.8	51.2	57.3	6.1	778
11:30	77.4	60.4	67	41.8	67.8	51.3	57.7	6.4	780
11:35	77.6	60.7	67.3	42.5	68	51	57.6	6.6	788
11:40	77.6	61.2	67.7	41.9	68.5	52.1	58.2	6.1	778
11:45	77.7	62.1	66.3	42.7	66.6	51.9	58	6.1	773
11:50	78.2	62.8	65.1	43.3	64.2	51.8	57.9	6.4	570
11:55	78.5	63.8	66.3	42.2	64.7	52.8	58.9	6.1	800
12:00	78.5	63.8	64	41.8	62.4	55.4	60.1	4.7	779
12:05	78.2	63.8	64.9	43.2	60.5	55.7	61.3	5.6	774
12:10	77.7	63.7	64.8	43.2	60.8	54	59.7	5.7	769
12:15	77.7	63.8	62.2	42.7	60	53.2	59.1	5.9	813
12:20	77.4	64.1	62.1	43.1	60.9	54	59	5	762
12:25	77.6	62.1	62.3	43.7	61.1	53.9	58.8	4.9	755
12:30	76.9	64.4	61.9	45.5	61.3	53.2	57.9	4.7	890

Table A.3: The experimental results of the flat plate solar collector with working fluid (Water) (30– 5 – 2017)

Mass flow rate 2 Lpm

Time (minutes)	T-plate (1) [°c]	T-pipe (2) [°c]	T-space (3) [°c]	T-ambient (4) [°c]	T-glass (5) [°c]	T-in (6) [°c]	T-out (7) [°c]	$\Delta T = T7-T6$ [°c]	Solar Radiation [W/m^2]
10:00	74.6	51.7	63.7	37.9	58.2	41.9	44.8	2.9	710
10:05	73.4	52.1	62.7	38.1	57.9	42.9	46	3.1	727
10:10	73.5	53.3	62.5	38.1	56.7	43.7	46.7	3	736
10:15	73.5	53.8	62.5	40.3	56.6	44.5	47.7	3.2	753
10:20	73.5	54.2	62.5	38.3	57	45.3	48.5	3.2	758
10:25	73.7	54.9	62.4	40.2	56.9	46	49.7	3.7	759
10:30	73.7	55.7	62.5	38.2	56.1	46.1	50.2	4.1	750
10:35	74.3	56.4	63.2	38.2	56.7	46.5	50.5	4	782
10:40	74.7	57	63.8	38.6	57.1	47.2	51.5	4.3	791
10:45	75.1	57.5	64	38.4	57.1	48	52.5	4.5	789
10:50	75.4	58.2	64.3	38.9	55.5	48.3	53	4.7	800
10:55	75.6	58.6	64.6	38.5	56.3	50.1	54.8	4.7	710
11:00	75.9	59.1	65	38.5	55.8	50.2	55.1	4.9	796
11:05	75.8	59.6	65.3	39.3	56	50.3	55.3	5	827
11:10	76.7	62.5	66	39.7	56.3	50.4	55.5	5.1	830
11:15	77.2	60.6	66	39.7	55.7	51.8	56.8	5	744
11:20	76.8	60.7	66.3	40.1	57.3	52.4	57.5	5.1	843
11:25	76.9	61.1	66.9	39.9	57.8	52.9	58.1	5.2	870
11:30	76.8	61.3	67	40.9	58.2	53.3	57.6	4.3	820
11:35	77.1	61.3	67	42.8	58.7	53.8	58.3	4.5	848
11:40	76.7	61.4	66.9	42.6	58.7	54	58.7	4.7	843
11:45	76.7	61.8	66.6	43.9	59.3	54.4	59.3	4.9	859
11:50	77	62.6	67.4	43.7	59.7	54.6	59.6	5	863
11:55	77.1	63.4	67.7	42.3	59.2	54.9	59.4	4.5	853
12:00	77	63.6	67.8	42.9	58.7	55.5	59.8	4.3	490
12:05	76.9	63.9	68.2	43.6	59.1	55.8	60.3	4.5	829
12:10	76.6	64.1	67.6	43.4	59.1	56	60	4	832
12:15	76.4	64.8	68.1	43.2	58.8	56.5	60.8	4.3	701
12:20	76.4	64.7	68.3	41	59.1	56.9	61.5	4.6	810
12:25	76.2	64.7	68.3	41.7	59.3	57.3	61.8	4.5	804
12:30	76.1	64.8	68.1	42.2	59.2	57.6	62.2	4.6	796

Table A.4: The experimental results of the flat plate solar collector with working fluid (Water) (31– 5 – 2017)

Mass flow rate 3 Lpm

Time (minutes)	T-plate (1) [°C]	T-pipe (2) [°C]	T-space (3) [°C]	T-ambient (4) [°C]	T-glass (5) [°C]	T-in (6) [°C]	T-out (7) [°C]	$\Delta T = T7-T6$ [°C]	Solar Radiation [W/m^2]
10:00	69.3	51.7	60.1	33.2	52.1	39.2	41.3	2.1	755
10:05	68.2	48.7	58.2	35.4	52.3	40.3	42.5	2.2	752
10:10	67.7	49.1	57.3	34.8	51.1	40.9	43.7	2.8	776
10:15	67.6	49.6	56.8	34.8	51.2	41.5	44.9	3.4	781
10:20	67.9	50.2	57.5	34.1	51.1	42.1	44.8	2.7	780
10:25	68.1	50.9	57.4	35.7	51.7	42.8	45.9	3.1	776
10:30	68.5	51.4	57.6	35.6	51.5	43.3	45.8	2.5	790
10:35	68.7	51.9	57.7	35.9	51	43.8	46.8	3	618
10:40	69	52.5	58.4	35.2	52.2	44.4	47.9	3.5	782
10:45	69.3	53.1	58.7	36.1	52.8	45	47.5	2.5	808
10:50	70.1	53.8	59.4	35.4	52.3	45.1	48.2	3.1	741
10:55	70.2	54	59.4	35.4	52.7	46	49.7	3.7	749
11:00	70.5	54.6	59.5	35.7	52.4	46.6	49.3	3.3	808
11:05	70.8	55	59.7	36.3	53	47.1	50.9	3.8	825
11:10	71	55.3	60.1	36.3	53.2	47.3	51.3	4	779
11:15	71.4	55.6	60.5	35.9	53.2	47.9	50.7	2.8	814
11:20	71.2	55.9	60.9	37.9	53.3	48.4	51.2	2.8	760
11:25	70.9	56.1	61.2	37.3	53.8	48.7	51.5	2.8	855
11:30	71.3	57	62.8	37.9	53.7	50	53.3	3.3	850
11:35	71.5	57.2	63.6	37.8	53.2	50.2	53.8	3.6	728
11:40	71	57.2	63.8	38.7	53.2	50.1	53	2.9	846
11:45	70.6	57.7	63.5	39.6	52.7	50.2	53	2.8	835
11:50	70.7	58.4	63.9	38.3	53.3	50.7	54.1	3.4	828
11:55	70.6	58.3	64.2	39.1	53.6	51.4	54.3	2.9	900
12:00	70.6	58.2	64.6	38.4	53.1	51.6	54.5	2.9	826
12:05	70.3	58.2	64.7	38.7	53.2	51.8	54.8	3	821
12:10	69.8	58.1	64.6	38.5	52.8	52	55.3	3.3	920
12:15	69.8	58.7	64.8	39	52.7	52.2	55.7	3.5	828
12:20	69.2	58.8	64.8	39.7	53.3	52.5	55.9	3.4	807
12:25	69.1	59.3	65	37.1	52.3	52.9	56.4	3.5	821
12:30	68.6	59.2	65.3	38.3	53.4	53.2	56.7	3.5	903

Table A.5: The experimental results of the flat plate solar collector with working fluid (Nano-fluid CuO 0.1 % vol.) (4 – 6 – 2017)

Mass flow rate 1.5 Lpm

Time (minutes)	T-plate (1) [°c]	T-pipe (2) [°c]	T-space (3) [°c]	T-ambient (4) [°c]	T-glass (5) [°c]	T-in (6) [°c]	T-out (7) [°c]	$\Delta T = T7-T6$ [°c]	Solar Radiation [W/m^2]
10:00	68	37.9	60	31.4	50.4	32.2	37.1	4.9	710
10:05	68.8	44.8	60.1	36.3	55.4	33.7	37.2	3.5	725
10:10	68.7	45	60.3	36.3	55.5	33.8	37.7	3.9	736
10:15	68.9	45.8	59.9	37.1	54.3	34.1	38.9	4.8	755
10:20	68.5	46.4	59.8	37.3	53.4	34.5	39.5	5	759
10:25	68.9	46.8	59.6	36.8	52.9	34.9	41	6.1	758
10:30	69.4	47.4	59.7	37.2	52	35.1	41.6	6.5	761
10:35	69.6	47.5	60.1	37	51.2	35.9	42.7	6.8	781
10:40	69.8	47.9	60.7	37.6	52.3	36.9	44	7.1	805
10:45	69.9	48.3	61.1	38	53.6	38.1	45.4	7.3	803
10:50	70	50.1	61.5	37.4	53.6	38.9	46.2	7.3	622
10:55	70	52.7	62.4	37.8	54.5	39.5	47.1	7.6	818
11:00	71.3	53.3	63.8	38.1	53.5	39.9	47.6	7.7	819
11:05	70.5	53.8	63.1	38.2	53	41.3	49.1	7.8	825
11:10	70.8	54.4	63.3	38.5	52.2	41.8	49.6	7.8	816
11:15	70.9	54.1	63.6	38.2	52.8	42.3	50.2	7.9	811
11:20	71.3	54.5	64.4	37.2	52.8	42.5	50	7.5	813
11:25	71.1	54.8	64.3	38.3	53.3	43.1	5.4	7.3	819
11:30	71	55	64.7	37.9	54.2	42.8	50	7.2	699
11:35	71	55.1	64.7	39.1	53.8	42.9	49.9	7	711
11:40	71.7	55.3	65.1	40.4	54.4	42.4	48.9	6.5	790
11:45	71.3	55.3	64.6	38.9	49.2	41.8	48.1	6.3	722
11:50	71.7	55.4	65.3	39.7	51.7	41.2	48.3	6.1	815
11:55	72.1	55.7	64.7	42.8	51.4	40.7	46.2	5.5	799
12:00	72.6	55.9	65.6	41.3	53.7	40.2	45.4	5.2	804
12:05	71.8	56	66	40.9	54.7	39.8	44.9	5.1	790
12:10	71.8	56.1	66.6	39.6	54.9	39.2	44.3	5.1	781
12:15	70.9	56.3	65.8	40.4	54.3	39.3	44.3	5	709
12:20	70.7	56.2	65.7	39.5	53.4	39.8	44.7	4.9	772
12:25	69.9	56.3	66.1	40.1	52.5	38	42.8	4.8	887
12:30	70.7	56.7	66	39.4	54.7	38.6	43.4	4.8	890

Table A.6: The experimental results of the flat plate solar collector with working fluid (Nano-fluid TiO₂ 0.1 % vol.) (8 – 6 – 2017)

Mass flow rate 1.5 Lpm

Time (minutes)	T-plate (1) [°c]	T-pipe (2) [°c]	T-space (3) [°c]	T-ambient (4) [°c]	T-glass (5) [°c]	T-in (6) [°c]	T-out (7) [°c]	$\Delta T = T7-T6$ [°c]	Solar Radiation [W/m^2]
10:00	72.5	51.1	63.6	37.2	56.2	39.2	42.3	3.1	693
10:05	71.2	50.6	62.7	38.8	55.7	42.4	44.4	2.9	715
10:10	71.4	52.5	63.1	38.2	54.6	42.5	46.1	3.6	738
10:15	71.4	53.5	62.7	37.3	54.4	43.4	48.1	4.7	759
10:20	71.5	54.1	62.7	37.6	54	43.9	48.8	4.9	750
10:25	71.9	55.2	63.1	39.7	54.6	44.4	49.9	5.5	730
10:30	72.4	55.5	64	38.9	55.4	45.2	51.1	5.9	770
10:35	72.7	56.1	64.3	38.1	55.3	45.9	52	6.1	782
10:40	73.5	58.6	65.3	37.9	54.4	46.1	52.5	6.4	786
10:45	73.8	57.3	65.6	39.3	56.4	47.1	53.6	6.5	803
10:50	74.3	58	66.1	38.8	56.9	48	54.7	6.7	817
10:55	75.2	61.2	67.3	39.5	57	47.9	54.8	6.9	810
11:00	76.3	60.7	68.3	40	57.3	48.5	55.4	6.9	825
11:05	75.7	59.7	68.3	39.9	57.7	49.4	56.4	7	800
11:10	75.8	62.2	68.2	41.2	57.5	50.1	57.2	7.1	788
11:15	76	61.5	68.8	41.5	57.6	50.3	56.8	6.5	818
11:20	76.4	61.2	69.1	40.7	58.9	50.4	56.1	6.1	842
11:25	76.7	62.2	69.8	39.9	58.6	50.6	55.8	5.2	835
11:30	76	61.2	69.3	41.1	57.7	50.1	55	4.9	829
11:35	75.8	61.4	69.2	41.3	57.3	49.9	54.5	4.6	876
11:40	75.7	62.7	69.4	42	57.2	49.6	54.1	4.5	821
11:45	76.9	63.6	70.7	42.7	58.3	49.1	53.4	4.3	830
11:50	76.4	64.2	70.3	40.4	58.9	49	53.1	4.1	889
11:55	76.8	64.1	71.3	40.7	60	48.5	52.5	4	818
12:00	76.9	64.1	71.7	40.3	59.1	48.3	52.2	3.9	678
12:05	77.1	64.4	70.9	40.9	58.5	48.1	51.9	3.8	790
12:10	77.3	64.9	70.8	44	58.8	47.8	51.3	3.5	745
12:15	76.6	64.4	71.4	43.7	59.3	47.3	50.7	3.4	801
12:20	76.2	64.7	72	42.2	59.6	47.1	50.3	3.2	855
12:25	76.5	64.9	72.3	42.3	59.9	46.8	49.9	3.1	799
12:30	76.5	65.1	71.6	42.2	56.2	46.7	49.7	3	776

Table A.7: The experimental results of the flat plate solar collector with working fluid (Nano-fluid CuO 0.2 % vol.) (11 – 6 – 2017)

Mass flow rate 1.5 Lpm

Time (minutes)	T-plate (1) [°C]	T-pipe (2) [°C]	T-space (3) [°C]	T-ambient (4) [°C]	T-glass (5) [°C]	T-in (6) [°C]	T-out (7) [°C]	$\Delta T = T7-T6$ [°C]	Solar Radiation [W/m^2]
10:00	71.3	74	69.4	36.9	55	41.5	45.8	4.3	712
10:05	71.5	54.9	64.9	37.6	54.4	46.5	50.4	3.9	749
10:10	72.3	56.5	63.3	36.9	51.8	47.9	51.1	3.2	759
10:15	72.2	57.1	63.1	37.7	53.4	49.6	53.7	4.1	770
10:20	72.6	58.8	63.4	37.5	53.7	50.2	55	4.8	750
10:25	73.1	59	64.3	39	53.5	51.2	56.3	5.1	771
10:30	73.2	59.8	64.1	37.2	53.6	52	57.4	5.4	784
10:35	73.5	60.5	64.6	38.6	53.8	52.9	58.5	5.6	790
10:40	74.6	62.2	65.7	38.8	54.6	53.6	59.5	5.9	798
10:45	75	62.1	66.5	38.3	55.4	54.6	60.8	6.2	804
10:50	75.7	63.6	67.2	38.3	55.7	55	61.8	6.8	822
10:55	75.9	63.5	67.7	39.6	55.6	55.8	63	7.2	819
11:00	76.8	65.3	68.1	38.2	55.7	55.9	63.4	7.5	810
11:05	77.7	68	69.4	38.9	56	56.2	63.7	7.9	820
11:10	77.4	65.4	69.7	39.5	57.5	57.4	65.5	8.2	830
11:15	77.5	66.1	70.2	38.1	54.7	58.2	66.6	8.4	825
11:20	77.8	66.5	69.6	40.1	56.2	58.1	66.1	8	831
11:25	77.9	66.5	70.4	39.2	57	58	65.8	7.8	835
11:30	78.1	68.5	70.9	38.5	57.3	57.9	65.4	7.5	812
11:35	77.5	67.2	70.8	39.6	55.2	56.3	63.6	7.3	824
11:40	77.2	68.1	71.4	39.2	56.7	56.1	63	6.9	840
11:45	77.1	67.1	71.6	39.2	57.4	55.6	62.3	6.7	812
11:50	77.8	69.4	72.2	39.1	57.5	55.3	61.8	6.5	799
11:55	78.5	68.2	71.8	38.8	57.2	55.1	61.5	6.4	811
12:00	78.2	69.8	72.9	39.3	58.9	54.8	61.1	6.3	801
12:05	77.4	68.2	72.3	40.1	57.7	54.5	59.9	5.4	809
12:10	76.5	69.8	72.5	39.3	56.7	54.3	59.6	5.3	826
12:15	75.5	67.9	71.9	41	56.5	52.9	58	5.1	820
12:20	74.8	68.8	71.7	40.1	56.2	52.5	57.9	5.1	809
12:25	76	69.7	71.8	42.8	56.2	52.3	57.3	5	800
12:30	76.1	69.4	71.2	41.7	50.3	52.1	57	4.9	790

Table A.8: The experimental results of the flat plate solar collector with working fluid (Nano-fluid CuO 0.2 % vol.) (12 – 6 – 2017)

Mass flow rate 2 Lpm

Time (minutes)	T-plate (1) [°C]	T-pipe (2) [°C]	T-space (3) [°C]	T-ambient (4) [°C]	T-glass (5) [°C]	T-in (6) [°C]	T-out (7) [°C]	$\Delta T = T7-T6$ [°C]	Solar Radiation [W/m^2]
10:00	71.4	59.7	63.6	38.6	53.9	39.8	44.4	4.6	698
10:05	72.6	57	62.8	38.9	54.2	48.7	52.6	3.9	737
10:10	72.6	57.8	63.3	39.2	54.3	49.5	52.7	3.2	729
10:15	72.7	58.6	63.3	39.5	54.7	50.4	53.5	3.1	751
10:20	73.3	57.2	64.2	39.7	54.9	51.4	55.1	3.7	760
10:25	73.6	56.5	64.9	40.8	54.9	52.1	56.3	4.2	772
10:30	73.9	55.3	65.4	40.2	55.2	52.5	57.2	4.7	770
10:35	74.2	57.5	66.3	40.3	55.7	53.2	58.1	4.9	796
10:40	74.7	57.9	67	40.9	56.4	54.6	59.2	4.6	801
10:45	74.8	58.7	67.3	41.3	56.9	55.4	60.7	5.3	800
10:50	74.9	59.4	68.3	41.5	57.7	55.5	61.3	5.8	807
10:55	75.1	60.3	68.8	41.7	57.9	56.4	62.5	6.1	804
11:00	75.3	64.9	69.5	41.9	58.2	56.8	63.3	6.5	810
11:05	75.3	67.8	70.1	42.4	58.4	57.3	64.2	6.9	807
11:10	75.9	67.2	70.9	42.7	58.7	57.9	65.4	7.5	799
11:15	76.4	65.9	70.6	42.8	58.9	57.3	64.5	7.2	819
11:20	76.8	67	71.5	42.9	59.1	57	63.9	6.9	825
11:25	76.9	66.8	71.1	43.1	59.4	56.7	63.1	6.4	812
11:30	77.3	66.5	71.1	43.3	59.9	56.5	62.6	6.1	820
11:35	77.5	68.9	71.5	43.3	58.1	56.1	62	5.9	818
11:40	77.7	67.4	72	43.2	58.5	55.9	61.6	5.7	795
11:45	77.8	68.8	72.4	43.5	58.7	55.6	60.9	5.3	816
11:50	78.3	68.7	72.1	43.4	58.1	55.4	60.4	5	669
11:55	78.5	67.4	71.8	43.6	58	54.2	57.1	4.9	803
12:00	78.2	68.1	71.4	43.6	57.8	54.1	58.6	4.5	798
12:05	78.4	67.8	71.7	43.4	58.6	53.6	57.8	4.2	790
12:10	78.6	67.4	71.9	43.6	59	53.3	57.2	3.9	782
12:15	78.9	69.7	72.6	43.7	57.9	53.1	56.8	3.7	787
12:20	79.5	68.5	71.3	43.6	57	53.1	56.7	3.6	708
12:25	79.8	70.2	72.1	43.8	56.7	52.9	56.1	3.2	781
12:30	79.9	68.7	71.3	43.8	56.5	52.7	55.8	3.1	769

Table A.9: The experimental results of the flat plate solar collector with working fluid (Nano-fluid CuO 0.2 % vol.) (13 – 6 – 2017)

Mass flow rate 3 Lpm

Time (minutes)	T-plate (1) [°c]	T-pipe (2) [°c]	T-space (3) [°c]	T-ambient (4) [°c]	T-glass (5) [°c]	T-in (6) [°c]	T-out (7) [°c]	$\Delta T = T7-T6$ [°c]	Solar Radiation [W/m^2]
10:00	83.9	81.8	75	39.6	60.6	43.5	47.4	3.9	681
10:05	83.3	80.7	69	39.9	59.1	49	52.5	3.5	692
10:10	76.7	73	67.7	41	58.4	53.4	56.6	3.2	726
10:15	75.7	65.9	67	40	57.4	54.6	58.9	4.3	745
10:20	75.6	60.6	67	40.2	56.2	54.8	59.4	4.6	761
10:25	76.1	61.8	67.7	39.9	55.2	55.6	60.3	4.7	750
10:30	75.7	62.2	67.3	40	56.1	55.8	60.7	4.9	742
10:35	76.1	62.9	67.8	40.8	57.4	56.4	61.4	5	755
10:40	76.8	63.8	68.4	41.6	57.6	57.6	62.8	5.2	760
10:45	77.3	64.6	69.1	42.2	58	57.9	63.3	5.4	765
10:50	77.4	65.4	69.4	40.8	55.6	58.1	63.8	5.7	757
10:55	77.6	65.6	70.2	40.8	57.9	58.4	64.1	5.7	771
11:00	77.8	65.4	70.7	41.8	59.1	58.6	64.5	5.9	759
11:05	78.3	67.1	71.2	40.9	58.3	58.9	65	6.1	775
11:10	79.5	69	71.9	42.3	59.8	59.1	65.3	6.2	771
11:15	79.1	67.8	72	42.1	60.3	59.2	65.4	6.2	763
11:20	79.1	68.1	71.9	41.4	59.5	60.8	67.1	6.3	779
11:25	79.1	68.8	71.9	40.9	59.6	59.5	65.6	6.1	785
11:30	78.8	68.5	72.3	42.6	60.2	59.1	65.1	6	703
11:35	78.9	68.8	72.8	43.5	60.2	58.8	64.6	5.8	785
11:40	79.2	69.9	73.3	42.7	60.6	58.4	64	5.6	769
11:45	78.9	69.4	73.2	41.7	60.8	58.1	63.5	5.4	790
11:50	79	70.4	73.4	41.2	59.3	57.9	63.1	5.2	802
11:55	78.7	69.9	73.3	41.3	59.7	57.5	62.5	5	784
12:00	78.2	69.5	73.1	42.6	60.1	57.2	61.8	4.6	760
12:05	78.5	69.9	73.5	41.2	60.9	57.1	61.4	4.3	734
12:10	78.2	69.9	73.8	41.8	60.9	56.8	60.9	4.1	769
12:15	78	70	74	42.9	61.1	56.5	60.3	3.8	789
12:20	78.1	70.9	74.4	44.3	61	56.3	59.9	3.6	760
12:25	78.2	71.2	74.1	43.1	61.1	56.2	59.6	3.4	779
12:30	77.8	70.4	74.3	42.6	61.1	56	59.3	3.3	790

Table A.10: The experimental results of the flat plate solar collector with working fluid (Nano-fluid CuO 0.3 % vol.) (14 – 6 – 2017)

Mass flow rate 1 Lpm

Time (minutes)	T-plate (1) [°c]	T-pipe (2) [°c]	T-space (3) [°c]	T-ambient (4) [°c]	T-glass (5) [°c]	T-in (6) [°c]	T-out (7) [°c]	$\Delta T = T7-T6$ [°c]	Solar Radiation [W/m^2]
10:00	76	73.1	66.4	39.7	60.1	41.7	45.8	4.1	680
10:05	76	71.9	66.5	40.4	59.1	47.7	51.4	3.7	695
10:10	75.6	63.8	66.4	39.5	58.6	50.5	53.6	3.1	703
10:15	75.6	60.9	66.2	40	58.4	51.8	56.4	4.6	713
10:20	76.5	62.2	67.6	40.9	58.8	52.9	58.2	5.3	722
10:25	77.1	63.5	68.3	40.1	59.5	53.6	59.5	5.9	729
10:30	77.8	64.5	69.4	39.9	59.7	54.7	61	6.3	730
10:35	78.3	65.3	69.8	42.4	60.3	55.4	62.3	6.9	739
10:40	78.6	64.8	70.5	42.8	60.7	57.1	64.6	7.5	743
10:45	79	66.2	70.8	41	60.5	57.7	65.5	7.8	750
10:50	79.5	66.8	71.3	42.4	60.9	58.7	66.8	8.1	768
10:55	80.1	67.9	72.3	42.6	61.1	59.4	68.3	8.9	760
11:00	80.8	68.9	72.7	42.4	61.4	60.1	69.6	9.5	778
11:05	81.6	69.6	73.7	42.2	62.3	60.8	70.6	9.8	785
11:10	82.3	70.3	74.1	43.1	63.3	60.7	70	9.3	773
11:15	82.4	71.3	74.9	43.5	62.7	60.5	69.6	9.1	780
11:20	82.6	71.8	75.3	42.5	63.2	60.1	68.9	8.8	783
11:25	82.8	72.6	75.6	41.8	62.8	59.5	67.8	8.3	790
11:30	82.4	71.2	75.2	43.5	62.9	59.2	67.1	7.9	788
11:35	82.7	71.7	75.3	43.7	62.8	58.7	66.3	7.6	792
11:40	82.8	71.9	75.7	44.1	63.8	58.3	65.5	7.2	785
11:45	82.2	72.4	75.6	43	63.2	58.1	64.9	6.8	795
11:50	83.2	75.2	76.7	43.3	63.9	57.5	63.8	6.3	782
11:55	83.2	73.4	77.1	43.3	64.6	57.3	63.4	6.1	800
12:00	82	73	76.5	44	64.3	57	62.9	5.9	780
12:05	81.4	72.9	76.2	43.8	63.9	56.8	62.2	5.4	773
12:10	82.1	73.1	76.2	43	63.3	56.5	61.7	5.2	788
12:15	81.3	73.8	76.3	43.5	63.4	56.4	61.3	4.9	769
12:20	81	73.8	75.9	43.6	63.2	56.1	60.8	4.7	752
12:25	80.8	73.5	76	43.1	63.6	55.7	60.4	4.7	749
12:30	81.3	73.6	76.1	44.3	63.5	55.6	60.1	4.5	738

Table A.11: The experimental results of the flat plate solar collector with working fluid (Nano-fluid CuO 0.3 % vol.) (15 – 6 – 2017)

Mass flow rate 1.5 Lpm

Time (minutes)	T-plate (1) [°C]	T-pipe (2) [°C]	T-space (3) [°C]	T-ambient (4) [°C]	T-glass (5) [°C]	T-in (6) [°C]	T-out (7) [°C]	$\Delta T = T7-T6$ [°C]	Solar Radiation [W/m^2]
10:00	78.3	55.2	62.1	39.5	52.4	39.2	43.1	3.9	669
10:05	77.8	55.9	62.4	39.9	52.9	43.3	46.5	3.2	684
10:10	80.3	56.8	61.8	39.2	52.1	44.9	47.8	2.9	702
10:15	77.9	56.9	60.6	40.3	51.5	46.5	50.7	4.2	700
10:20	73	57.2	60.9	40.2	51.8	48	52.9	4.9	710
10:25	70.3	57.5	61.4	40.1	51.8	48.7	54	5.3	721
10:30	70.7	58.1	62.3	40.5	50.8	49.4	55.3	5.9	741
10:35	71	58.7	62.4	41.1	51.9	50.3	56.5	6.2	731
10:40	71.4	59.7	62.7	40.3	51.5	51	57.8	6.8	752
10:45	72.1	60.3	63.6	40.3	52.7	51.7	58.9	7.2	763
10:50	72.7	61.3	64.5	40.2	53.2	52.2	60.1	7.9	770
10:55	73.3	61.7	65.4	40.2	53.9	52.7	61	8.3	756
11:00	73.6	61.9	66	41.3	53.9	53.4	61.9	8.5	771
11:05	73.7	63.7	66.3	40.4	54	52.6	61.3	8.7	754
11:10	74.1	62	66.7	40.7	54.2	54.2	63	8.8	760
11:15	73.8	62.6	66.5	41	54.1	54.9	63.8	8.9	768
11:20	74.1	63.2	66.7	41.5	54.3	54.5	63.1	8.6	790
11:25	74.6	64.4	67.5	41.8	55.3	54.1	62.2	8.1	782
11:30	75.3	64.8	68.1	41.9	55.9	54	61.8	7.8	778
11:35	75.4	65	68.6	42	56.2	53.7	61.2	7.5	770
11:40	75.4	65.4	68.5	41.9	56	53.5	60.8	7.3	751
11:45	75.5	66.4	68.6	42.3	56.6	53.2	60.3	7.1	767
11:50	74.9	65.5	68.7	42.1	55.6	52.9	59.7	6.8	779
11:55	74.8	65.6	69	42.1	56.1	52.7	59.2	6.5	755
12:00	75.1	66.3	69.6	42.2	55.5	52.4	58.7	6.3	760
12:05	74.8	66.2	69.5	42.3	56.2	52.1	58.2	6.1	747
12:10	74.3	66.4	69.5	42	55.8	51.9	57.2	6	739
12:15	74.3	66.7	69.3	42.6	55	51.7	57.6	5.9	722
12:20	74.6	66.1	69.5	42.5	56	51.5	57.2	5.7	712
12:25	73.8	66.6	69.4	42.5	56.3	51.3	56.6	5.3	699
12:30	73.8	66.5	68	42.4	54.6	51.3	56.4	5.1	710

Table A.12: The experimental results of the flat plate solar collector with working fluid (Nano-fluid CuO 0.3 % vol.) (18 – 6 – 2017)

Mass flow rate 2 Lpm

Time (minutes)	T-plate (1) [°C]	T-pipe (2) [°C]	T-space (3) [°C]	T-ambient (4) [°C]	T-glass (5) [°C]	T-in (6) [°C]	T-out (7) [°C]	$\Delta T = T7-T6$ [°C]	Solar Radiation [W/m^2]
10:00	76.8	65.2	64.4	39	53.7	38.2	42.3	4.1	655
10:05	75.2	63.6	65.8	38.7	54.6	47.9	51.5	3.6	665
10:10	73.4	57.1	65	39.6	55.6	49.5	52.7	3.2	680
10:15	72.9	58.5	65.3	39.4	56.3	50.6	55.3	4.7	701
10:20	73.2	59.5	65.6	39.7	56.2	51.6	56.9	5.3	711
10:25	73.7	60.5	66	39.7	56.9	52.6	58.5	5.9	725
10:30	74.3	61.3	66.4	41.3	56.9	53.5	59.7	6.2	741
10:35	74.8	62	66.9	41.3	57.7	54.4	61.2	6.8	745
10:40	75.4	63.1	67.7	41.4	58.1	55.3	62.4	7.1	728
10:45	76	64.1	68.2	41.4	58.5	56	63.5	7.5	750
10:50	76.5	64.7	68.8	42.1	58.5	56.8	64.7	7.9	760
10:55	76.9	65.3	69.3	42.2	58.7	57.7	65.9	8.2	778
11:00	77.1	65.8	69.8	42.4	58.9	58.3	61.8	8.5	755
11:05	77.1	66.3	70.1	42.5	59	58.1	66.4	8.3	781
11:10	77.6	67.6	70.8	42.9	58.9	57.8	66	8.2	759
11:15	77.8	67.3	70.9	42.9	59.3	57.5	65.5	8	765
11:20	76.4	67.5	71.9	43.1	60.1	57.2	64.8	7.6	748
11:25	76.6	67.8	72	43.2	60.2	57.1	64.4	7.3	769
11:30	78.3	68.2	72.4	43.2	60.5	56.8	63.9	7.1	751
11:35	78.7	68.5	72.8	43.6	60.9	56.5	63.4	6.9	782
11:40	78.9	68.9	73.1	43.7	60.6	56.3	62.9	6.6	772
11:45	79.1	69.1	73.6	43.7	61.4	56.1	62.3	6.2	799
11:50	78.8	68.7	73.3	41.9	61.2	55.7	61.8	6.1	763
11:55	78.4	68.3	73.6	42.3	61.8	55.4	61.2	5.8	749
12:00	78.7	68.4	73.9	42.2	61.7	55.2	60.8	5.6	744
12:05	78.8	69.7	73.7	42.3	61.4	54.7	60	5.3	738
12:10	78.9	71.2	74	41.2	62.3	54.5	59.6	5.1	729
12:15	79.3	71.5	74	41.8	62	54.3	59.2	4.9	704
12:20	79.9	71	74.6	40.7	62.4	54.2	58.9	4.7	719
12:25	78.5	71.2	74.8	42.7	62.3	53.9	58.4	4.5	710
12:30	78.9	71.1	74.1	41.3	61.9	53.7	57.9	4.2	722

Table A.13: The experimental results of the flat plate solar collector with working fluid (Nano-fluid CuO 0.3 % vol.) (19 – 6 – 2017)

Mass flow rate 3 Lpm

Time (minutes)	T-plate (1) [°C]	T-pipe (2) [°C]	T-space (3) [°C]	T-ambient (4) [°C]	T-glass (5) [°C]	T-in (6) [°C]	T-out (7) [°C]	$\Delta T = T7-T6$ [°C]	Solar Radiation [W/m^2]
10:00	72.3	58.9	67.3	39.2	55.8	45.3	49.1	3.8	713
10:05	74.9	59.5	67.7	38.9	56.9	50.5	53.9	3.4	725
10:10	75.5	60.5	66.3	38.9	57.3	51.8	54.7	2.9	730
10:15	75.9	61.4	65.7	38.8	57.5	52.5	57.1	4.6	750
10:20	76.2	62	65.6	38.7	58.1	53.3	58.5	5.2	761
10:25	76.5	62.8	66.2	38.9	58.4	54.1	59.8	5.7	755
10:30	76.8	62.9	66	40.1	58.9	54.9	60.8	5.9	770
10:35	75.2	63.3	66.7	42.5	58.8	55.8	62.1	6.3	760
10:40	72.9	64.6	68.1	40.3	57.4	56.5	63	6.5	790
10:45	77.7	65.5	68.9	39.7	56.4	57.3	64	6.7	806
10:50	75.7	65.9	69	42.7	58.2	58.1	65.3	7.2	810
10:55	78.5	66.7	70.1	40.4	58.6	58.8	66.2	7.4	820
11:00	79.5	67.7	71	40.5	58.4	59.4	66.9	7.5	822
11:05	79.4	68.2	71.7	40.6	58.3	59.9	67.5	7.6	819
11:10	79.4	68.5	71.3	40.5	58.4	59.5	66.9	7.4	830
11:15	79.5	69	72.1	39.6	57.6	59.1	66.2	7.1	821
11:20	79.4	69.5	72.2	40.7	58.4	58.7	65.6	6.9	827
11:25	79.2	68.7	72.5	40.4	58.5	58.5	65.1	6.6	816
11:30	78.9	68.5	72.9	40.7	58.6	58.4	64.7	6.3	810
11:35	79.6	69.4	72.1	40.4	58.5	58.2	64.3	6.1	802
11:40	79.1	69.5	72.4	41.4	59.4	58	63.8	5.8	798
11:45	78.8	70.2	71.7	42	59.9	57.9	63.5	5.6	790
11:50	78.5	70.5	71.9	39.6	57.4	57.6	62.9	5.3	795
11:55	77.8	70.6	72.2	40	55.2	57.3	62.5	5.2	789
12:00	77.2	71.1	71.6	39.4	55.3	57.1	62.3	5.2	799
12:05	76.1	71.4	71.5	41	56.5	56.8	61.8	5	785
12:10	75.7	71.7	72.5	41	57.4	56.6	61.4	4.8	780
12:15	75.5	71.9	71.7	40.4	56.7	56.4	60.9	4.5	775
12:20	75.2	69.2	72.1	41	55.9	56.3	60.7	4.4	769
12:25	74.8	69.9	71.3	40	56.5	55.9	60.2	4.3	760
12:30	74.6	70.8	71.8	39.9	56.6	55.7	59.8	4.1	755

APPENDIX-B: Nanografi Nano Techonogy



Nanografi Nano Technology

Copper Oxide (CuO) Nanopowder CuO, 99.9%, 20-60 nm

Technical Properties:

Purity % : 99.9+

Color : black

AVERAGE PARTICLE SIZE (nm): 20-60 nm

SPECIFIC SURFACE AREA (m²/g): 35

Bulk Density (g/cm³) : 0.8

True Density (g/cm³) : 6.5

Elemental Analysis:

Fe : 0.008

Ca: 0.003

Mn: 0.003

Mg : 0.007

Co: 0.006

Applications:

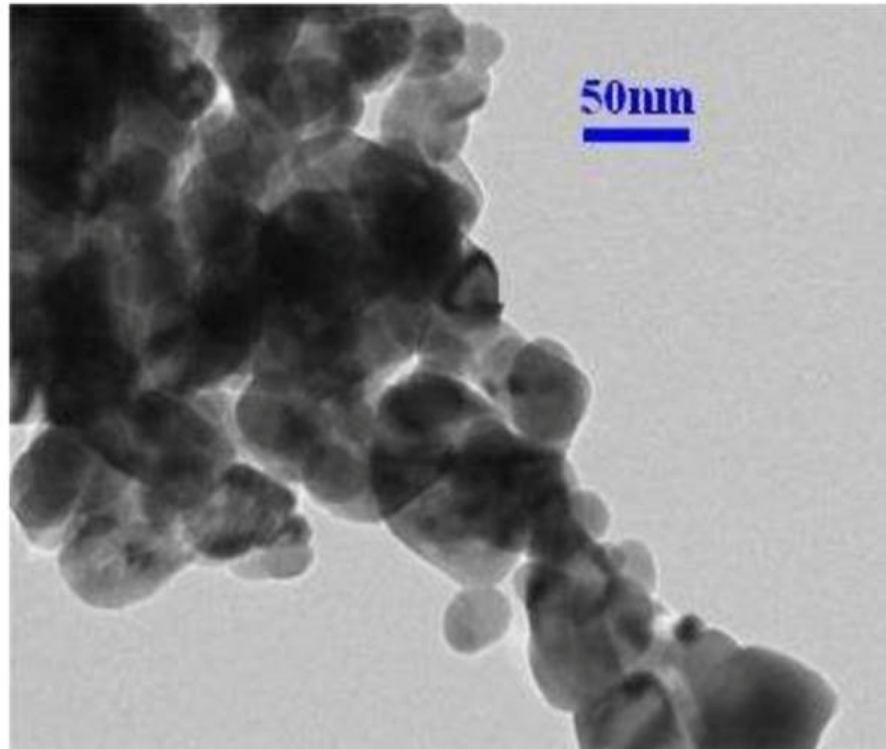
Copper Oxide nanoparticles has wide applications in different materials. It is applied to thermoelectric materials, superconducting materials, sensing materials, catalysts, ceramics, and glass. For example it is applied in the folloeing: near infrared tilters, magnetic storage devices, semicundoctors, gas sensors, photoconductors and photothermal applications, and solar energy transformation. In catalysis, it is used as rocket propellant combustion catalyst. It segnificantly can improve the homogeneous propellant burning rate and lower pressure index.

info@nanografi.com

PROPERTIES OF NANO-FLUIDS



Nanografi Nano Technology



nanografi

info@nanografi.com

**Titanium Oxide Nanopowder TiO₂, rutile, high purity,
99.9+%, 20 -60 nm**

Technical Properties:

Purity % : 99.9+

Color : White

AVERAGE PARTICLE SIZE (nm): 20-60 nm

SPECIFIC SURFACE AREA (m²/g): 50

Bulk Density (g/cm³) : 0.3

True Density (g/cm³) : 4.5

Morphology : nearly spherical

Elemental Analysis:

Al : 0.003

Ca: 0.005

Si: 0.003

S : 0.005

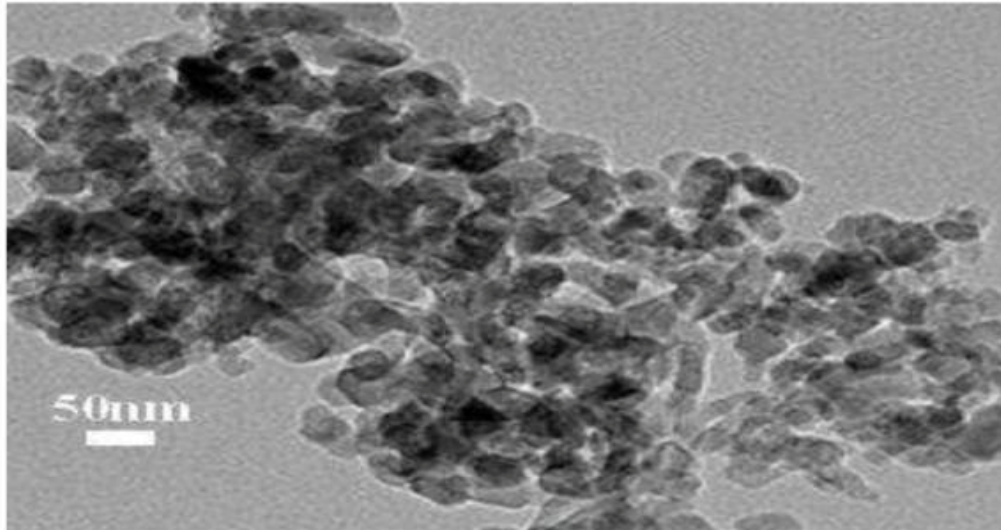
Mg : 0.01

W: 0.01

Applications:

Titanium oxide nanoparticles has wide applications in chemical industry. It is used in products such as cosmetics, beauty and whitening cream, vanishing cream, skin protecting cream, natural white moisture protection cream, powder make-up, and other cosmetic cream products. It has applications in

coatings such as coating for plastics, foods packing material, and in printing inks. It has also applications in photocatalysts, UV-resistant material, antibacterial materials, sewage treatment, and self-cleaning glass and ceramics. Titanium oxide nanoparticles is used in metallurgical, paper, and astronautics industry. It is used for improving the impressionability and opacity of papers, and in producing titanium, ferrotitanium alloy, carbide alloys.



nanografi

CURRICULUM VITAE

PERSONAL INFORMATION

Name, Surname : Hassn Jalel
Nationality : Iraqi
Date and Place of Birth : 10 June 1983, Iraq- Baghdad
Marital Status : Married
Phone : +90 539 791 78 95
Email : hassndams@gmail.com



EDUCATION

High School : AL-Markazya Secondary School, 2000 / 2001.
Undergraduate : AL-Mustansiriya University College of Engineering/
Mechanical Department, 2005.

WORK EXPERIENCE

Year : 2006- Present
Place : Iraqi Ministry of Water Resources/ Commission for Dams
& Reservoirs Office.

FOREIGN LANGUAGE

English